Dynamic ab initio study towards new hydrocarbon pool cycles for MTO-conversion in H-SAPO-5

Thomas Deconinck

Supervisors: Prof. dr. ir. Veronique Van Speybroeck, Prof. dr. ir. Karen Hemelsoet
Counsellors: Kristof De Wispelaere, Samuel Moors, Jeroen Van der Mynsbrugge

Master's dissertation submitted in order to obtain the academic degree of
Master of Science in Chemical Engineering

Department of Applied Physics
Chairman: Prof. dr. ir. Christophe Leys
Faculty of Engineering and Architecture
Academic year 2013-2014

UNIVERSITEIT
GENT

Dit onderzoekswerk werd uitgevoerd binnen het Centrum voor Moleculaire Modellering.

Dankwoord

Een thesisjaar is altijd heel verschillend van alle jaren ervoor. Het is het eindpunt van een loopbaan als student. Het is het drukste, maar zeker ook boeiendste jaar van die loopbaan geweest. Dit jaar kreeg ik de kans om nieuwe aspecten binnen mijn opleiding te ontdekken. Het uitvoeren van onderzoek is een uitdagende en unieke ervaring, wat een grote meerwaarde heeft betekend voor mijn opleiding. Ik stond gelukkig niet alleen voor deze nieuwe opdracht. Vele mensen hebben mij geholpen en gesteund en ik wil hen daarvoor graag van harte bedanken.

In de eerste plaats wil ik mijn beide promotoren Prof. Dr. ir. Veronique Van Speybroeck en Prof. Dr. ir. Karen Hemelsoet bedanken om mij de kans te geven dit onderzoek uit te voeren binnen het CMM. Zij zorgden voor een persoonlijke begeleiding en stonden altijd klaar om te helpen bij de onvermijdelijke obstakels die optreden tijdens het maken van een thesis. Daarnaast betekende het veel voor mij om als thesisstudent te mogen meegaan naar het NCCC congres te Noordwijk (NL). Het voorstellen van mijn eigen onderzoekswerk op een grote conferentie was een unieke ervaring.

Ik zou in het bijzonder Jeroen, Kristof en Sam willen bedanken. Hun geduld, inzet en motivatie wordt ten zeerste geapprecieerd! Zij stonden steeds voor mij klaar ondanks het vele werk dat ze hadden voor hun eigen onderzoek. Zonder hen was ik nooit zover gekomen.

Ik wil zeker ook alle andere CMM'ers bedanken voor de open en hulpvaardige sfeer die leeft in de onderzoeksgroep. Die sfeer is zeker ook te danken aan mijn bureaugenoten. De gezellige babbels tijdens de middag, het gelach tussen het werken door en het samen oplossen van problemen zorgden ervoor dat het werken aangenaam werd.

Bovendien wil ik ook mijn vrienden en de hele klasgroep van de chemische technologie en materiaalkunde bedanken. Ik wens hen veel succes met hun verdere loopbaan en hoop dat onze paden zich nog zullen kruisen! In het bijzonder wil ik mijn vriendin bedanken voor alle steun en liefde.

Tot slot wil ik ook mijn ouders bedanken voor alle begrip, hulp en kansen die zij mij geboden hebben, zowel dit jaar als doorheen mijn hele leven.

Dynamische ab initio studie naar nieuwe hydrocarbon pool cycli voor MTO-conversie in H-SAPO-5

Thomas Deconinck

Masterproef ingediend tot het behalen van de academische graad van
Master in de Ingenieurswetenschappen: Chemische Technologie
Academiejaar 2008–2009

Promotoren: prof. dr. ir. Veronique Van Speybroeck, prof. dr. ir. Karen Hemelsoet
Begeleiders: ir. Kristof De Wispelaere, dr. Samuel Moors, dr. ir. Jeroen Van der Mynsbrugge

Faculteit Ingenieurswetenschappen – Universiteit Gent

Centrum voor Moleculaire Modellering

Samenvatting

Het methanol to olefins proces is niet afhankelijk van olie gebaseerde grondstoffen en is daardoor een veelbelovende techniek voor de productie van lichte alkenen. Gedetailleerd inzicht in het mechanisme van dit zeolietgekatalyseerde proces is cruciaal voor de procesoptimalisatie op industriële schaal. In de kanalen of poriën van de zure zeoliet of zeotype katalysator zijn er koolwaterstoffen aanwezig die als co-katalysatoren fungeren. Deze zijn essentieel om een hoge conversie te bereiken. In deze thesis wordt de invloed van de zuurtegraad van de katalysator op de adsorptie van belangrijke reactanten in de AFI gestructureerde katalysatoren onderzocht door middel van moleculaire modellering. Verder worden ab initio moleculaire dynamica simulaties gebruikt om de belangrijkste mechanismen voor productie van alkenen met aromatische koolwaterstoffen te vergelijken, namelijk het side chain en paring mechanisme.

Trefwoorden: MTO, adsorptie, hydrocarbon pool mechanisme, moleculaire dynamica, metadynamics, ab-initio modellering

Dynamische ab initio studie naar nieuwe hydrocarbon pool cycli voor MTO-conversie in H-SAPO-5

Thomas Deconinck

Promotoren: prof. dr. ir. Veronique Van Speybroeck, prof. dr. ir. Karen Hemelsoet

Begeleiders: ir. Kristof De Wispelaere, dr. Samuel Moors, dr. ir. Jeroen Van der Mynsbrugge

Abstract—**Het methanol to olefins proces is niet afhankelijk van olie gebaseerde grondstoffen en is daardoor een veelbelovende techniek voor de productie van lichte alkenen. Gedetailleerd inzicht in het mechanisme van dit zeolietgekatalyseerde proces is cruciaal voor de procesoptimalisatie op industriële schaal. In de kanalen of poriën van de zure zeoliet of zeotype katalysator zijn er koolwaterstoffen aanwezig die als co-katalysatoren fungeren. Deze zijn essentieel om een hoge conversie te bereiken. In deze thesis wordt de invloed van de zuurtegraad van de katalysator op de adsorptie van belangrijke reactanten in de AFI gestructureerde katalysatoren onderzocht door middel van moleculaire modellering. Verder worden ab initio moleculaire dynamica simulaties gebruikt om de belangrijkste mechanismen voor productie van alkenen met aromatische koolwaterstoffen te vergelijken, namelijk het side chain en paring mechanisme.**

Trefwoorden—**MTO, adsorptie, hydrocarbon pool mechanisme, moleculaire dynamica, metadynamica, ab initio modellering**

I. Inleiding

De vraag naar basischemicaliën zoals ethyleen en propyleen is aan het stijgen, maar de oliereserves zijn aan het slinken. Er is duidelijk nood aan alternatieve grondstoffen om de wereld te voorzien van essentiële chemicaliën. Lichte alkenen worden momenteel geproduceerd door stoomkraken van een dure olie gebaseerde voeding. Onderzoek naar alternatieve bronnen voor het produceren van lichte alkenen is noodzakelijk om de range aan grondstoffen te verruimen. Het methanol to olefins (MTO) proces is één van de meest veelbelovende alternatieven om aan de toekomstige marktvraag te voldoen.

Het MTO mechanisme is reeds het onderwerp van vele experimentele en theoretische studies geweest en de grote complexiteit ervan staat vast.[1] De methanolconversie wordt gekatalyseerd door een zeoliet of zeotype katalysator met Brønsted zure sites. Het hydrocarbon pool model wordt nu algemeen aanvaard als het MTO mechanisme. Volgens het dit model zijn er in de kanalen of poriën van de katalysator koolwaterstoffen aanwezig die fugneren als co-katalysatoren. Deze koolwaterstoffen zijn cruciaal voor het MTO proces. Er bestaan twee grote categorieën van actieve co-katalysatoren, de alkenen enerzijds en de aromatische verbindingen anderzijds. Katalytische cycli met deze koolwaterstoffen kunnen afzonderlijk werken, maar ze zijn met elkaar verbonden door nevenreacties. Dit concept wordt het dual cycle mechanisme genoemd (zie Figuur 1). Er zijn veel parameters die de reactiviteit van deze cycli beïnvloeden; afhankelijk van de katalysatortopologie, zuursterkte, temperatuur en druk, kan het relatieve belang van beide cycli verschillen. Door het verschil in selectiviteit naar lichte alkenen tussen de twee cycli is het productspectrum ook afhankelijk van deze parameters.[2]

T. Deconinck behoort tot het Centrum voor Moleculaire Modellering , Universiteit Gent (UGent), Gent, België. E-mail: thomasm.deconinck@UGent.be

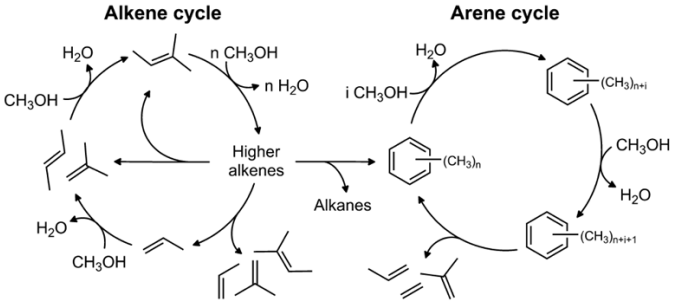

Fig. 1. Het voorgestelde dual cycle mechanisme.[2]

Westgård Erichsen et al. hebben recent experimenten uitgevoerd in AFI gestructureerde katalysatoren, namelijk H-SAPO-5 en H-SSZ-24.[3] Dergelijke experminenten worden voornamelijk uitgevoerd aangezien er vele gelijkenissen zijn tussen H-SAPO-5 en H-SAPO-34, één van de belangrijkste MTO katalysatoren gebruikt op industriële schaal. De AFI topologie heeft ééndimensionale kanalen die co-voedingsexperimenten mogelijk maken, deze kunnen extra inzicht verschaffen in het actieve mechanisme. De invloed van de zuursterkte op het MTO proces werd geëvalueerd door het vergelijken van de isostructurele materialen H-SAPO-5 en H-SSZ-24. Ze concludeerden dat de zuurdere katalysator H-SSZ-24 leidde tot een hogere selectiviteit naar etheen, propeen en aromaten. De areen cyclus werd eerder al in verband gebracht met de productie van de lichtere olefinen, in tegenstelling tot de alkeen cyclus die hoofdzakelijk C_3+ componenten levert.[1] De invloed van de zuursterkte op de relatieve reactiviteit van de twee cycli opent de mogelijkheid om de selectiviteit naar lichte alkenen aan te passen door een katalysator met geschikte zuursterkte te gebruiken. Verder gebruikten ze ^{13}C labeling experimenten om een onderscheid te maken tussen twee mechanismen met aromatische co-katalysatoren, namelijk het paring en side chain mechanisme.[4] Het labeling patroon dat ze terugvonden in de producten was consistent met het paring mechanisme. Goede kennis van het actieve mechanisme op de moleculaire schaal leidt tot een intelligenter design van het industriële proces. Verder onderzoek op dit gebied is dus relevant.

In deze thesis wordt de adsorptie van relevante reactanten in zowel H-SSZ-24 als H-SAPO-5 gemodelleerd om de invloed van de zuursterkte te onderzoeken. In een tweede luik worden

moleculaire dynamica simulaties gebruikt om het side chain en paring mechanisme te vergelijken in H-SAPO-5 startend van het heptamethylbenzenium ion.

II. Theoretische methodes

De simulaties werden uitgevoerd met het CP2K softwarepakket. Dichtheidsfunctionaaltheorie (DFT) werd gecombineerd met Gaussian plane wave basis sets. De revised-PBE functionaal wordt gebruikt met GTH pseudo potentialen. Periodieke randvoorwaarden worden toegepast op een supercel die bestaat uit 48 T-atomen en 1 Brønsted zure site. Ab initio moleculaire dynamica wordt gebruikt voor het simuleren van de reactantenvallei om zodanig ook de invloed van de temperatuur en de roosterflexibiliteit in rekening te brengen. De simulaties zijn uitgevoerd bij 623 K en metadynamica zorgt ervoor dat er een efficiënte sampling van de barrière mogelijk is.[5] Metadynamica is een krachtig hulpmiddel om nieuwe reactiepaden te onderzoeken door een set van collectieve variabelen te definiëren die een interessante regio op het potentiële energie oppervlak beschrijven. Deze simulaties geven inzicht in de vrije energie van de reactie (ΔG_r), de evenwichtsconstante (K_{eq}) en de oriëntatie van de molecules gedurende de reactie bij de gegeven temperatuur.

III. Resultaten en discussie

De adsorptie van dimethylether (DME), methanol en benzeen in H-SAPO-5 en H-SSZ-24 wordt onderzocht. Benzeen wordt gekozen als representatieve component voor de aromatische koolwaterstoffen. De adsorptie op zowel de zure site als een naburige site (boven een zuurstofatoom dat niet verbonden is met de zure site) wordt beschouwd. Co-adsorptie van benzeen met één en twee methanol molecules wordt eveneens bestudeert om een prereactief complex te simuleren voor de methylatie van benzeen. Het effect van clustervorming van methanol wordt ook in beschouwing genomen.

De belangrijkste resultaten zijn samengevat in Figuur 2. Polaire molecules zoals methanol en DME adsorberen veel sterker op de zure site in H-SSZ-24 dan in H-SAPO-5 omdat dit een zuurdere katalysator is. Op de naburige sites is het effect van de zuursterkte minder uitgesproken omdat de adsorptie daar gedomineerd wordt door dispersie-interacties in plaats van elektronische interacties. Voor de adsorptie van benzeen is de bijdrage van dispersie-interacties altijd sterker dan de elektronische bijdrage, hierdoor is het verschil tussen beide sites beperkter. Er is echter nog steeds een sterkere adsorptie op de zure site dankzij de interactie tussen de π-orbitalen van benzeen en het Brønsted zure proton. De coadsorptie simulaties tonen aan dat een methanoldimeer een proton kan opnemen van de katalysator, in het bijzonder in H-SSZ-24, deze clustervorming is energetisch bevoordeeld ten opzichte van het splitsen van deze cluster (zie Figuur 2). Bij de zuivere adsorptie van methanol wordt een sterke gefysisorbeerde toestand teruggevonden als optimale structuur waarbij waterstofbrugbindingen de structuur van het complex bepalen. Bij de adsorptie van het dimeer wordt echter een gechemisorbeerde toestand teruggevonden, de protonaffiniteit van het dimeer is duidelijk veel sterker dan die van een enkele methanol molecule. De coadsorptie is voor zowel benzeen als methanol sterker dan de zuivere adsorptie, de nabijheid van een ander molecule zorgt dus voor extra stabilisering van het reactantencomplex.

Om een onderscheid te kunnen maken tussen de verschillende

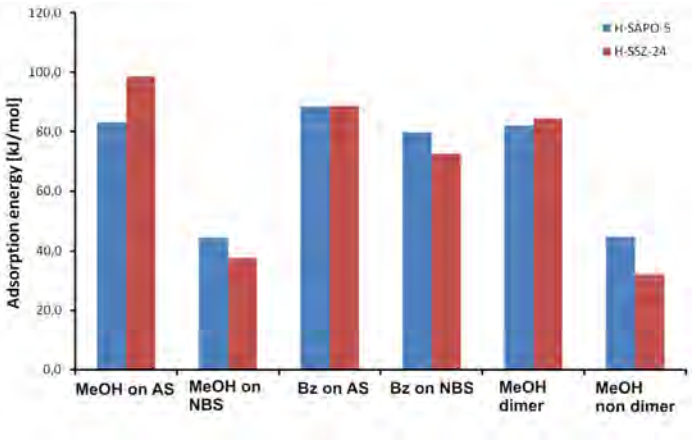

Fig. 2. Berekende adsorptie-energiën van methanol (MeOH) en benzeen (Bz) op zowel de zure site (AS) als de naburige site (NBS) in H-SAPO-5 and H-SSZ-24 en een vergelijking van clustervorming van methanol met het breken van de cluster

mechanismes met aromatische koolwaterstoffen, worden moleculaire dynamica simulaties gebruikt. Sterk gemethyleerde benzeencomponenten zoals heptamethylbenzenium ($heptaMB^+$) zijn de meest reactieve species in katalysatoren met grote poriën zoals H-SAPO-5.[6] Daarom wordt $heptaMB^+$ gekozen als modelcomponent van waar de simulaties zullen vertrekken. Er bestaan hoofdzakelijk drie katalytische cycli voor de alkeenproductie met aromatische componenten als intermediairen. Deze zijn het side chain mechanisme, het paring mechanisme dat begint met een ringcontractie en het paring mechanisme dat start met een ringexpansie.[7][8]

Na verscheidene methylatiestappen van benzeencomponenten wordt het $heptaMB^+$ kation gevormd. Deze component kan een deprotonering ondergaan die resulteert in een exocyclische dubbele bindingen die verder gemethyleerd kan worden. Er kan ook ringcontractie tot een vijfring doorgaan of een ringexpansie die een zevenring oplevert. Dit zijn de drie reacties die bestudeert worden in deze thesis om te bekijken of er al een groot verschil is tussen de mogelijke mechanismes in deze eerste stappen. Een overzicht van de bestudeerde reacties wordt getoond in Figuur 3. Het kan noodzakelijk zijn om de volledige katalytische cyclus te simuleren om te bepalen welk mechanisme dominant is bij de productie van alkenen, maar desalniettemin is deze eerste stap interessant omdat deze reacties bottlenecks zijn in hun respectievelijke cycli.

De reacties zijn gesimuleerd bij 623 K. De barrière voor de ringcontractie is 141 kJ/mol en de barriè voor de deprotonering is 166 kJ/mol. De vrije energie profielen van de reacties worden getoond in Figuur 4. De resultaten van de ringexpansie ontbreken aangezien de keuze van de collectieve variabelen niet optimaal was. Statische berekeningen en literatuur wijzen er echter op dat deze reactie van ondergeschikt belang is.[8] Voor de deprotonering van $heptaMB^+$ zijn er twee verschillende reactiepaden geobserveerd; ofwel wordt het proton overgedragen aan methanol terwijl simultaan methanol zijn proton doorgeeft aan de katalysator (deze is afgebeeld in Figuur 4), ofwel wordt het proton afgestaan aan een cluster van methanol molecules. De rechtstreekse overdracht van $heptaMB^+$ naar de katalysator en de overdracht naar een ongebonden methanol molecule worden dus niet teruggevonden. Dit suggereert dat deze reac-

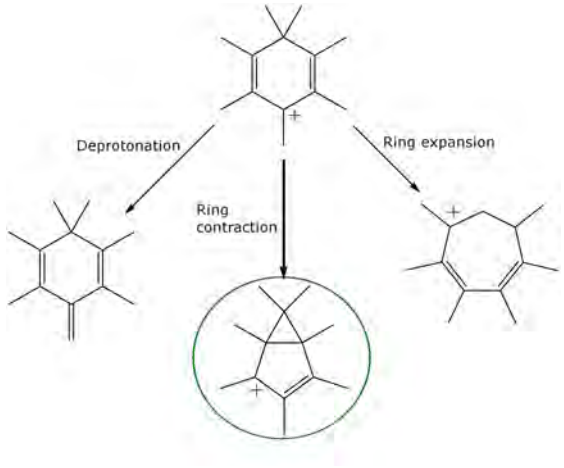

Fig. 3. Verschillende reacties startend van $heptaMB^+$ die bestudeerd worden in deze thesis in H-SAPO-5

tiepaden een hoge activeringsenergie hebben. Methanol dient als een brug tussen de katalysator en $heptaMB^+$ voor de deprotonering om op die manier te reactie vlotter te laten verlopen. De reactiebarrières tonen aan dat de ringcontractie kinetisch bevoordeeld is. De evenwichtsconstante voor de deprotonering K_{eq} is 2.0 $\times 10^{-9}$ en die voor de ringcontractie is 8.2 $\times 10^{-4}$. Onder evenwichtscondities is het ringcontractie mechanisme dus veel waarschijnlijker omdat $heptaMB^+$ zich altijd in zijn geprotoneerde vorm bevindt. Het ringcontractiemechanisme is dus zowel kinetisch als thermodynamisch bevoordeelt.

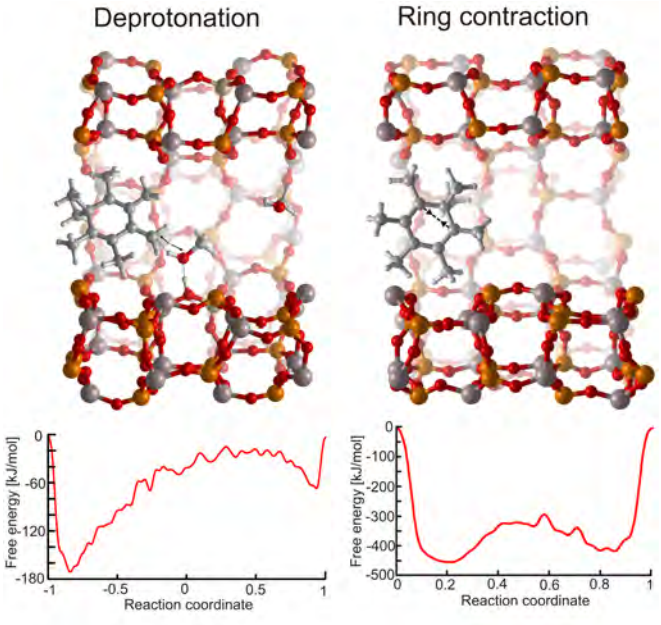

Fig. 4. Links staat de transitietoestand afgebeeld voor de deprotonering van $heptaMB^+$ geassisteerd door een methanol molecule die gebonden is aan de zure site in H-SAPO-5. Het vrije energie profiel is eronder terug te vinden. Rechts is de transitietoestand voor de ringcontractie van $heptaMB^+$ afgebeeld en het vrije energie profiel staat eronder.

IV. Conclusies

Moleculaire modellering is toegepast om de invloed van de zuursterkte op de adsorptie van belangrijke reactanten te onderzoeken in H-SAPO-5 en H-SSZ-24. Deze isostructurele materialen hebben de AFI topologie, gekenmerkd door zeer ruimte één-dimensionale kanalen. Polaire moleculen zoals methanol en DME adsorberen sterker in de zuurdere H-SSZ-24 katalysator omdat hun adsorptie gedomineerd wordt door elektronische interacties. Voor de adsorptie van apolaire moleculen, zoals benzeen, is de dispersie-interactie het belangrijkste en deze is daarom minder gevoelig aan veranderingen in zuursterkte. Coadsorptie simulaties toonden aan dat methanol dimeer vorming energetisch bevoordeeld is en dat de aanwezigheid van andere moleculen een extra stabilisering aan het complex geeft. Geavanceerde moleculaire dynamica simulaties worden gebruikt om het paring en side chain mechanisme te vergelijken startend vanaf $heptaMB^+$ in H-SAPO-5. Metadynamica is een krachtig hulpmiddel om deze complexe reacties te simuleren en levert informatie over de mogelijke reactiepaden, de reactiebarrière en de evenwichtsconstante. Deze simulaties zijn geen routineberekeningen, een intelligente keuze van de collectieve variabelen is nodig om realistische resultaten te bekomen. Het ringcontractie paring mechanisme heeft zowel een gunstigere reactiebarrière als evenwichtsconstante voor de eerste cruciale stap van de katalytische cyclus. Deze theoretische bevindingen bevestigen de experimentele resultaten.[4]

Dankbetuigingen

Prof. U. Olsbye, Prof. S. Svelle en M. Westgård Erichsen (inGAP Centre of Research Based Innovation, University of Oslo) worden bedankt voor hun experimentele resultaten die bijgedragen hebben tot deze thesis. De computationele infrastructuur (Stevin Supercomputer Infrastructure) en diensten die in dit werk gebruikt zijn werden voorzien door het VSC (Vlaams Supercomputer Centrum), gesponsord door de Universiteit Gent, de Hercules stichting en de Vlaamse overheid - afdeling EWI.

References

[1] K. Hemelsoet, J. Van der Mynsbrugge, K. De Wispelaere, M. Waroquier, V. Van Speybroeck, ChemPhysChem 14 (8).
[2] U. Olsbye, S. Svelle, M. Bjørgen, P. Beato, T. V. W. Janssens, F. Joensen, S. Bordiga, K. P. Lillerud, Angew. Chem. Int. Ed 51 (24) (2012) 5810–5831.
[3] M. Westgård Erichsen, S. Svelle, U. Olsbye, J. Catal. 298 (2013) 94–101.
[4] M. Westgård Erichsen, S. Svelle, U. Olsbye, Catal. Today 215 (2013) 216–223.
[5] A. Laio, F. L. Gervasio, REP. PROG. PHYS. 71 (12) (2008) 126601.
[6] A. Sassi, M. A. Wildman, H. J. Ahn, P. Prasad, J. B. Nicholas, J. F. Haw, J. PHYS. CHEM. B 106 (9) (2002) 2294–2303.
[7] T. Mole, G. Bett, D. Seddon, J. Catal. 84 (2) (1983) 435–445.
[8] B. Arstad, S. Kolboe, O. Swang, J. PHYS. CHEM. A 109 (39) (2005) 8914–8922.

Dynamic ab initio study towards new hydrocarbon pool cycles for MTO-conversion in H-SAPO-5

Thomas Deconinck

Supervisors: prof. dr. ir. Veronique Van Speybroeck, prof. dr. ir. Karen Hemelsoet

Counsellors: ir. Kristof De Wispelaere, dr. Samuel Moors, dr. ir. Jeroen Van der Mynsbrugge

Abstract—**The methanol to olefins process, which does not depend on oil-based feeds, is a very promising technique for the production of light olefins. Detailed understanding of the mechanism behind this zeolite-catalyzed process is crucial for the process optimization on an industrial scale. Inside the pores of the acidic zeolite or zeotype catalysts there are hydrocarbon pool species present which act as co-catalysts and are essential to reach a high conversion. In this thesis, the influence of catalyst acidity on the adsorption of important species in AFI-structured catalysts is investigated by means of molecular modeling. Furthermore ab initio molecular dynamics simulations are used to compare the main mechanisms for olefin production involving aromatic species, namely the side-chain and paring mechanisms.**

Keywords—**MTO, adsorption, hydrocarbon pool mechanism, molecular dynamics, metadynamics, ab initio modeling**

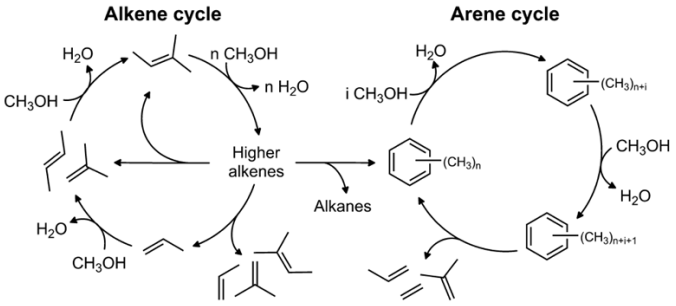

Fig. 1. The proposed dual cycle mechanism.[2]

I. Introduction

As the demand for base chemicals keeps growing and oil reserves continuously diminish, the need for alternative feedstocks to provide the world with base chemicals is evident. Light olefins are currently produced by steam-cracking of an expensive oil-based feed. In order to diversify the feedstock, research towards alternative sources to produce light olefins is necessary. The methanol to olefins (MTO) process is one of the most promising alternatives to fulfill the market's demand in the future.

The MTO mechanism has been the subject of many experimental and theoretical studies, and has proven to be very complex.[1] The methanol conversion is catalyzed by a zeolite or zeotype catalyst with Brønsted acid sites. Experimental evidence has lead to the general acceptance of the hydrocarbon pool model for the MTO mechanism. In this model the hydrocarbon species present inside the pores of the catalyst act as co-catalysts and are crucial for the MTO conversion. There exist two main categories of active co-catalysts, the alkenes and the aromatic compounds. Catalytic cycles with these co-catalyst can operate individually, but they are linked to each other by secondary reactions, this concept is called the dual-cycle mechanism (see Figure 1). There are many parameters influencing the reactivity of these cycles; depending on the catalyst topology, acidity, temperature and pressure, the relative importance of both cycles can differ. Due to the difference in selectivity towards light olefins between both cycles the product spectrum is also dependent on these parameters.[2]

Recently, Erichsen et al. have performed experimental work on catalysts with the AFI-structure, namely H-SAPO-5 and H-SSZ-24, because of the similarities between H-SAPO-5 and H-SAPO-34.[3] The AFI topology has one dimensional pores that are open to co-feeding experiments, which can lead to additional insight on the operating mechanism. The influence of the acidity on the MTO-process was evaluated by comparing the isostructural catalysts H-SAPO-5 and H-SSZ-24. They concluded that the more acidic H-SSZ-24 gave rise to a higher selectivity towards ethylene, propylene and aromatics. The catalytic cycle with aromatic compounds as co-catalyst has previously already been linked to the production of the lighter olefins, while the alkene cycle predominantly produces C_3+ products. This difference in reactivity between both cycles due to the difference in acid strength opens the possibility to tune the selectivity towards lighter olefins by adapting the acidity of the catalyst. Furthermore, they used carbon labeling experiments to distinguish between two aromatic based mechanisms, namely the paring and side-chain mechanism.[4] They observed products with a labeling pattern consistent with a paring type reaction mechanism. A good understanding of the mechanisms on the molecular scale can lead to a smarter and better design of the industrial process, thus further research on this topic is very interesting.

In this thesis the adsorption of relevant reactant species on both H-SSZ-24 and H-SAPO-5 is modeled to investigate the influence of the acidity on a theoretical level. Next, molecular dynamics simulations are used to compare the paring and side-chain mechanism in H-SAPO-5 starting from the heptamethylbenzenium ion.

II. Theoretical methods

Simulations were performed with the CP2K simulation package on the DFT level of theory and with Gaussian plane wave basis sets. The revised-PBE functional is used with GTH pseudo potentials. Periodic boundary conditions were applied with a super cell consisting of 48 T-atoms and one Brønsted acid site. Equilibrium ab initio molecular dynamics were used for the simulation of the reactant state basin to take the influence of temperature and framework flexibility into account. Metadynamics

T. Deconinck is with the Center for Molecular Modeling, Ghent University (UGent), Gent, Belgium. E-mail: thomasm.deconinck@UGent.be

simulations at 623 K are performed to achieve computationally efficient sampling of the reaction barrier.[5] Metadynamics is a powerful tool to explore reaction paths by defining a set of collective variables which describe an interesting region of the potential energy surface. These simulations will give insight into the reaction free energy (ΔG_r), the equilibrium constant (K_{eq}), the reaction rate (k) and also the orientations of the molecules on the reaction path at the given temperature.

III. Results and Discussion

The adsorption of dimethylether (DME), methanol and benzene was investigated on H-SAPO-5 and H-SSZ-24. Benzene is chosen as a representative compound of the arene based hydrocarbon pool. Adsorption on both the acid site and a neighbouring site (on top of a bridging oxygen atom, not connected to the acid site) is evaluated. Co-adsorption of benzene with one and two methanol molecules is investigated as well to simulate the pre-reactive state for a methylation reaction and to examine the effect of a cluster of methanol molecules.

The adsorption of the polar molecules, methanol and DME, on the acid site is stronger in H-SSZ-24 than in H-SAPO-5 due to the stronger acidity of the latter. On the neighbouring site this effect is less pronounced as the adsorption interaction on this site is dominated by dispersion interactions rather than electronic contributions. The adsorption of benzene is always driven by dispersion interactions, thus the difference between both sites is less pronounced, there is however still a stronger adsorption on the acid site due to the interaction between the π-orbitals of benzene and the Brønsted proton. Moreover, the co-adsorption simulations show that a methanol dimer is able to abstract a proton from the catalyst, especially in H-SSZ-24 and that this cluster formation is energetically favored. The pure adsorption of methanol showed a strong physisorbed methanol molecule, bonded to the framework with hydrogen bonds, but chemisorption only occurred in the presence of a second methanol molecule. These simulations further indicate that co-adsorption induces some additional stability of the reactants, both for methanol as for benzene. The most important results are shown in Figure 2.

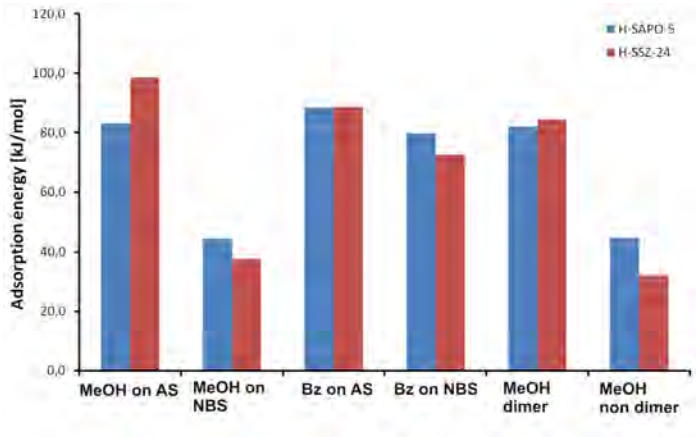

Fig. 2. Important adsorption energies for the MTO process in H-SAPO-5 and H-SSZ-24 involving methanol (MeOH) and benzene (Bz) on both the acid site (AS) and neighbouring site (NBS) and a comparison between methanol cluster formation and breaking

To distinguish between the different mechanisms involving aromatic hydrocarbon pool species, molecular dynamics simulations are applied. Heavily methylated benzenes such as heptamethylbenzenium ($heptaMB^+$) are the most reactive aromatic compounds in large pore catalysts such as H-SAPO-5.[6] Therefore $heptaMB^+$ was chosen as the model compound to start the simulations from. There exist three main catalytic routes for the olefin production with aromatic compounds as intermediates, the side-chain mechanism, the paring mechanism starting with a ring contraction and the paring mechanism starting with a ring expansion.[7][8]

After several methylations of benzenic compounds, the $heptaMB^+$ cation is formed. This compound can undergo either deprotonation, leading to an exocyclic double bond that can be methylated, or undergo a ring contraction leading to a five membered ring with an isopropyl side chain or a ring expansion leading to a seven membered ring. In this thesis these three reactions are simulated to see if there is already a large difference between the various mechanisms in these first steps. An overview of these steps is shown in Figure 3. Although simulation of the entire catalytic cycles might be necessary to determine which mechanism dominates product formation, it is instructive to study the first step of each mechanism since these steps are important bottlenecks for their respective catalytic cycle.

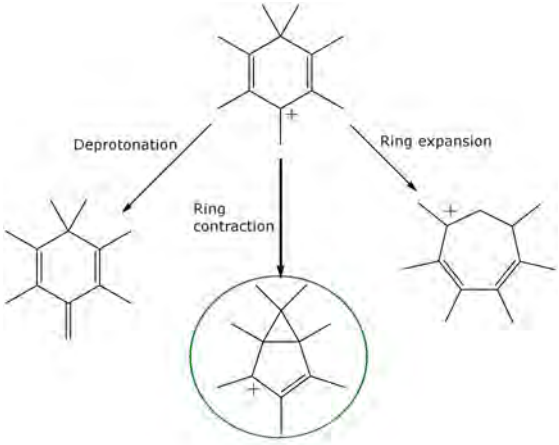

Fig. 3. Different reactions starting from $heptaMB^+$ relevant for MTO chemistry in H-SAPO-5

The reactions are simulated at 623 K. The barrier for the ring contraction is 141 kJ/mol, while the reaction barrier for the deprotonation is 166 kJ/mol, the reaction profiles are displayed in Figure 4. For the ring expansion the results are missing due to a suboptimal choice of the collective variables. Static optimizations and literature data however indicate that this reaction path is less important.[8] For the deprotonation reaction two different reaction routes are observed; either the methanol which substracts the proton of $heptaMB^+$ immediately transfers its own proton to the framework (as is depicted in Figure 4) or it has to have a hydrogen bond with the second methanol molecule before reaction can occur. Neither transfer directly to the framework or transfer to an unbonded methanol molecule has been observed and these reactions are thus most likely highly activated. Methanol acts as a bridge between $heptaMB^+$ and the framework to facilitate the reaction. The reaction barriers indicate that kinetically the ring contraction is slightly favored. In equi-

librium conditions the deprotonation has a K_{eq} of 2.0 $\times 10^{-9}$, while for the ring contraction this constant is 8.2 $\times 10^{-4}$, which clearly favors the ring contraction since $heptaMB^+$ will remain in its protonated form. The ring contraction is thus thermodynamically favored as well.

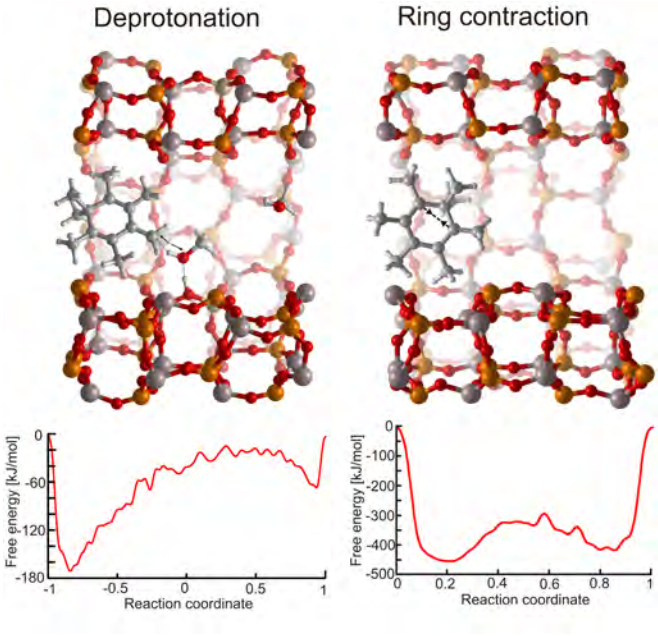

Fig. 4. On the left side the transition state for the deprotonation of $heptaMB^+$ by a methanol molecule bonded to the acid site of H-SAPO-5, with below the free energy profile. On the right side the transition state for the ring contraction of $heptaMB^+$ with its corresponding free energy profile shown below

IV. Conclusions

Molecular modeling is used to investigate the influence of catalyst acidity on the adsorption of species that are important for the MTO process in H-SAPO-5 and H-SSZ-24. Co-adsorption complexes representing a pre-reactive state are simulated. Polar molecules such as methanol and DME adsorb stronger in the more acidic H-SSZ-24 catalyst because their adsorption is dominated by the electronic interaction with the acid site. The adsorption of apolar molecules such as benzene is governed by their dispersion interaction and therefore less sensitive to the catalyst acidity. Advanced molecular dynamic simulations are performed to compare the ring contraction, ring expansion and side-chain mechanisms starting from $heptaMB^+$ in H-SAPO-5. Metadynamics has proven to be a very powerful tool to simulate complex reactions resulting in information about the possible reaction paths, the reaction barrier and the equilibrium constant. The ring contraction mechanism has both a lower reaction barrier and a more favorable equilibrium constant for the first crucial step of the catalytic cycle, confirming the experimental results.[4]

Acknowledgements

Prof. U. Olsbye, Prof. S. Svelle and M. Westgård Erichsen (inGAP Centre of Research Based Innovation, University of Oslo) are acknowledged for providing experimental data related to this research. The computational resources (Stevin Supercomputer Infrastructure) and services used in this work were provided by the VSC (Flemish Supercomputer Center), funded by Ghent University, the Hercules Foundation and the Flemish Government department EWI.

References

[1] K. Hemelsoet, J. Van der Mynsbrugge, K. De Wispelaere, M. Waroquier, V. Van Speybroeck, ChemPhysChem 14 (8).
[2] U. Olsbye, S. Svelle, M. Bjørgen, P. Beato, T. V. W. Janssens, F. Joensen, S. Bordiga, K. P. Lillerud, Angew. Chem. Int. Ed 51 (24) (2012) 5810–5831.
[3] M. Westgård Erichsen, S. Svelle, U. Olsbye, J. Catal. 298 (2013) 94–101.
[4] M. Westgård Erichsen, S. Svelle, U. Olsbye, Catal. Today 215 (2013) 216–223.
[5] A. Laio, F. L. Gervasio, REP. PROG. PHYS. 71 (12) (2008) 126601.
[6] A. Sassi, M. A. Wildman, H. J. Ahn, P. Prasad, J. B. Nicholas, J. F. Haw, J. PHYS. CHEM. B 106 (9) (2002) 2294–2303.
[7] T. Mole, G. Bett, D. Seddon, J. Catal. 84 (2) (1983) 435–445.
[8] B. Arstad, S. Kolboe, O. Swang, J. PHYS. CHEM. A 109 (39) (2005) 8914–8922.

Contents

List of abbreviations

AIMD	ab initio molecular dynamics
AS	acid site
Bz	benzene
CHA	chabazite
CN	coordination number
CSVR	canonical sampling through velocity rescaling
CV	collective variable
DFT	density functional theory
DME	dimethylether
FCC	fluid catalytic cracker
GGA	generalized gradient approximation
GTO	Gaussian type orbital
$heptaMB^+$	heptamethylbenzenium
HMMC	1,2,3,3,4,5-hexamethyl-6-methylene-1,4-cyclohexadiene
HP	hydrocarbon pool
LDA	local density approximation
MD	molecular dynamics
MeOH	methanol
MM	molecular mechanics
MTO	methanol to olefins
MTP	methanol to propylene
NBS	neighbouring site
NMR	nuclear magnetic resonance
OCP	olefin cracking process
PA	proton affinity
QM	quantum mechanics
SAPO	silico-aluminophosphate
STO	Slater typer orbital
TS	transition state
US	United States

List of symbols

β	J^{-1}	thermodynamic beta
ΔE_{ads}	kJ/mol	adsorption energy
ΔE_{co-ads}	kJ/mol	co-adsorption energy
ΔE_r	kJ/mol	reaction energy
ΔG	kJ/mol	free energy difference
$\Delta G^{\ddagger}$	kJ/mol	free energy reaction barrier
ΔG_r	kJ/mol	Free energy of reaction
h	J s	Planck constant
k	s^{-1}	reaction rate constant
k_b	JK^{-1}	Boltzmann constant
K_{eq}	-	equilibrium constant
R	$\frac{J}{molK}$	gas constant
T	K	temperature
t	s	time
V_G	kJ/mol	potential energy surface

There is nothing noble in being superior to some other man,
true nobility is being superior to your former self.

- Hindu proverb -

Chapter 1

The MTO process

1.1 Introduction

As the demand for base chemicals keeps growing and oil reserves continuously diminish, the need for alternative feedstock to provide the world with base chemicals is clear to everyone.[1] Light olefins, which are the most important base chemicals, are currently produced by steam-cracking of the expensive oil-based feed. In order to diversify the feedstock, research towards alternative sources to produce light olefins is necessary.

The polymer market consumes large amounts of these olefins every year, but the demand is shifting. Propylene is becoming more and more important. At the moment ethylene is mainly produced by steam cracking of either natural gas, naphta or heavier oil fractions. Propylene was originally a side product of the ethylene production. Propylene is formed together with the ethylene, but there are only a few processes that deliver on purpose production of propylene. Lately, propylene prices have increased more than the ethylene prices which has been another driving force towards new processes that are able to produce propylene, preferably independent of the oil market.

The demand for propylene has increased due to the superior quality of its corresponding polymer compared to polyethylene. While the demand for ethylene also rises the demand for propylene increases faster as can be seen in Figure 1.1. The annual demand growth of propylene is 0.5% larger than the growth in demand for ethylene. In the US and the Middle-East there are new ethane crackers because of the cheap feedstock that is readily available.[2] [3] These ethane crackers produce large amounts of ethylene but little to no propylene. The traditional steam crackers which are still cracking naphta are not capable to vary the propylene production to a large extend. The overall result is that propylene prices are rising and on-purpose production of propylene is of utmost importance.

To satisfy the need of the market in the upcoming years the methanol to olefins (MTO)

process is a very promising technique.[4] This process is able to take advantage of both the rise in propylene demand and the depletion of oil reserves. As the name explains, the MTO process is able to convert methanol into a wide range of light olefins. Since methanol can be produced from various sources independent of oil it can use a cheap feedstock to produce very valuable products. Another advantage of the MTO process is its flexibility: the product spectrum can be varied to satisfy the needs of the market. This is one of the most promising techniques for industrial production of the light olefins when oil prices are soaring.[5]

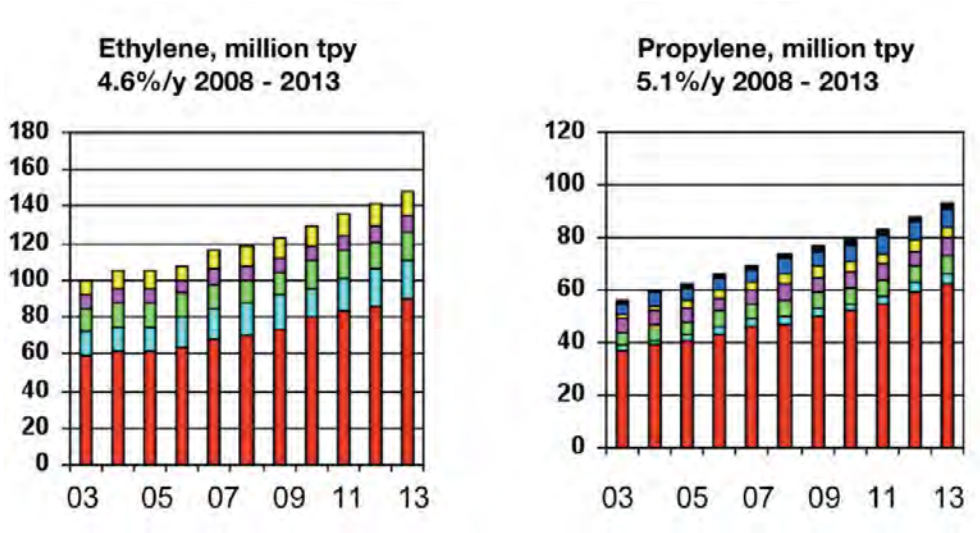

Figure 1.1: The evolution of the ethylene and propylene demand in 2008-2013 (million tpy)[6]

1.2 Methanol production

Worldwide methanol production capacity is increasing strongly the last 15 years, going from 30 million tonnes/year in 1995 to 90 million tonnes/year in 2011.[7] As can be seen in Figure 1.2, China has grown a lot in this market, holding over 50% of the production capacity. The capacity is however not fully used in China, but it adapts itself to fulfill the market demand.

For the production of methanol there are one-step and two-step processes. It is possible to convert methane over a Cu-zeolite to form methanol in a single step, but usually a two-step process is preferred.[7] This process uses syngas as an intermediate which will be further converted to methanol. Syngas or synthesis gas is defined as a gaseous mixture of hydrogen and carbon monoxide. An important characteristic to define this mixture is the hydrogen/carbon ratio. This ratio has an influence on the energy content of the mixture and on its reactivity towards different product types. Depending on the

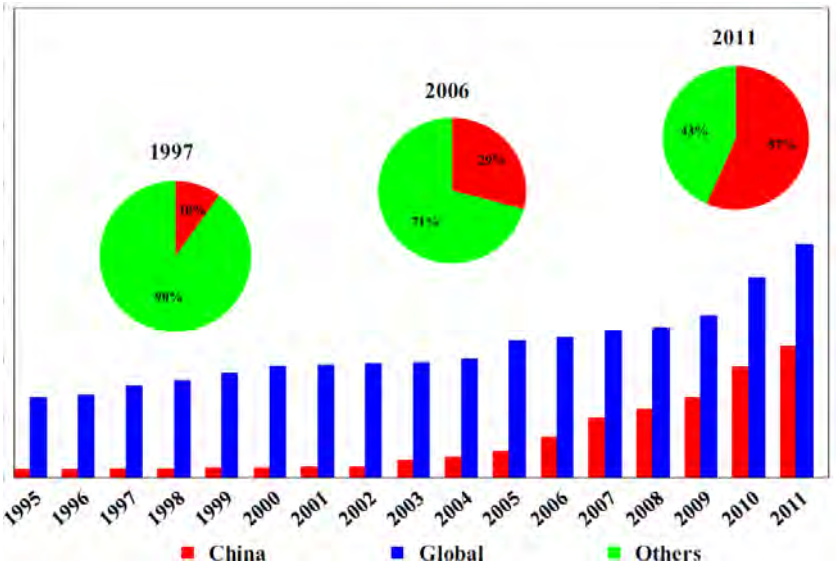

Figure 1.2: Evolution of methanol capacity in the world and in China [7]

source of the syngas the obtained ratio will be different. There are often traces of carbon dioxide remaining in the mixture due to it being produced by oxidation reactions.

There are three main resources for syngas: natural gas, coal and biomass. The main reason for choosing a specific resource is its price. Natural gas and coal are readily available in some parts of the world and are thus an obvious choice in those regions. [3]

Natural gas can be converted into syngas by a combination of steam reforming and partial oxidation. In steam reforming the feedstock is catalytically converted in the absence of oxygen with the addition of steam and possibly carbon dioxide, leading to a mixture of CO, CO_2 and H_2. In partial oxidation, reaction with oxygen leads to a mixture of CO and H_2. In a combination of the two processes a quarter of the natural gas stream is subjected to steam reforming. The remainder passes with the reformed gas to an autothermally operated reformer in which the natural gas is partially oxidized by oxygen. [7] The advantage of this process is its simplicity and high-purity products.

Coal is still abundant in many regions of the world. Therefore it can be a very cheap and interesting resource. [3] In China 50 million tonnes/year of methanol are produced. [8] The share of this production that is reserved for MTO and MTP processes is growing every year and will be more than 17% by 2017. [9] China has a large overcapacity of methanol, but can adapt its production to fulfill the market demand. In particular during times where oil prices are peaking this can be very lucrative. [5] Steam reforming and partial oxidation of coal result in a syngas with a rather low H_2/CO ratio. Therefore the watergas shift reaction is very important in this case to obtain enough hydrogen (see

further). It is also important to note that the steam reforming reaction of carbon is endothermic and thus the partial oxidation is needed to provide enough energy. The overall carbon balance is rather low for this process, but since coal is a very cheap resource this is not an issue.

A final source for syngas is biomass. Biomass is a very promising renewable carbon source that is widely available. It is the resource with the lowest CO_2 emissions in its life cycle. There is a debate on whether it is ethical to use biomass and crop land for non-food purposes. This debate can however be avoided by using low value biowaste. Before this biomass can be gasified multiple treatment steps are necessary. Drying can increase the energy efficiency of the following steps. Torrefaction or pyrolysis of the biomass can be required to pulverize the feedstock.[10] There are many different gasification methods available, such as heated entrained flow, fluidized bed gasification and atmospheric or pressurized gasification. The advantages and disadvantages of all the technologies, together with a more elaborate description are reported by Olofsson et al.[11]. The syngas produced in this way requires some final gas cleaning steps before it is ready for synthesis purposes. There are demonstration units planned for this technology but due to the complexity of the systems and the energy cost of the different endothermic processes this technology is more expensive.[12]

The final step is the conversion of syngas to methanol. This conversion is performed over a copper-zinc-aluminum catalyst. The optimal H_2/CO ratio for this reaction is 2, but in practice a slightly higher ratio is used to control the by-product formation.[13] The watergas shift reaction is the most important reaction to influence this ratio. This reaction can be seen below. A water-gas-shift reactor changes the composition of the feed to acquire the optimal H_2/CO ratio. Methanol synthesis reactors operate at a pressure between 50-100 bar and a temperature of 230-270°C.[12]

$$CO + H_2O \leftrightharpoons CO_2 + H_2$$

1.3 The MTO plant

The MTO-process is very interesting because it provides a production route for olefins that is independent of oil. There are however more reasons why this process is being studied. In contrast to the traditional steam crackers the MTO plant can be designed for a wider range of outlet compositions. In particular the propylene production can be favored over the production of ethylene. The ratio of propylene production to ethylene production is limited to 0.53-0.6 in naphta and gas oil crackers.[14] The new ethane crackers in North America and the middle east produce even less propylene while the average annual demand growth for propylene is higher than the annual demand growth

rate of ethylene (see Figure 1.1). Therefore 20% of the annual demand for propylene will have to be produced by on-purpose processes such as MTO.[15]

The process is operated in a fluidized bed reactor and 80% of the methanol is converted into ethylene and propylene. In this reactor a zeolite catalyst is present, industrially H-SAPO-34[16] and H-ZSM-5[17] are often used.[18] The small pores of H-SAPO-34 result in a high selectivity towards the light olefins, because branched and larger molecules are being hindered. The larger openings in H-ZSM-5 result in a lower light olefins yield. Methanol is dehydrated and converted to light olefins over this catalyst. An intermediate which is formed in the dehydration step is dimethylether (DME). This intermediate is never fully converted and will have to be removed from the product stream.

The pressure in the reactor is usually chosen according to the mechanical strength of the materials.[19] Lower partial pressures of methanol can lead to a higher yield towards light olefins and in particular light olefins. A feed of methanol with 20% water can thus improve this yield.[19] The temperature is the main control variable, higher temperatures lead to a higher selectivity towards ethylene. Operating conditions can thus vary depending on the preferred product distribution, but in general a relatively low pressure around 1 bar and temperatures between 300-500°C are applied.[20]

The relatively high temperatures of this process will inevitably result in coke formation. This coke deposition will lower the activity of the catalyst and the conversion while changing the product spectrum, in particular hydrogen and alkanes are being formed.[21] H-ZSM-5 will deactivate on a timescale of 10-60 minutes depending on the process conditions.[22] H-SAPO-34 undergoes even faster deactivation.[23] This is why the fluidized bed setup with a continuous regeneration section is used. The operation is thus very similar to that of a fluidized catalytic cracker unit (FCC).

Since the products of the MTO-process are similar to these of a steam cracker the separation section is also similar to the cold box separation section found in those processes. The main difference is that there's the need for an oxygenate removal section beforehand due to the high amount of DME and water in the effluent. There are also less light ends present in the effluent compared to a traditional cracker effluent; therefore it is usually not economically viable to recuperate hydrogen.

In 1995 Norsk Hydro constructed a demonstration unit to study the continuous operation of the fluidized-bed MTO reactor/regeneration system.[24] The unit is able to convert 0.75 ton methanol per day. For over 15 years the unit has been a valuable resource for confirming the performance of the MTO process technology and its catalyst performance and stability. The development of the unit led to an improvement of the cost effective design of the established MTO process technology. Optimization of technical characteristics, e.g. high single-pass olefin yield and low byproduct yields, was realized by the use

of the demonstration unit. The unit, which was the first of his kind, continues to be an excellent asset for testing new ideas and improvements for the MTO process. The setup of the unit is shown in Figure 1.3.

Figure 1.3: Pilot MTO plant [24]

1.4 The MTO/OCP setup

A disadvantage of this process is that there is a side product stream of C_{4+} species. These C_{4+} species are unwanted since they have a lower value than ethylene and propylene. However since these C_{4+} components are usually also olefins, they are an ideal feed for the olefin conversion process (OCP) [25] [24] developped by Total and UOP . This process will convert the higher olefins into the more valuable C_2 and C_3 species. There exists a demonstration unit in Feluy, Belgium that proves the combination of the MTO process with the OCP process. This demonstration unit proved useful enough to make plans for a large production site in China.

In the OCP process there is a dimerization of the C_{4+} components, forming large (C_{8+}) compounds. These components are afterwards converted into the desired ethylene and propylene via cracking reactions. The process is performed over a MFI-structured catalyst, such as H-ZSM-5, at atmospheric pressure. This process also uses the fluidized bed technology to overcome the coke deposition problems that occur.

This process can be integrated with the MTO-process but can also be used in combination with the traditional naphta steam crackers. Conversion of the C_{4+} stream towards high amounts of propylene and some ethylene can be beneficial. It helps to control the propylene/ethylene production ratio which is a very interesting characteristic. As can be seen in Figure 1.4, the combination of MTO and OCP can vary the propylene/ethylene ratio from 1.25 to 1.8 while maintaining a high carbon yield.[24] The total integration of these two schemes can be seen in Figure 1.5. This full integration is not that straightforward due to the presence of oxygenates and the amount of water present in the process. However the demonstration unit of Total Petrochemicals has proven to maintain high yields and conversion for hundreds of days.[26] A good separation and operation of a MTO/OCP unit is thus possible.

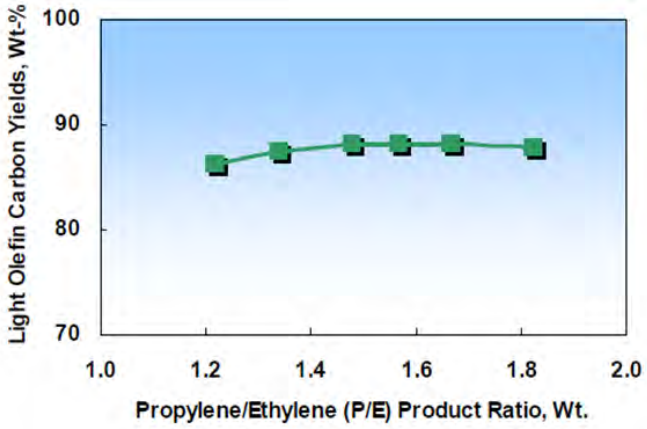

Figure 1.4: Attainable carbon recovery in function of the propylene/ethylene ratio[24]

A downside of this integration is that the OCP process introduces more light end components into the system which can be very costly to separate due to the need for very low temperatures in the separation section. This is only a small cost compared to the added benefit which this process can provide. The demonstration plant of Total in Feluy has proved the feasibility of this combination, but it also proved that the light olefins are pure enough to produce polymers. Usually oxygenates are feared in polymerization plants due to their toxicity towards the catalyst. But despite the presence of DME and water in the MTO-reactor effluent the light olefins can be produced at the high purities which are desired for polymerization.[26]

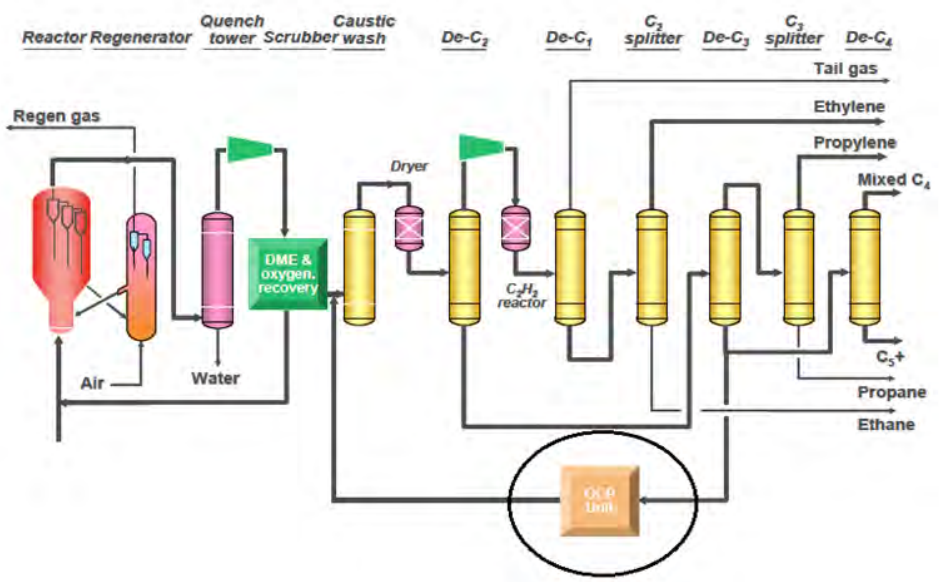

Figure 1.5: Setup of a MTO/OCP plant [24]

1.5 The MTO catalyst

There are many zeolite and zeotype catalysts that show activity for the MTO-process. There are however distinct differences between them because of their respective properties. As mentioned before the two most important catalysts for industrial purposes are H-ZSM-5 and H-SAPO-34. The other catalyst are usually less interesting from an industrial point of view, but can nonetheless provide insight for experimental and academic work.

Zeolites consist of tetrahedral building blocks with a silicon atom at the center and oxygen atoms at the corners. A certain fraction of these silicon atoms is being substituted by aluminum atoms. Since aluminum has one valence electron less than silicon there is an effective negative charge being introduced into the structure. This charge can be compensated by a proton which will be bonded to one of the four bridging oxygen atoms surrounding this aluminum atom, hereby forming Brønsted acid sites. Another type of catalysts are zeotype materials or the silico-aluminophosphates. Those consist of the same structure as the zeolites but have alternating a aluminum or phosphorus atom at the center of the tetrahedrals. When phosphorus is substituted by silicon , again a negative charge is induced in an analogous way as with the zeolites and a proton can compensate this charge. Next to their composition, zeolites can be divided in different groups according to their topology. This section will discuss the structures that are relevant for the MTO-process.

1.5.1 The MFI topology

The MFI-structured catalyst H-ZSM-5 (Figure 1.6) is industrially one of the most interesting catalysts especially in the MTO-process. It consists of a network of intersecting sinusoidal and straight channels. The channels both have 10-ring channels with an elliptic cross section. Benzene molecules with up to four methyl substituents are able to diffuse through the channels, but larges species are only able to reside at the intersections of the channels.

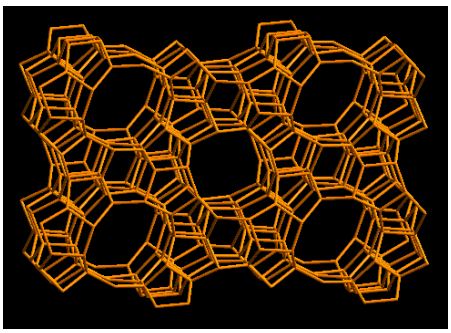

Figure 1.6: The MFI structure[27]

H-ZSM-5 is strongly acidic which results in a lot of secondary reactions. During methanol conversion the selectivity towards light olefins is rather low due to these secondary reactions. However the large pores have as an advantage that large molecules are still able to diffuse out of the catalyst and deactivation is much slower compared to other catalysts.

1.5.2 The CHA topology

The chabazite (CHA) topology is characterized by large 20-hedral cages connected by narrow 8-ring channels (see Figure 1.7). These small pores prohibit large or branched species from diffusion, for example iso-butene is unable to diffuse through these pores.[28] The large cages however provide the required space for reaction and the formation of methylated benzenes. H-SAPO-34 is a silico-aluminophosphate with this structure and H-SSZ-13 is the isostructural zeolite variant.
H-SAPO-34 is known for its very high selectivity towards light olefins. This is due to the small pores, as branched hydrocarbons are unable to leave the cages and are stuck inside. In Figure 1.8 the product distribution of both H-ZSM-5 and H-SAPO-34 are shown next to their structures.[19] This clearly illustrates that smaller pores result in a higher selectivity towards light product. Thanks to the moderate acidity of the H-SAPO-34 catalyst the occurrence of secondary reactions is being reduced, but the activity of the catalyst is high enough for industrial purposes. The rate of deactivation is however

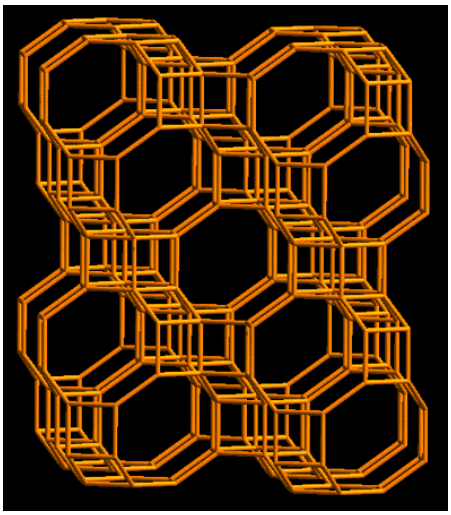

Figure 1.7: The CHA structure[27]

still higher than in H-ZSM-5 and frequent regeneration is necessary. H-SSZ-13 which only differs from H-SAPO-34 in its composition has a much higher acid strength than the latter. Therefore the deactivation occurs too fast for industrial purposes and this catalyst is only used from an academic point of view in the MTO-process.

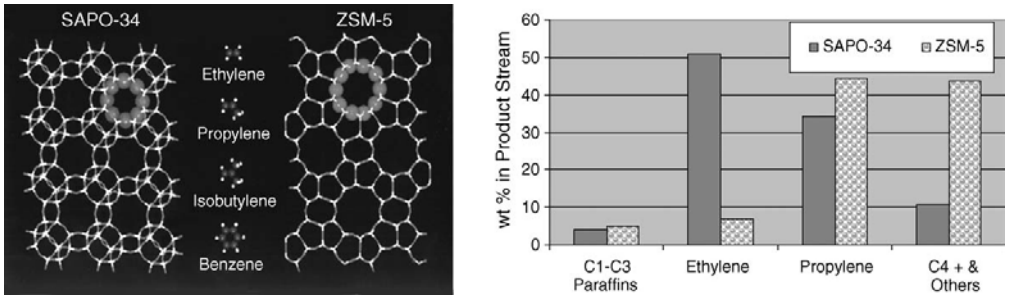

Figure 1.8: The smaller pores of H-SAPO-34 result in the higher selectivity towards light olefins[19]

1.5.3 The BEA topology

H-beta is another catalyst which shows activity for the MTO-process. This catalyst is a zeolite with the BEA topology which is shown in Figure 1.9. This structure consists of large 12-ring channels crossing each other. This catalyst is very sensitive to deactivation and is therefore irrelevant from an industrial point of view. This catalyst is however very interesting from an experimental point of view, thanks to the large pores of the catalyst it is possible to perform co-feeding experiments of methanol with voluminous

hydrocarbons. The reasoning behind these experiments is that although the topology of the catalyst is different the intrinsic chemical mechanism behind the process is identical and thus experiments will lead to detailed mechanistic insight that can be extrapolated to other catalyst topologies.

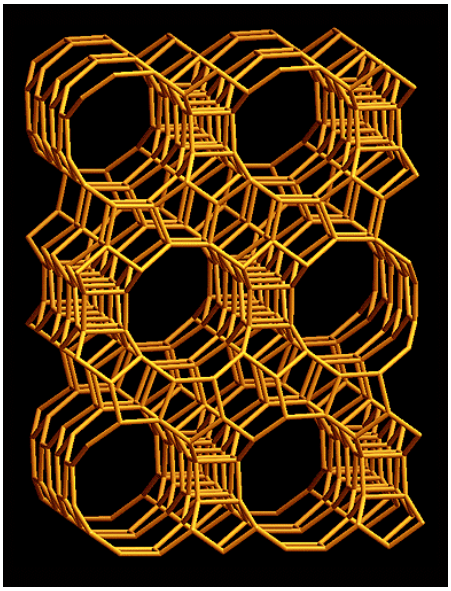

Figure 1.9: The BEA structure[27]

1.5.4 The AFI topology

The AFI structure, which is shown in Figure 1.10, consists of large 12-membered ring one dimensional pores which have a diameter of 7.42 Å. The two catalyst with this topology are H-SAPO-5 and H-SSZ-24, but they are usually not used in context of the MTO-process, certainly not for industrial purposes. ALPO-5, the non-acidic variant of H-SAPO-5, is however used together with transition metals for the selective oxidation of hydrocarbons such as propylene, cyclohexane and toluene.[29] [30]

Recently MTO experiments with H-SAPO-5 and H-SSZ-24 have been performed by Erichsen et al.[31] As a follow-up of a study of Yuen et al.[32] they investigated the influence of acid strength on the MTO-process. H-SAPO-5 has a similar acid strength as H-SAPO-34 and similar pore diameters, but the pores are accessible for co-feeding of bulky components. This is a very interesting characteristic from an experimental point of view. The zeolite H-SSZ-24 is more acidic, but has the same topology as H-SAPO-5.

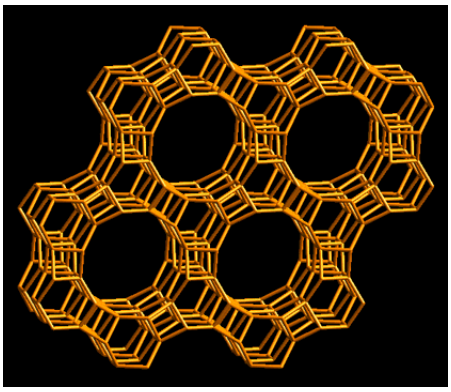

Figure 1.10: The AFI structure[27]

1.5.5 The TON topology

Another type of catalyst with one dimensional pores are those with the TON topology. H-ZSM-22 has the TON topology and has shown some limited MTO-activity. However deactivation in this catalyst can occur quite fast.[33] A comparative study between H-ZSM-22 and H-ZSM-12 (MTW-topology) showed that small changes in the pore size of the catalyst can have a large influence on the behavior for the MTO-process.[34] This is due to the mechanism that is very sensitive to the available space inside the catalyst, which will be explained later on. The limited amount of space inside the pores has its implications on the active mechanism, but experiments showed that this catalyst does have a certain activity.[35]

Chapter 2

The MTO-mechanism

The MTO process converts methanol to light olefins. The composition of these olefin products depends on the utilized catalyst. MTO processes are catalyzed by a zeolite or zeotype catalyst with Brønsted acid sites. In practice the most commonly used catalysts are H-SAPO-34 and H ZSM-5. The H-SAPO-34 catalyst specifically exhibits a high selectivity towards ethylene and propylene, but this is not a general trend, other catalyst also produce higher olefins.[23] Due to the wide range of products and amount of possible reactions it is difficult the unravel the exact mechanism. Knowledge of this reaction mechanism is however very useful for the optimization of the process.

Experimental research showed that the first step of the methanol conversion is the formation of an equilibrium mixture of dimethylether, water and methanol.[18] This mixture is subsequently converted to the desired olefins. Further reaction leads to the formation of long alkanes and aromatics. These heavier fractions are crucial in the deactivation of the catalyst.[22] The exact mechanism that leads to the formation of the olefins remains uncertain and has proven to be depending on the catalyst as well.

2.1 Proposed mechanism

2.1.1 Direct coupling

The first propositions for the reaction network that led to these products involved a direct coupling between two methanol molecules. The two carbon atoms of the two methanol molecules would form a carbon-carbon bond on which more methanol can add. This would thus lead to the synthesis of a carbon chain of varying length. This length is limited by the space available inside the pores of the catalyst. The mechanism is thus one of chain growth, very similar to a polycondensation reaction.

There have been many propositions for this direct coupling mechanism. There are mecha-

nisms with a surface associated carbenium ion, oxonium-ylide mechanisms, carbocation mechanisms or mechanisms with radicals.[28] However recent theoretical studies have proven that every possible reaction that utilizes this direct coupling has at least one intermediate which is too unstable or has a very high reaction barrier.[36]

Experimentally there are also many indications that this mechanism does not describe the process accurately. At the start of an experiment there is a period with almost no olefin production. It is only after a certain time that the catalyst is able to achieve a reasonable and stable conversion until the catalyst gets deactivated. Dessau et al. performed co-feeding experiments with ^{13}C labelled methanol and unlabeled ethylene. If ethylene is exclusively formed by reaction between two C_1 molecules then all the produced ethylene should be doubly labeled, the presence of unlabeled ethylene should not influence this. There was however a large amount of single labeled ethanol which ended up in the product stream, this means that there is label scrambling between the methanol and ethylene from the feed.[37]

2.1.2 Hydrocarbon pool mechanism

The auto-catalytic effect of the MTO process was quickly established and is in accordance with the kinetic induction period which is observed at the start of the experiments. In 1982 Mole performed experiments where toluene and other hydrocarbons are co-fed with methanol. With these experiments they proved there was a clear co-catalytic effect of the aromatic compounds such as toluene, benzene and xylene, but no such effect was observed for n-hexane.[38] [39]

A new reaction model including a pool of hydrocarbons acting as a co-catalyst was proposed by Dahl and Kolboe.[40] [41] These hydrocarbons have to be formed before the catalyst can be reactive and both aromatics and aliphatics can ast as hydrocarbon pool species, depending on the catalyst topology. Instead of a direct coupling between methanol molecules, olefin production is described by a series of reactions of these hydrocarbon pool species.

The formation of these co-catalyst molecules is still not fully understood. While it has been proven that direct C-C coupling is not the active process during steady state operation with a high conversion it remained a possibility for the formation of this very first C-C bond. Haw et al. performed experiments with highly purified methanol which contained thirty times less ethanol than reagent methanol. They observed a longer delay for the induction period where no olefins were produced.[42] One possibility is thus that impurities are the source of these first C-C bonds. Ethanol is a common impurity in the methanol feed, but also the carrier gas and the calcinated solid acid itself can be sources of hydrocarbon species. Naphtalene, phenantrene and other impurities have been detected

in H-SAPO-34 after conventional calcination procedures.[42] It is however not generally accepted that these impurities are the source for the first C-C bond or at least not for all catalysts. Experiments in zeolite H-Y performed by jiang et al. showed that purification of the feed had little impact on the formation of hydrocarbons.[43] Theoretical studies in a finite cluster model have shown that cyclic HP species can be formed inside the framework of H-ZSM-5 starting from methanol and light hydrocarbons by a ship-in-a-bottle mechanism. They also showed that the catalyst environment is crucial in order to evaluate the stability of the intermediates.[44]

After the formation of the equilibrium mixture of water, dimethylether and methanol, there is not yet any production of olefins since there is no co-catalyst present yet. The formation of this co-catalyst is difficult, slowly there are hydrocarbons being formed inside the pores of the catalyst. These hydrocarbon pool molecules can differ in activity depending on the catalyst, for example in H-SAPO-34 and H-Beta heavily methylated benzenic compounds are most active[21] [45] [46] while in H-ZSM-5 alkene compounds are active as well.[47] [48] Cages inside the catalyst, such as in H-SAPO-34, provide the necessary volume for these hydrocarbons to form and react. Due to the smaller size of the SAPO-34 pores the larger molecules are further hindered from diffusion and will remain inside these pores untill the catalyst is regenerated.[21]

Once a critical amount of hydrocarbon pool species is available the reaction is able to start. There are many variables that influence the mechanism and structure of the hydrocarbon pool mechanism. In particular the catalyst topology, pore sizes and acidity have an impact on the activity of the different species, but also the operating conditions will have their influence on the mechanism.

The product distribution that results from the MTO-mechanism depends on many factors. There are of course the proces conditions, but the catalyst and co-catalyst have a big influence on the distribution as well, as Figure 2.1 illustrates for H-SAPO-34 and H-ZSM-5. Clearly the amount of aromatics formed in both catalysts under identical conditions is very different. The cages of H-SAPO-34 can hold large molecules but they are unable to diffuse out of the cages. As a result ethene and propylene are the main components in the product stream.

The type of hydrocarbon which is active as co-catalyst is very important for the product distribution as can be seen in Figure 2.2[31] where the influence for addition of benzene in the feed is shown for H-SAPO-5. These product distributions show clearly that when the aromatic species are being favored as co-catalyst (because more of them are present) the selectivity towards C_2 and C_3 increases at the expense of C_4+ products. This has previously been discussed in literature in a comparative study between H-ZSM-5 and H-beta where Svelle et al. showed that lower methylated benzenes produce more ethylene

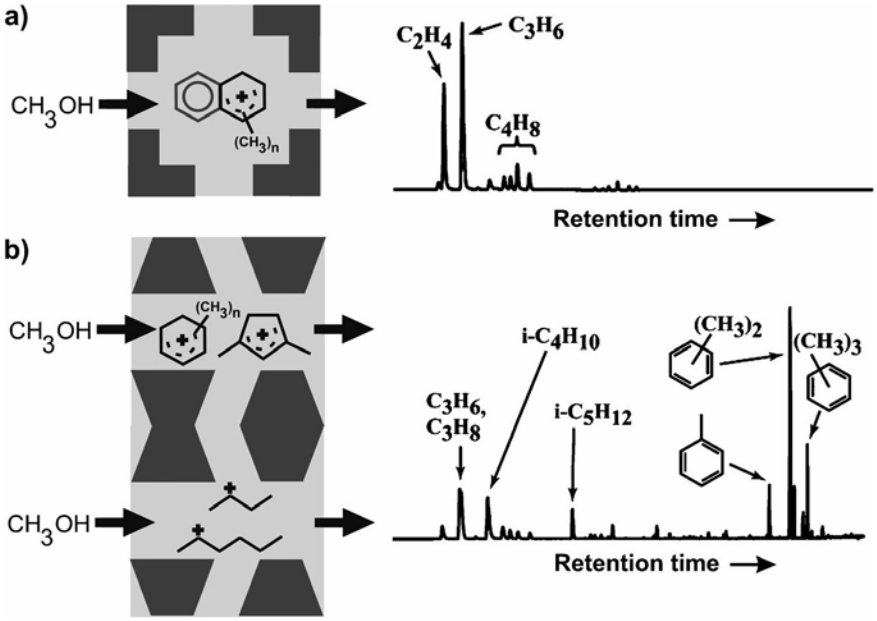

Figure 2.1: The product distribution found for H-SAPO-34 (a) and H-ZSM-5 (b) [4]

than propylene and that the arene cycle is the only real source of ethylene. [49]

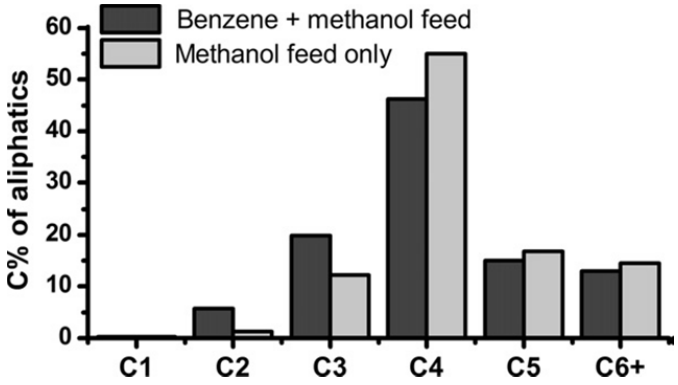

Figure 2.2: The product distribution found experimentally in H-SAPO-5 with and without benzene in the feed. [31]

2.2 Aromatics based HP cycles

This section will discuss the mechanisms that involve aromatic hydrocarbon pool species and the catalysts in which aromatic compounds are important as co-catalyst. The two main routes that have been proposed are the ring contraction paring mechanism and the side-chain mechanism as can be seen in Figure 2.3 [23]. A third, less popular mechanism

which has been proposed is the ring expansion mechanism and has its similarities with the ring contraction paring mechanism. It is shown in Figure 2.4. In all these mechanisms an aromatic compound is considered to be the active co-catalyst which gets methylated multiple times. The main differences lie in the exact mechanism for the elimination of the products.

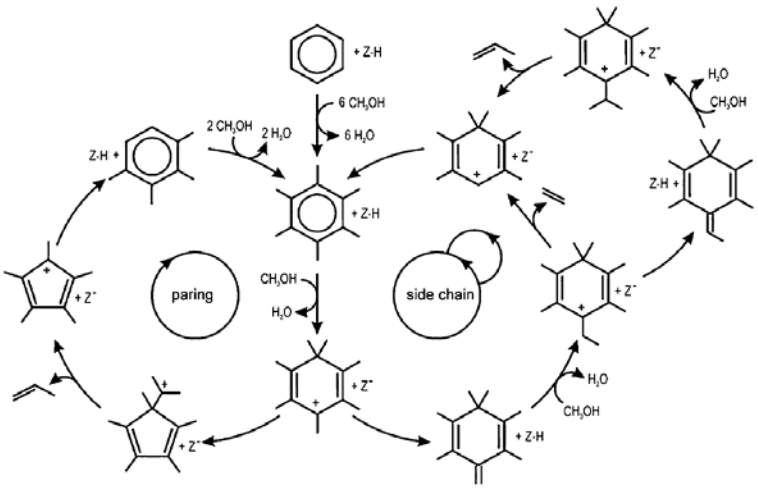

Figure 2.3: Overview of the paring and side-chain schemes for MTO conversion based on aromatic hydrocarbon pool species [23]

The proposition of the side-chain mechanism came in 1983 by Mole and co-workers. [39] In this theory the aromatic compound is deprotonated to form an exocyclic bond on which subsequently methanol addition can occur. An elimination reaction will then release the olefin from the aromatic compound. Many additions have been made to this theory such as stating that additional substitutions on the benzene compound are beneficial for the process. [51] The shown mechanism starts with a benzene ring that is highly substituted because those have proven to be most reactive in large pore catalysts such as H-Beta and H-SAPO-5. [46]

The paring mechanism that involved ring contraction has been proposed earlier. [52] It states that the aromatic compound, after being methylated, undergoes a ring contraction, elimination and ring expansion step. A big benefit of this proposal is that it is able to explain the observed isotope scrambling. [53] [31] During co-feeding experiment with ^{13}C labeled methanol and unlabeled benzene it was observed that ^{13}C was incorporated into the ring of benzene and ^{12}C labels into the products. This can not be explained by the side-chain mechanism but can be a consequence of these subsequent ring contraction and expansion steps.

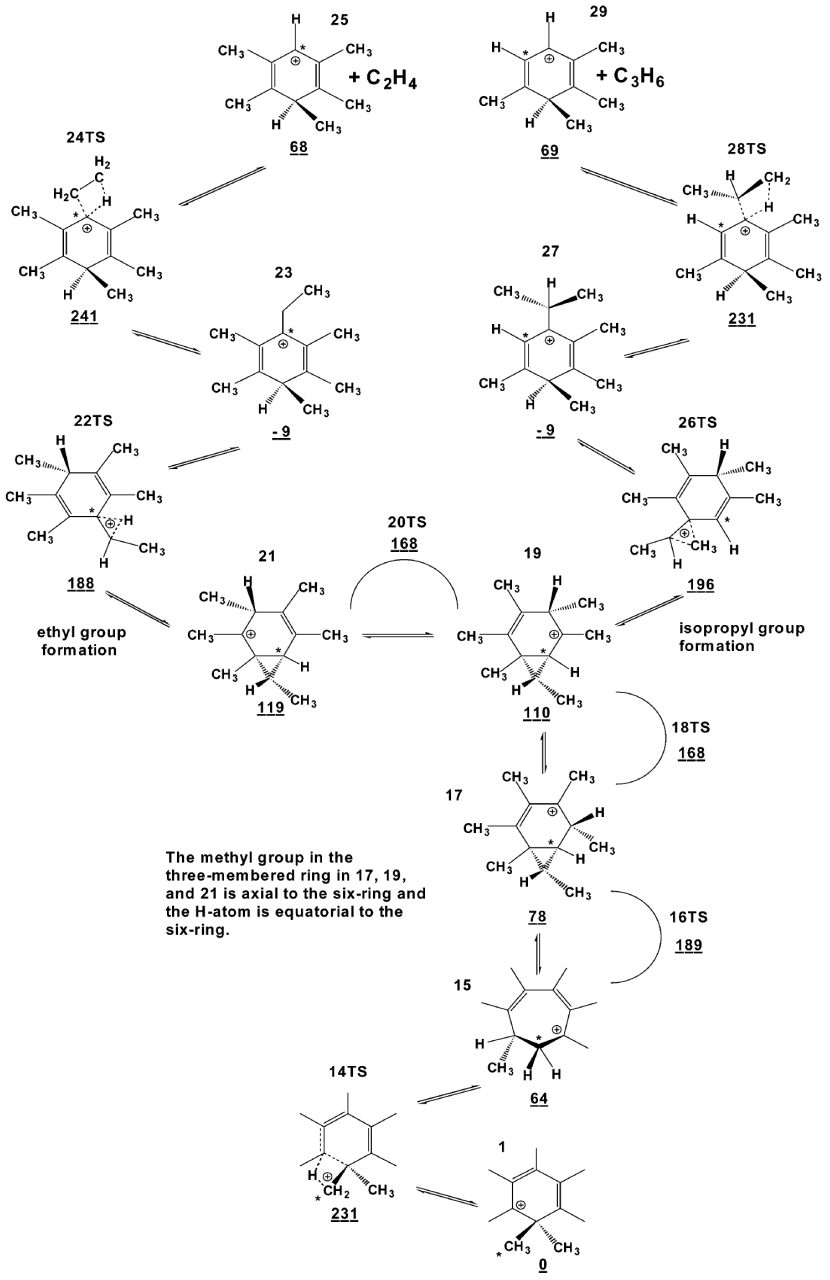

Figure 2.4: Proposed ringexpansion mechanism[50]

The third mechanism (see Figure 2.4) has its similarities with the ring contraction mechanism. In this mechanism the aromatic compound first undergoes a ring expansion to form a tropylium ion like structure, followed by a ring contraction to a rearranged form which is more suitable for elimination.

A lot of research has been performed on all these mechanisms, but due to the complexity of the process and the variety of parameters such as topology, acidity and reaction con-

ditions no single mechanism has proven to be correct one to explain product formation. Theoretical studies have shown the feasibility of each path, but full catalytic cycles often have some bottlenecks such as high barriers.[50]

For H-SAPO-34 studies have shown that the reactivity of the aromatic compound and its selectivity towards propene increase with the number of substituents.[54] The species with fewer substitutions lead primarily to ethylene while the highly substituted and more reactive species lead predominantly to propylene. Hexamethylbenzene has therefore been pointed out as the most critical compound in this catalyst and has been observed in multiple experiments.[55] Theoretical calculations in H-SAPO-34 and H-SSZ-13 came to the same conclusion and derived a difference in reaction rate of up to 6 orders of magnitude.[56] A similar effect has been found for napthalenic compounds, they are also active as co-catalyst, though with a much lower activity. The position of the substitutions is very important here, too many substitutions will lead to deactivation.[56] Naphtalenic compounds result primarily in ethylene formation which is likely to be caused by their low degree of substitution similar to how lowly substituted benzenes preferably produce ethylene.[57] While naphtalenic species are indeed active, there is thus a subtle balance with the deactivation process as they can also be regarded as coke precursors as shown by Hemelsoet et al.[58]

Investigation of both side-chain and the paring mechanism lead to the conclusion that the side-chain mechanism would preferably form propene due to the high barrier for ethylene elimination.[59] Recent research proved however that a complete low barrier side-chain route for ethylene production is possible with barriers lower than 100 kJ/mol. The difference being that stabilizing effects occured when simulating the carbon center of the intermediate as an sp^3 carbon and taking the alkyl-benzene interaction into account.[60] The major bottleneck for the ringcontraction paring mechanism is the regeneration of six-membered cyclic structure.[61]

When steric hindrance is not an issue, the heptamethylbenzenium ion has shown to be the most reactive compound such as in H-Beta.[62] [49] Since hexamethylbenzenium has a high proton affinity (860.6 kJ/mol[62]) it is easily methylated to form this compound when it is possible in the catalyst pores. Ethyl and iso-propyl substituted methylbenzenes were experimentally found in the product stream of H-Beta. They could be regarded as intermediates, but can also be the effect of secondary reactions of the produced alkenes with the aromatics that are present in the catalyst.[46]

In H-ZSM-5 there is more steric hindrance, resulting in a preference for lower methylated compounds.[63] NMR spectroscopy showed that next to these organic compounds and their lower-methylated forms also methylated cyclopentenyl cations are present during MTO-conversion on H-ZSM-5.[64] These five membered rings are another possibility as

reaction center in H-ZSM-5. For all these hydrocarbon species the protonated forms are assumed to be the most reactive. The proton affinities of the components in gas phase has been used as a measure for their stability. Macht et al. showed that the reaction barriers are not only determined by the acid strength of the catalyst, but that the proton affinities have a crucial role in the formation of the transition state. [65]

This catalyst is the one that got the most theoretical attention. In a joint experimental and theoretical effort a complete catalytic route for MTO conversion has been reported. [61] Starting from toluene and going up to the elimination of the olefins and restoring of the co-catalyst everything has been simulated and no major bottleneck has been found for the paring mechanism, the main product being formed was propylene. Investigation of the side-chain mechanism by Lesthaeghe et al. showed that chain growth is possible, but that olefin elimination is difficult. This route may thus very well lead to deactivation of the catalyst rather than olefin production. [66] There is the possibility that the low barrier reaction path, proposed by De Wispelaere et al. in H-SAPO-34 could also work for H-ZSM-5, but this is to be investigated.

2.3 The dual cycle

Since the aromatic based cycles were not able to describe all the observations, in particular for H-ZSM-5, other routes involving alkenes have been proposed. In contrast to experiments in H-SAPO-34, experiments showed that ethylene and propylene were reactive as co-catalyst in H-ZSM-5. [67] [41]

It has been proposed that there are two different cycles that interact with each other, the so-called dual cycle concept. This concept was first introduced for H-ZSM-5 [68], but is also applicable to other catalysts. Isotopic labelling studies on H-ZSM-5 investigated the rate of ^{13}C uptake by the different products. After a switch to feed with ^{13}C was done the effluent was analysed on its ^{13}C content. As can be seen from Figure 2.5, there are two distinctly different groups. This lead to the conclusion that the mechanism behind the formation of these products will be different as well. [68] The authors proposed a dual cycle mechanism where there are two different types of co-catalyst active in two different mechanisms that interact with each other. [69]

There is an autocatalytic cycle which uses alkenes as co-catalyst, while there is also a cycle using aromatic compounds as co-catalyst. [47] This is shown in Figure 2.6 [23]. In the arene cycle methylations of lower alkenes produce higher alkens which can subsequently crack into two lighter alkenes. In the arene cycle methylations occur on a benzenic compound. Light olefins can be eliminated from this compound and restore the benzenic compound in its first form. Due to the difference in uptake of ^{13}C content between the

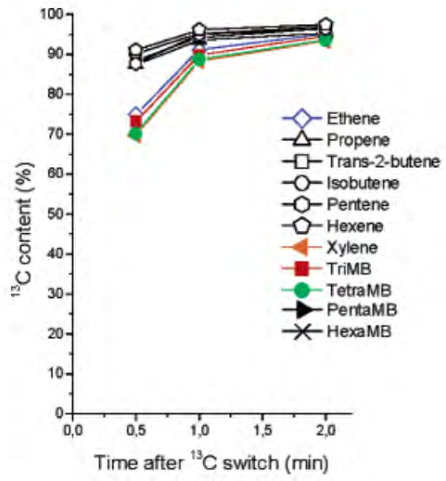

Figure 2.5: evolution of ^{13}C content in the different components of the effluent in function of time [47]

two groups it was also concluded that ethylene will be primarily formed in the arene cycle, while propene and heavier olefins are all part of the alkene cycle.

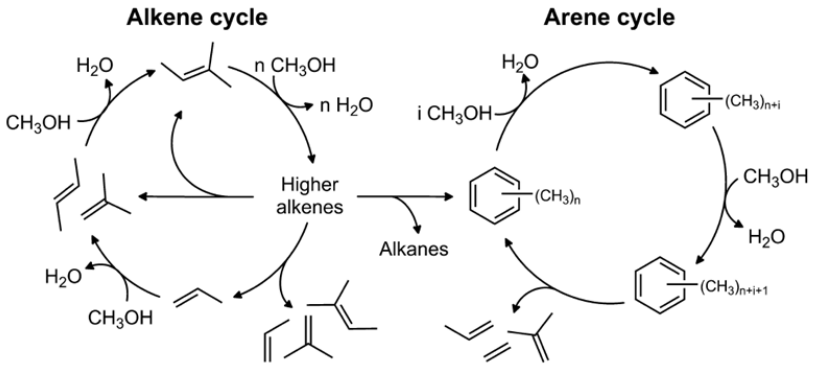

Figure 2.6: The proposed dual cycle mechanism [23]

This separation of the mechanisms behind ethylene and propylene formation seem to give opportunities into varying the ethylene to propylene yield of the process. The cycles are however not fully separated. The arene cycle is producing alkenes which can be used as a co-catalyst in the alkene cycle, ethylene is not considered to be reactive, nor are they a product of the alkene cycle, but propylene and other larger olefins are. The alkenes which are also continuously being formed in the alkene cycle can undergo secondary reactions such as cyclizations and hydride transfers. This will result in the formation of cyclic and aromatic hydrocarbons which act as co-catalyst in the arene cycle. These

two cycles, which are able to operate independent of each other are thus in fact strongly correlated.

The dual cycle mechanism has also been investigated on a theoretical level. Lesthaeghe et al. simulated the alkene cycle in H-ZSM-5 and were able to reproduce the experimental findings very well, they found a lower barrier for propene formation compared to ethene formation and barriers for methylation of 60-80 kJ/mol.[70] Together with their earlier simulations of the side-chain[66] and paring mechanism[61], both cycles have now been simulated on H-ZSM-5.

There are many other zeolites and zeotype materials that show activity for the MTO process, they are usually divided into categories by their acid strength and pore size. Both parameters are assumed to have a large influence on the MTO reactions.

H-ZSM-22 which has 10-ring one dimensional pores (TON topology) has been shown to produce nearly no ethylene. This was ascribed to the small pores of the catalyst which provided too little room for the aromatics to exist.[71] H-ZSM-22 produced primarily C_{5+} branched hydrocarbons. This was found to be very interesting to produce clean fuels because there are almost no aromatics present in the product stream. Therefore further research was performed on similar one dimensional 10-ring zeolites. However they found surprisingly that these very similar catalyst were able to produce aromatics.[72] As reported before in a similar study involving H-ZSM-22 they found that a very small difference in pore diameter (of up to 0.3 Å) could completely change the activity of the catalyst. The most active co-catalyst apparently must be around the size of these pores because it is present in one catalyst but not in the other.[34]

Recently more work has been performed on H-SAPO-5, which has the AFI topology, by Erichsen et al. because of the similarities between H-SAPO-5 and H-SAPO-34.[31] H-SAPO-5 and H-SAPO-34 have similar acid strengths and pores sizes, with the difference that the one dimensional pores of H-SAPO-5 are open to co-feeding experiments. This is of course very interesting, because the reactions that take place in H-SAPO-5 are likely to be very similar to those in H-SAPO-34, but H-SAPO-5 allows for these additional experiments. H-SAPO-5 can be regarded as a one dimensional variant of H-SAPO-34, it is also a common impurity in the synthesis of H-SAPO-34. They performed a comparative study with the isostructural catalyst H-SSZ-24 to unravel the effect of acid strength on the MTO reaction mechanism. They showed that the more acidic H-SSZ-24 had a larger production of aromatics, ethene and propene. The combination of ethene and propene with the aromatic cycle is in agreement with the results in other catalyst as described before. They suggested that the acidity of a catalyst could be tuned in order to influence the dominating reaction cycles (aromatics/alkene) and hence the product selectivity. It must be noted that during co-feeding experiments with methanol and

benzene they proved that H-SAPO-5 certainly is able to use aromatics as a co-catalyst since they observed a significant increase in the production of the light olefins. Either the acid strength influences the interplay between the two cycles, cyclization reactions and hydride transfer reactions are a link between the two cycles, or the difference in acid strength promotes one cycle over the other.

In the same study by Erichsen et al. labelled methanol experiments were performed. The labelling patterns for isobutene were typical for an alkene cycle in H-SAPO-5, while being typical for an arene cycle in H-SSZ-24. Co-feeding experiments with unlabelled benzene and labelled methanol showed that label scrambling occurs. This is shown in Figure 2.7, the paring mechanism incorporates scrambling of the atoms from the methyl substituents to the aromatic ring, while the side-chain mechanism does not. This scrambling could however also be the result of a ring expansion mechanism or other secondary reactions.

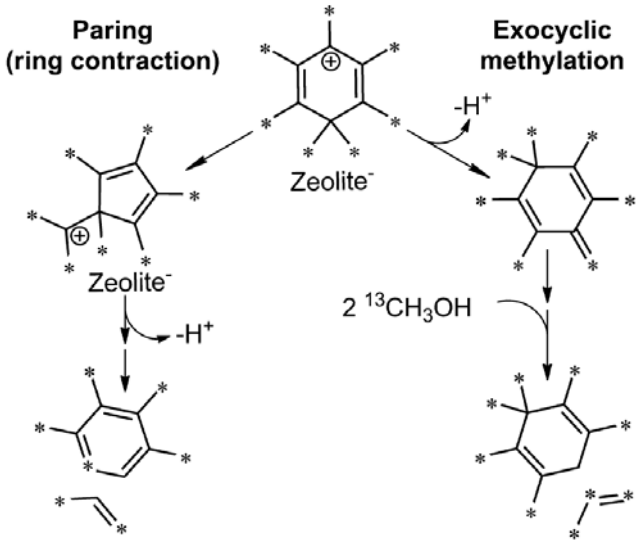

Figure 2.7: The difference in labeling between side chain mechanism and paring mechanism. [31]

As discussed above methylation reactions occur in every scheme and are crucial steps in all these mechanisms since they lead to chain growth. Multiple propositions exist for the mechanism, there is a stepwise and a concerted mechanism. [73] Both mechanisms can be seen in Figure 2.8. In the stepwise mechanism (top two rows of Figure 2.8) there is first the formation of a framework bound methoxy group which adds to the hydrocarbon pool compound in a second step. The concerted mechanism describes the reactions as a one step mechanism which is acid catalysed, water is eliminated while the carbon-carbon bond between methanol and the hydrocarbon compound is being formed. In most theoretical studies the physisorbed methanol and the co-adsorbed hydrocarbon compound are assumed to follow the concerted mechanism. These theoretical results

have been in good agreement with experimentally obtained data for H-ZSM-5. [74] [75] [76]

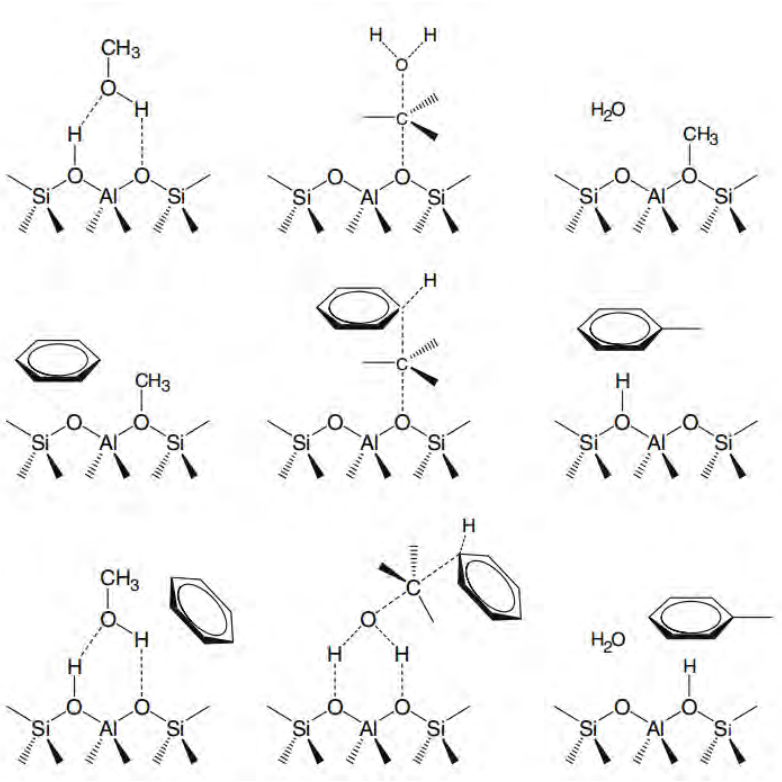

Figure 2.8: Two proposals for the methylation mechanism, stepwise mechanism (top and middle row) and concerted mechanism (bottom row) [73]

While the alkene and arene cycle are being studied the most, other propositions for the intermediates can also be found in literature. Carbene like intermediates have been observed by means of IR spectroscopy during reaction of ethene and methoxy groups over H-ZSM-5 [77], but these will not be discussed in more detail here.

2.4 Deactivation

The previous sections described the mechanisms that give rise to olefin production. Chain growth and methylation of aromatic compounds are very important and occur frequently. However these methylations, together with secondary reactions, can lead to undesired effects. The intermediates can continue to grow into larger coke species. These coke species can block the pores or poison the catalyst. Coking is a serious issue in most processes involving hydrocarbon chemistry due to the loss in acitivity of the catalyst. Another effect of this deactivation proces is that it shifts the product spectrum.

Cokes are in general heavy hydrocarbons that lead to the deactivation of the catalyst.[78] Cokes often have a polyaromatic structure but all the hydrocarbon species that do not diffuse out of the catalyst and lead to catalyst poisoning are considered to be cokes. The methylated benzene species which are the important active compounds in the MTO process are precursors for these coke species. The methylated naphtalenic compounds are also coke precursor while still having some reactivity towards the desired olefins.[79] Phenantrenic compounds on the other hand are considered coke-precursor without a significant activity.[58] Which species are exactly still active or not-active is dependent on the catalyst. Smaller pores can be blocked more easily and are thus more sensitive to deactivation.

The deactivation reaction depends strongly on the temperature of the reaction, the acidity and topology of the catalyst.[80] Higher temperatures are usually detrimental for coke formation.[81] At every temperature coke formation is very rapid at the start of the reaction, but higher temperatures will increase the rate of overall coke formation. In H-SAPO-34 the deactivation is related to polyaromatic compounds trapped in the cages, while in H-ZSM-5 there are large aromatic compounds forming at channel intersections.[68] [82] At high temperatures there are not only cokes forming inside the pores, but there is also a graphite like layer forming at the external surface of H-ZSM-5.[22] In H-SAPO-34 coke formation starts at the edges of the catalyst crystal and propagates towards the center.[83]
The more acidic catalysts are more susceptible for coke formation. In particular the concentration of acid sites and their acid strength is important for the coke formation.[28] Due to this fact some catalysts are being prepared with a transition metal incorporated in the structure to reduce the acidity of the catalyst. Incorporation of Cr or Ni will enhance the durability of the catalyst and its selectivity towards ethylene.[84] [85] The effect of acid site density has been examined by comparing H-SAPO-34 with H-SSZ-13.[86] The conclusion was that acid site density was more important than the acidity of the catalyst. A higher Al/Si ratio gives rise to more Brønsted acid sites but with a lower acid strength, experiments have shown that in this case the acid site density is the most important factor.[87] Experiments with H-SAPO-34 and H-SSZ-13 with the same acid site densities, performed by Bleken et al., showed that the more acidic H-SSZ-13 has a higher deactivation rate, but also a higher production rate of olefins. H-SSZ-13 had the highest conversion capacity out of these two catalysts.[88]

Another way to reduce the coke formation is to change the feed composition, for example water has a stabilising effect on the lifetime of a catalyst. The addition of water also increases the selectivity towards ethylene. The reasoning behind these findings is that water adsorps on the acid sites, thus reducing the possibility for secondary reactions.[89] When the deactivation of the catalyst has become too severe the catalyst has to be

regenerated by removing the cokes. The cokes are being burned at high temperature. This oxidative process can have a negative influence on the structure of the catalyst, therefore the decoking can be done in two steps, one at low temperature and one at higher temperature. Jiang et al. showed that for H-SAPO-34 two hours purging with synthetic air would eliminate most of the cokes from the catalyst. [90]

2.5 Goal of this thesis

In a first part of this thesis advanced molecular simulations will be used to optimize adsorption complexes and calculate adsorption energies of important reactant molecules of the MTO process. In particular the adsorption of methanol, DME and benzene are investigated in H-SAPO-5 and H-SSZ-24. The adsorption on both the acid site and a neighbouring site, on top of bridging oxygen atoms not connected to the acid site, are considered. These calculations provide insight on the interactions governing the adsorption for the various complexes. Co-adsorption of benzene with up to two methanol molecules represent a pre-reactive state for a methylation step which are crucial steps in the MTO process. The formation of a methanol dimer and its effect on the proton affinity of the adsorbates is addressed. Adsorption steps are a crucial first stage of the process before reaction can occur, insight in the preferred complexes and interaction strengths are important for the entire catalytic cycle.
In the second section of this thesis a distinction is made between the different proposed aromatic based mechanisms. Therefore, dynamic molecular simulations are applied. Heptamethylbenzenium has proven to be the most reactive compound and was therefore chosen as the model compound to start the simulations from. There exist three main catalytic routes for the olefin production with aromatic compounds as intermediates, the side-chain mechanism, the paring mechanism starting with a ring contraction and the paring mechanism starting with a ring expansion. Heptamethylbenzenium is the state from where all the mechanisms start to differ, the first crucial step is being investigated to see if it is possible to make a distinction between the mechanisms at this stage.

Chapter 3

Quantum chemical simulations

This chapter will elaborate on the use of quantum chemical simulations in heterogeneous catalysis. The basic principles and techniques will be explained and also the usage in this thesis.

3.1 The quantum chemical methods

Quantum mechanical methods describe a system by solving the Schrödinger equation for the many-body problem. To do this the Born-Oppenheimer approximation is used to separate effects from the cloud of electrons and the nucleus.[91] There are many different methods available. They can be divided in three main categories: ab-initio methods, density functional methods and semi-empirical methods.

3.1.1 Ab-initio methods

Ab-initio methods describe the system starting from the basic physical laws. There are no further assumptions made to solve the Schrödinger equations. They are often used for comparison and validation due to their theoretical soundness.[91]

The simplest example of an ab-initio method is the Hartree-Fock method. The main issue in solving the many-bodem problem is the interaction between the multiple electrons. The Hartree-Fock method approximates the system as an independent particle model wherein the interaction is substituted by a mean-field interaction. The exact N-body wave function is approximated by a single Slater determinant.

The Hartree-Fock equations contain a new operator, the Fock operator. This operator contains two contributions to the energy. The first contributions are those that can be calculated exactly namely the kinetic energy of the electrons, the attraction energy between electrons and nuclei and the repulsion energy between nuclei. The second term

is the repulsion energy between the electrons described by the mean field approximation. The electron correlation energy is completely neglected. The result is that Hartree-Fock methods will always result in a too high energy since part of the stabilization is not taken into account. The obtained energy is an upper limit and the difference between the calculated and real energy is the electron correlation energy. Numerical methods are needed to solve the Hartree-Fock methods since there is a self consistent field, the solution of the Hartree-Fock equations is needed to calculate the mean-field and thus iterations are performed until a minimum in the energy is found. [91]

More sophisticated methods include parts of the correlation energy to obtain a better result. these methods are called post-Hartree-Fock methods. A group of examples are the Moller-Plesset pertubation methods. These methods use additional terms to the Fock operator. These pertubations include the two body interactions. Another example is the coupled cluster method. These methods are more accurate but requite a high computational effort.

3.1.2 Density functional theory

The starting point of density functial theory (DFT) is that the density function of the ground state is equivalent with the wave function of the ground state. Every property of the ground state can be calculate from this density function. A big advantage of this way of describing a system is that the number of coordinates is 3 instead of 3N. The description of a system by its density function is done by solving the Kohn-Sham equations. These equations will describe the system exact if the correlation-exchange potential is known. [91]

An approximation is needed for the exchange-correlation potential. Some functionals use empirical input, while others do not. Note that this is the first step in the theory where experimental input is used. Strictly speaking the DFT-methods are thus semi-empirical methods, but the empirical input is very limited. One must however always be wary when using parameters fitted to experiments. Leaving the system for which the parameters were fitted can lead to errors. This is the point where DFT-methods differ from the Hartree Fock methods. Where an ab-initio energy will always be an upper limit the energy obtained by DFT-methods can be lower due to overestimation of the correlation energy. In practice the functionals for the correlation energy and exchange energy are often split in two. One can then make combinations of any two functionals, one for the electron correlation and another one for the exchange energy. There are many functionals available, they can be divided into subclasses depending on their computational complexity and accuracy. More complex functionals are also more accurate.

The most simplistic functionals are only dependent on the electron density in a single point. This is called the local density approximation, they are computationally interesting, but not very accurate since there can be a large underestimation of the exchange energy.

A first step of improvement is to include the gradient of the density function into the functional. Examples of semi-empirical functionals which utilize the gradient are the Becke exchange functional and the LYP correlation functional. PBE and revisedPBE are two functionals which do not try to satisfy as many exact conditions as possible, which is often done for other functionals such as PW91, but minimizes its parametrization by only describing the conditions that are important for the energy of the system. [92]

Hybrid methods are a different class of functionals which try to use the fact that the Hartree Fock method has a correct implementation of the exchange energy without any correlation. An example of these hybrid functionals is the B3 functional. It consists of a Becke (gradient exchange), LDA and Hartree-Fock part. By combining the Hartree-Fock with the other functionals the overestimation of the exchange energy can be compensated. [91] B3LYP is a very widespread and often used functional for theoretic calculations. A next step in complexity for the functionals is inclusion of the second derivative of the electron density in essence this is the non-interacting kinetic energy density (τ). These functionals are called meta-GGA-functionals. tHCTH is an example of such a method.

The hyper-GGA-functionals combine the exact exchange energy with the meta-GGA-functionals. There are even more advanced functionals under development using a complete description of the Kohn-Sham orbitals. This would lead to a full ab-initio description of the correlation and exchange energy. However due to the complexity of such systems they aren't available yet. The main limitation to the DFT system is their lack of correct description of long distance correlation energy. This problem is due to localized character of the functionals. Gradients do not describe the long distance interactions which are crucial for dispersion interaction. Computationally it is very demanding to implement the correct interaction. Therefore Grimme suggested a different scheme called DFT-D. It included a semi-empirical correction to the energy of the system by the use of a R^{-6} term (with R the internuclear interaction). Because the dispersion energy is calculated separately from the DFT energy the computational cost is very low but the results are very good. This implementation allows description of systems where dispersion energy is the main stabilization factor. [93]

3.1.3 Semi-empirical methods

The most rigorous approach to solve the many-body problem is to replace the difficult two body interaction integrals with empirically parameterized functions. These functions are computationally much less demanding than the full analytical integrals. Depending on the specific semi-empiric method there are certain atoms for which the method is better parameterized and thus more accurate. The resulting energies obtained in these calculations are not very reliable. They are however very adequate to optimize the geometry of the system. A common practice is thus to use a semi empirical method such as PM6[94] to get a geometry which is close to its optimum. This geometry is then used in a second calculation with more sophisticated and more theoretical methods to obtain a reliable energy calculation. This will result in a lower computational cost with the same energy qualities as in a full optimization with the more advanced method.

3.2 The basis set

The goal of solving the Schrödinger equation is to find the energy of the ground state. This results in an eigenvalues problem with as eigenfunctions the wave function of the molecule.

To solve this problem the wave function is first expressed as an infinite sum of basis set functions. It is not possible in practice to work with an infinite set of basis functions thus the set will have to be limited. There should be enough functions available in order to guarantee a high accuracy. A logical basis set to use are the atomic orbitals. In principle this means that every basis function is a Slater determinant. This method is computationally very demanding. Since there is no restriction on the form of the basis set it is also possible to choose other functions. A good alternative is to approximate the Slater type orbitals (STO) with one or multiple Gaussian type orbitals (GTO). These functions are computationally very interesting. They are also able to resemble the STO to a certain extend.

Another modification which is often performed is separating the description of core electrons from the valence electrons. This is because the most interesting part of the calculations is situated in these valence electrons. A correct description of these electrons is thus essential and the computational cost can be reduced by simplifying the description of the core electrons. Furthermore there is also the possibility to introduce diffuse functions to describe the long distance interactions better. Polarization functions can be added to allow deformation of the orbitals which can be very interesting to describe reactions.

The Pople basis sets are often used and are an easy example to explain the previous. For

example the 3 21+G* basis set implies that each core atomic orbital function consists of three primitive gaussian functions. The valence orbitals are described by a double-zheta basis function. This implies that every orbital consists of two basis functions from which one consist of two primitive Gaussian functions and the second one is a single primitive gaussian. The other symbols indicate the presence of the diffuse functions and the polarization functions. It's also possible to further extend on this example and use triple or quadruple zheta basis sets.[91]

Another class of basis sets which are not fully localized are the plane waves. These can be very interesting when working with periodic boundary conditions. They describe the electron density with augmented plane waves while the Kohn-Sham orbitals are expanded in Gaussian functions. This localization that is incorporated into the basis functions reduces the necessary amount of basis set functions by a factor of five compared to normal plane waves.[95] There is still a cutoff for the planar waves, but the usage for these basis sets in periodic calculation is very natural and straightforward while still desribing the parts localized close to the nuclei by gaussians to ensure fast convergence. Further information about the implementation of Gaussian plane waves in the quickstep algorithm, as implemented in CP2K and which will be used in this thesis, has been described by Van de Vondele et al.[96]

3.3 Application of Quantum chemical simulations to heterogeneous catalysis

In heterogeneous catalysis experimental work can be challenging due to the limited access to the reaction center. In particular this is true for zeolite catalysis where an acid site is situated inside the catalyst and thus hard to observe with experimental techniques. A second difficulty is the investigation of a specific reaction mechanism with experiments. To do this all side reactions should be suppressed as much as possible. This is not always possible and the results can thus be influenced by unwanted effects.

Simulating a reaction with quantum chemical methods has the advantage that there is full control over the system which is studied. One should however reassure himself that all necessary effects are taken into account when performing simulations. Simulations of unrealistic systems are possible but the results are not valuable. The specific challenge in heterogeneous catalysis is thus a correct description of the catalyst. In reality this catalyst is a crystalline structure with a well-defined unit cell which is repeated in all directions for a high, but finite amount of times.

3.3.1 Finite cluster approach

The first attempts to simulate reactions over a zeolite were confronted with severe limitations on the available computational power. Therefore a simplified model of the catalyst was necessary and only the most essential parts of the catalyst were taken into account. A zeolite cluster is usually denoted as an nT cluster with n the number of tetrahedral atom (Si, Al and P). The earliest clusters consisted of five T-atoms. These included the substituted atom that lead to the acid site and the four surrounding atoms connected by their oxygen bridges. To saturate the four surrounding T atoms usually hydrogen atoms are used. This 5T-clusters are able to show catalytic activity but don't take any topology aspects into account.

Thanks to the increased computational power and more advanced methods (with a lower computational cost for a similar accuracy) it became possible to simulate larger cluster that included the topology effects. The amount of tetrahedral atoms that is optimal to reach a balance between accuracy and computational cost is dependent on the structure but clusters of 45 T atoms are often used. Hydrogen atoms are used as substitutes for the oxygen bonds that were cut by using a finite cluster. To implement the effect of the surrounding cages that are not included in the simulations these terminal hydrogen atoms are fixed in space. Zeolites are known to have some flexibility in their structure, the bonds are able to twist and deform a bit from their optimal position. This 'breathing' effect of the zeolite is hindered by the fixation of the hydrogen atoms.

There are ingenious techniques available to effectively reduce the added cost of increasing the size of the cluster such as QM/MM and QM/QM methods.[91] Since the most interesting part of the simulation is the center of the cluster where the actual reaction occurs. These methods use this fact by using a multi layered system where the most important part of the system is described on a high level of theory, while the surroundings which are important for the topology effects are described on a lower level of theory. An example is to describe the center 5T-cluster on a high level of theory and use a force field technique for the surroundings which reduces the computational cost significantly while still obtaining near chemical accuracy. This is a QM/MM technique which is very interesting for practical purposes.[97] [44]

It is also possible to describe the surrounding with a less computationally demanding quantum mechanics technique. Such techniques are called QM/MM methods. The ONIOM method can be used as QM/MM and QM/QM method and is thus very flexible and interesting for a cluster approach.[98]

In a perfect world it would be possible to simulate a very large finite cluster on a high level of theory which could incorporate effects such as impurities, defects and effects due to the surface of a zeolite particle. In practice this is not possible yet and thus idealized

structures are used.

3.3.2 Periodic approach

The alternative working method to the finite clusters is the periodic approach. This technique utilizes the fact that the zeolites have a well-defined crystal structure with a unit cell that is periodically repeated. A unit cell is implemented and periodic boundary conditions are implemented to represent an infinite crystalline material. One must be careful though that there are no unphysical interactions between the different periodic images. This is in particularly important in zeolites with a small unit cell.

This approach seems to be an ideal representation of the reality at first. However there are effects that are not accounted for in the periodic approach. In reality the catalyst is not infinitely big and there are definitely effects of these boundaries of the catalyst particles on the neighboring active sites. The periodic approach will also represent a perfect crystal structure, in reality there are defects present and the substituted atoms will not be perfectly homogeneously divided.

3.4 Dynamic simulations

In the past, simulations were mostly done on stationary systems obtained after geometric optimization of the potential energy surface at 0K. These simulations can give valuable information such as adsorption energy, proton affinity and reaction barriers. Transition state theory can link the information from these simulations with macroscopic quantities of the reactions. There are however more effects that come into play for a reaction.

For an accurate description of complex reaction environments and to take into account some crucial dynamical effects, the static approach is not sufficient. Every reaction is characterized by the movement of certain atoms. Therefore it is obvious that dynamic effects can play an important role if one tries to describe a reaction. A thorough sampling of the potential energy surface will lead to insights into the different possible stable structures and the transitions between them (see Figure 3.1). There might be a specific pre-reactive conformation which has to be achieved before reaction can occur. Therefore there is more and more interest in dynamic simulation. These calculations can take many more factors into account, such as the temperature effect, the framework flexibility, entropic effects and it is also easier to investigate the influence of assistant molecules. The more molecules participate in a reaction, the more complex the potential energy surface becomes and hence requiring a good sampling with molecular dynamics.

In practice the time-dependent Born-Oppenheimer approximation is often used [91]. This approximation only allows for the description of the ground state. Since the atom cores

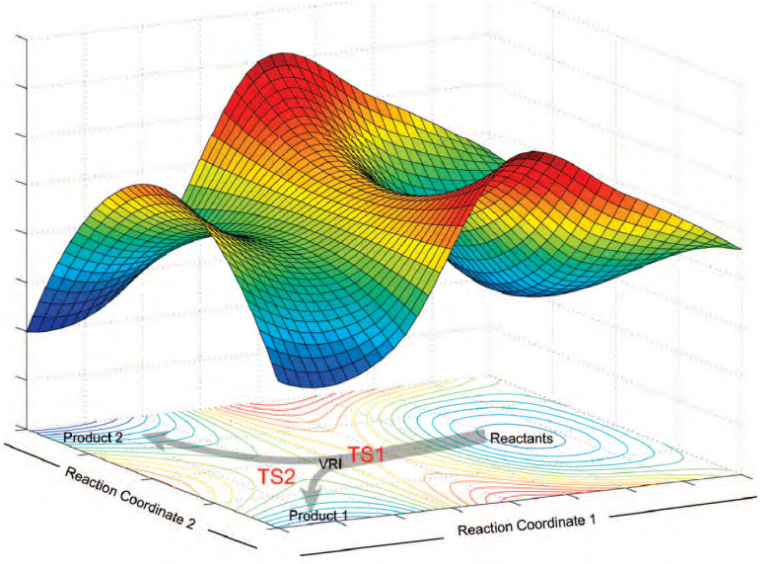

Figure 3.1: Example of a potential energy surface

are much heavier than the electrons, they move on a larger timescale. One assumes that the electrons rearrange themselves fast enough to adapt to nuclear motion. The movement of the atom cores is being described by the classical Newton's law of motion.

$$M_I \times \overrightarrow{a_I} = \overrightarrow{F_I} = -\overrightarrow{\nabla} V$$

In this equation $\overrightarrow{a_I}$ is the acceleration of the atom nuclei and $\overrightarrow{F_I}$ is the force acting on the core. This equation is coupled to the many-particle equation due to the fact that the forces acting on the core are calculated by constructing the potential energy surface. The gradient of the potential energy surface gives the forces acting on the body.
In classical molecular dynamics the potential V is not described on a quantum mechanical level, but by using force fields. This approximation is valid when no bonds are being formed or broken. In quantum or ab initio molecular dynamics (AIMD), this classical equation of motion is coupled to an electronic structure method such as DFT.

The simulations starts with a starting structure and random initial velocities, then the forces acting on the different bodies are calculated by calculating the electronic structure. When the forces are known, the atoms are moved according to Newton's laws of motion and the new conformation for the next time step is obtained after integration of this equation of motion. An important parameter is thus the time step of the simulation, this has to be small enough in order to describe the reactions that one wants to see. Shorter time steps are however computationally more demanding and can make it unfeasible to

simulate for an extended period of time.
In every new conformation of the nuclei the electron configuration has to be calculated again on a quantum mechanical level. During a reaction the electronic structure of the molecules is subject to change, thus a correct description of the electrons is necessary before the forces can be evaluated. Once the wave functions are known the forces on the cores can be evaluated.[91]

The most straightforward method and correct method for molecular dynamics is to solve the electronic many-particles problem after every movement of the atom cores. This method is however very computationally demanding. The Car-Parinello approach leads to a serious reduction in computational effort while still evaluating the electronic structure on a quantum chemical level.[99] In this method there is a ficticious kinetic energy for the electrons introduced. This means that the laws of motion of the electrons and ions are being coupled, the degrees of freedom are being combined, resulting in a generalized Lagrangian for the system. Therefore deviations from the Born-Oppenheimer approximations can occur and excited states can be described. The Kohn-Sham equations are no longer calculated from scratch in every timestep, but are based on the previous ones. Only in the first step are they explicitly calculated according to the DFT method.[91] Opposed to Born-Oppenheimer MD, Car-Parinello MD allows to sample other states than the ground state.

The system is being described as a statistical ensemble, meaning every conformation is regarded as a possible state and that the simulation will eventually give the probability distribution for all the states of the system. Depending on the degrees of freedom a different ensemble is simulated. For example in a microcanonical ensemble (NVE) the system is simulated as fully isolated.[100] No energy exchange or particle exchange is allowed, resulting in a system with predetermined energy content. Another example is the canonical ensemble or the NVT ensemble in which the system is still closed and thus no particle exchange is allowed, but the system is in contact with a heat bath. The system is allowed to exchange energy with this heat bath, resulting in a system that doesn't have a constant energy but a constant temperature. In the isothermal-isobaric ensemble (NPT) the volume is allowed to change but the pressure is being controlled as well. This ensemble is very important for chemical reactions, because in practice the pressure is a process variable. There are multiple options to use as controllers. For example a well-known thermostat is a Nosé-Hoover heat bath, this introduces a new variable which rescales the kinetic energy of the system to more closely resemble the demanded temperature. Other options are a series of heat baths or a Nosé-hoover chain. There is also the CSVR (canonical sampling through velocity rescaling) with a transfer coefficient, this thermostat will rescale the velocities in the system in order to control the temperature.

Molecular dynamics can be computationally demanding, but can provide a lot of insight on the interactions and properties in the system. A correct description of the temperature effect and entropy is important, this can lead to differences in which structures are expected to be stable. [101] [102]

When one does not do the effort to perform dynamic calculations important properties can be missed or estimated wrongly as Benco et al. desribed in their comparative study between periodic, cluster and dynamic calculations. [103] They showed that large cluster calculations lacked the proper description of the framework flexibility, resulting in an overestimation of the reaction barrier. The harmonic oscillator approximation is not always valid and can lead to an underestimation of the loss of entropy upon activation. The anharmonic effects are intrinsicly incorporated in the dynamic simulations.

Depending on the length scale on which the reaction occurs and thus the level of detail that is required there are still limitations on the timescale which can be simulated. When large changes in the conformation of a protein occur there is no need to describe every atom with high accuracy and less computationally demanding force fields can be utilized. Thanks to these methods longer simulation times can be achieved. Force fields are however not very appropriate when bond breaking and formation is needed, then more advanced methods are necessary and the time scale of the simulation will have to be smaller, therefore the total simulation time which is feasible will be shorter. An overview of the level of detail and feasible simulation times is shown in Figure 3.2.

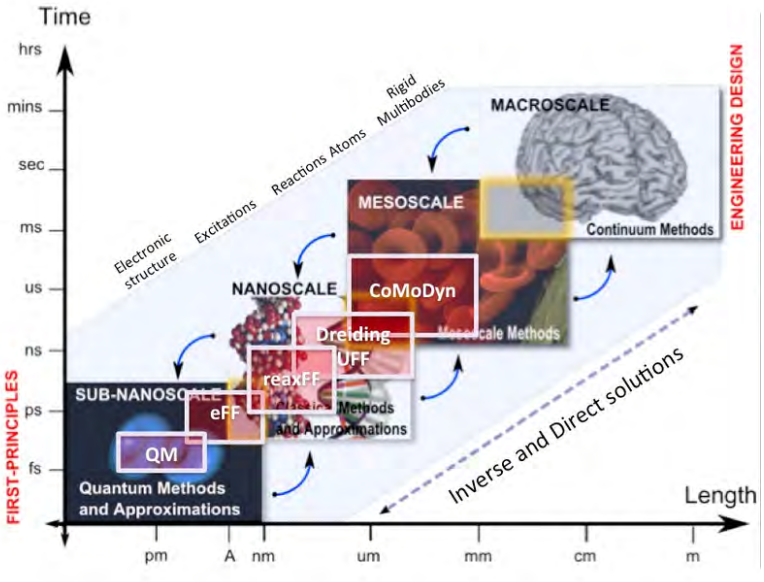

Figure 3.2: Feasible combinations of time scales and length scales for dynamic simulations [104]

3.5 Metadynamics

Due to the required accuracy in chemical reactions it can be very computationally demanding to achieve enough sampling of the reaction barriers in order to get a statistically relevant simulation. During the simulations a lot of states are being simulated but not all of them are relevant for the reaction which is being studied. The states which are higher in energy are less likely to be visited, the chance is proportional to a Boltzmann factor. While the transition state is one of the most interesting points it will thus rarely be simulated.

In metadynamics the simulation is biased by a bias potential that is constructed on the fly. This bias potential consists of a sum of gaussian functions with a predefined height (w) and width (δs) , the formula for this sum at any time step is shown in Equation 3.1. These gaussian hills are introduced in the simulation along some predefined collective variables and at a predefined frequency (t_G is the time between the addition of two hills).[105] they are fictive energy barriers which will be added to certain conformations of the structure as they occur more often. The result is that energy wells will be filled with these gaussian hills and the system will be forced out of a more stable conformation and reaction will be more probable. As an example look at Figure 3.3, where the simulation starts at x=0. When the potential energy well is filled with about 20 gaussian hills, the system is able to cross the energy barrier towards x=-4. After about 160 gaussian hills are added there is enough filling to push the system to the third minimum at x=4. After the addition of 320 gaussian hills the entire profile is filled with gaussian hills and all states are equally likely to be sampled.

$$V_G(S(x),t) = \sum_{t'=t_G,2tG,3t_G,..} w * exp(-\frac{(S(x)-s_{t'})^2}{2\delta s^2}) \tag{3.1}$$

The Gaussian hills are added along certain collective variables which describe the reaction coordinate for the particular reaction. As the energy well is being filled with Gaussian hills the probability of reactions increases. The placement of Gaussian hills is being tracked in order to reconstruct the potential energy surface afterwards. To achieve this free energy profile the added hills are being summed up and inversed. When the simulation has converged the potential well will be filled and the inverse of the summed up hills will result in the underlying free energy profile. Recrossing of the barrier is important to achieve sufficient sampling, else the filling of the potential wells will not be smooth.

Collective variable (CV) are parameters that will vary during the reaction and should properly describe the reaction coordinate. There are many options in choice for this CV, a few examples are a bond length, an angle, dihedral angle, but also more complex

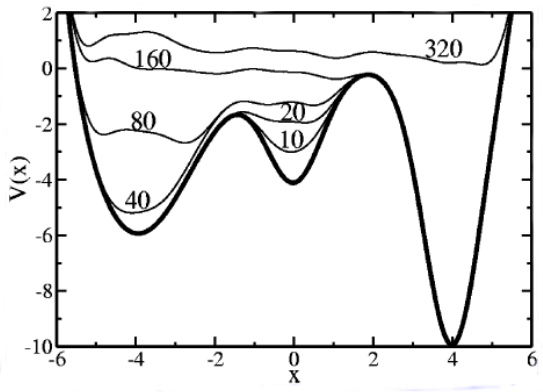

Figure 3.3: As the number of added gaussians increases the system is able to leave to local minimum in the middle and transfer to other minima. [106]

functions like sums of bond lengths can be used. A common function to be used is the coordination number (CN) shown in Equation 3.2. [107] In this formula r_0 is a reference bond length, which is typically set around the transition between a bonded and non bonded state. If this is done correctly the CN will be approximately be 1 in a bonded state, it will be 0 when there is no bond and be 0.5 around the transition state. The CN can be defined between multiple atoms and a specific one and will then indicate the amount of bonds which are formed with this specific atom.

$$CN_{ij} = \sum_{i,j} = \frac{(1 - \frac{r_{ij}}{r_0})^6}{(1 - \frac{r_{ij}}{r_0})^{12}} \tag{3.2}$$

Figure 3.4 illustrates an example on how to select the collective variables for the proton abstraction from hydroxonium ion to acetone. Since all three hydrogen atoms of the hydroxonium ion have a similar reactivity towards proton abstraction they could all be taken into account for the simulation of this reaction. Clearly for this reaction one O-H bond has to be formed, while another one has to be broken. To simplify things one can choose to focus on a single hydrogen atom since they would all show similar behavior. A good CV would then involve both the bond length of the first and second O-H bond. By taking the difference of these two bond lengths all states are defined in a unique way. Imagine the oxygen of acetone being O_1 and the one from hydroxonium ion O_2 and the CV being $CN(O_1 - H) - CN(O_2 - H)$. If a good r_0 is chosen for the coordination numbers then the CV will be approximately be 1 when the hydrogen atom is bonded to acetone and -1 when it is bonded to water.

The choice of the collective variables is very important. One could miss important effects that occur on other variables if they are not taken into account, but too many collective variables will make it slower to fill the potential energy well.

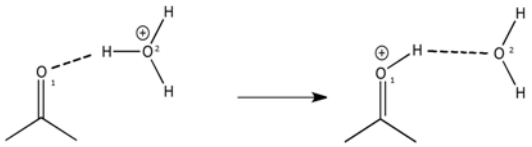

Figure 3.4: A proton transfer between hydroxonium ion and acetone

An example to show what can go wrong is given in Figure 3.5. In this case a simulation with only one collective variable would assume the reaction to occur on the diagonal of the picture with two collective variables (left pannel of Figure 3.5). Due to the form of the energy profile there will not be any reaction when one control variable is implemented untill there is large overfilling of the energy well, thus overestimating the energy barrier. For some more complex reaction paths it is very important to take multiple collective variables into account for an accurate description of the reaction.

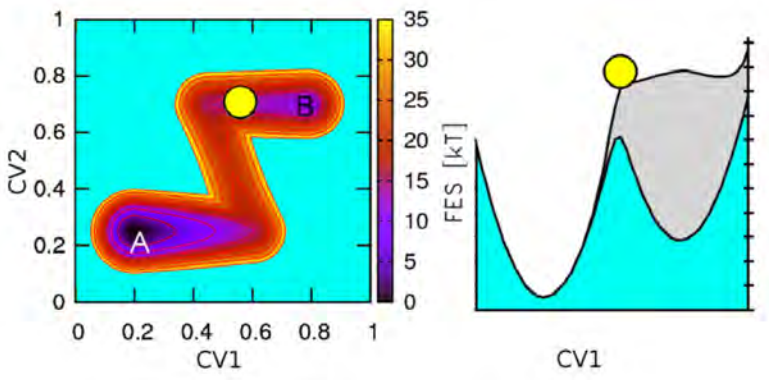

Figure 3.5: effect of not taking all the necessary control variables into account [105]

The choice of good simulation parameters is very important, i.e. the height and width of the hills and the time between the placement of two hills. This because overfilling could occur when the parameters of the simulations are not chosen correctly. The optimal case is where all the energy wells are being filled equally and there is no well where a high overfilling exists. When the height of the added Gaussian hills is too high and the rate of addition of these hills is too fast, the system will not be fully equilibrated before the next hill is added. This can result in one spot of the energy surface which is being sampled too much.

In a recent study of Moors et al. a comparison was made for the methylation of benzene between static calculations in gas phase, on a large finite cluster and dynamic calculations employing metadynamics. [108] Although static calculations on the 46-T cluster were able

to produce kinetic data with near chemical accuracy they showed that those calculations lack a proper description of the entropic effect. In a static calculation transition state theory is used where the transition state is modeled as a first order saddle point. It is only with dynamic simulations that the effect of temperature, framework flexibility and entropy can be truely investigated.
In the dynamic simulations the free energy barrier is calculated as the difference in free energy between the transition state ensemble and the free energy of the reactant region:

$$\Delta G^{\ddagger} = -\frac{1}{\beta} ln \frac{exp\{-\beta G(TS)\}}{\int_{-\infty}^{TS} exp\{-\beta G(s)\} ds}$$

where $\beta = \frac{1}{k_B T}$ and TS is the position on top of the reaction barrier along the reaction coordinate. Reaction rates are calculated using transition state theory:

$$k = \frac{1}{\beta h} exp(-\beta \Delta G^{\ddagger})$$

Like every computational method, there are some errors which will be part of the simulation. Many of these errors can not be quantified, examples are the errors caused by the choice of basis sets and functionals. There are however some errors which can be estimated. The statistical error of the free energy difference in metadynamics is approximately proportional to $\sqrt{\delta s w / \tau_G}$.
These parameters are in practice dependent on each other. The larger the size of the hills (w) the more time (τ_G) a system needs to relax. The next hill should only be added after the system has relaxed again. If the hills are added too fast after each other 'hill surfing' can occur. This is the phenomena where the collective variable continuously rides the tail of the last added hill. This will result in wrong results because there is a fraction of the energy well which isn't being sampled. On the other hand if the time for relaxation is too large the efficiency of the metadynamics simulation is partly lost.
The width of the hills (δs) and the height are also dependent on each other because they determine the steepness of the added hills. Since the forces acting on the system are calculated by taking the derivative of these hills a steep hill will lead to large forces.

Another error is the statistical error which is inherent to the finite time of simulation. This error can be estimated by generating the free energy surface at regular time intervals during the simulation. If the simulation has converged these will all lead to the same results, the variance on these results is an indication of the statistical error of the simulation.

3.5.1 Methodology in this thesis

In this thesis the calculations were performed using the CP2K package. CP2K is a freely available package for molecular simulations of solid state, liquid, molecular, and

biological systems. It is written in Fortran 95 and is frequently used for simulations with periodic boundary conditions.[109]

Previous experience with simulations on extended H-SAPO-5 cluster led to the conclusion that a large dipole moment negatively influenced the results. The dipole moment is inherent to the catalyst its structure because of its one dimensional channel, by making a finite cluster large dipole moments are obtained. Therefore it was opted to simulate the system with periodic boundary conditions. The primary unit cell of H-SAPO-5 is very small and only consists of 24 T-atoms, therefore the unit cell has been extended in the direction of the pores, the c-axis. This results in a super cell with 24 aluminum atoms, 23 phosphoros atoms and 1 silicon atom which can be seen in Figure 3.6. With period boundary conditions this will simulate a perfect crystal structure with a Si/(Al+P) ratio of 1/47. This ratio is important for the comparisson with other results because it is one of the variables that influences the acid strength of the catalyst. For H-SSZ-24 the silicon atom is substituted by aluminum and the aluminum and phosphorus is substituted by silicon, resulting in a Al/Si ratio of 1/47.

The calculation are performed on the DFT level of theory with the revised PBE functional and Gaussian plane waves basis sets.[110] [96] The DZVP-GTH basis set are used and dispersion interactions were taken into account by the addition of Grimme D3 corrections.[93] The GTH pseudopotentials are used to describe the complex motion of the core in a efficient manner.[111]

Static calculations

The geometry optimizations are used to calculate energy differences between different states and for the calculation of adsorption energies. For the calculation of the adsorption energies a difference in energy is taken between the adsorbed state and the empty framework and the adsorbate in gas phase. For the adsorbate in gas phase periodic boundary conditions were also used but this has little to no influence on the obtained values.

An important thing to note here is that the calculation of the energy of the framework and geometry optimization has to be repeated for every adsorption even though the framework is essentially identical. When the adsorbed state is optimized small changes to bridging oxygens may occur, corresponding with relatively high energy differences. Therefore the optimization of the framework is being redone by reoptimizing from the optimized adsorbed state, but deleting the adsorbate from the input structure. This ensures that the reference point will always be as accurate as possible.

For the cell parameters of the adsorption energies optimized values were used from a NPT MD simulation with one methanol molecule inside the framework at 623K. The

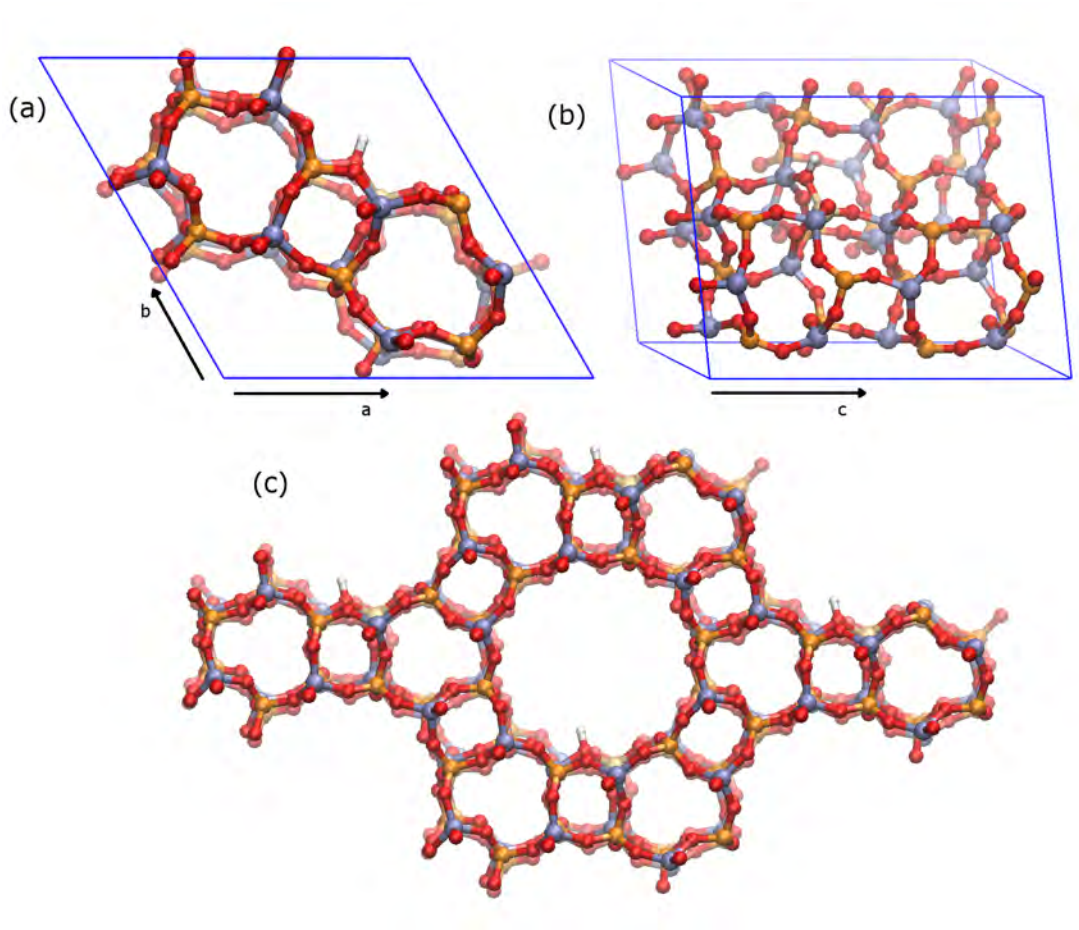

Figure 3.6: An overview of the unit cell for H-SAPO-5 with 1 acid site from the different angles, looking along the axis of the pores (a) a side view (b) and an overview of the unit cell which has been extended in the a and b direction (c)

framework parameters for H-SSZ-24 and H-SAPO-5 are thus different, but during all the different geometry optimizations with different adsorbates they are identical.
The energy calculations performed within the CP2K package did not involve vibrational analyses nor do they incorporate zero point energy corrections. They will thus result in ΔE values as the adsorption energy.

Molecular dynamics and metadynamics simulations

The dynamic simulations were all performed on a temperature of 623K and all time steps were 0.5 fs. This time step is small enough in order to see the important details of the reaction. The metadynamics simulations are performed in the NVT ensemble, therefore there is first the need for an average volume.
First a simulation of the system in the NPT ensemble is used and after a certain equi-

libration time the volume is being averaged. The volume of the unit cell may vary according to the molecule(s) present inside the pores.

In the metadynamics simulations the most important characteristics are the height of the gaussians, their width and the frequency of placing a gaussian. The frequency is always set at once every fifty timesteps, being every 25 fs. The width of the gaussians is set at 0.02 and the height is adapted depending on the specific circumstances. If atoms with low inertia, i.e. hydrogen, are part of the collective variables the height of a gaussian will be lowered. More detailed information on the applied parameters will be given with the discussion of the results.

After every recrossing of the reaction barrier the height of the gaussians is halved. This allows for a rapid filling of the potential wells at the start of the simulation and an improvement of the accuracy at the end of the simulation.

Chapter 4

Adsorption in the AFI topology

In heterogeneous catalysis there are active sites where reactions occur. In the case of the MTO-process it has been shown that proton transfer from the framework to methanol is very important, since it is this Brønsted acid proton which is mainly responsible for the activity of the catalyst.[4] This site can however only be occupied by one molecule at a specific time. Evidently, molecules with a higher interaction strength will be more favorable to reside on the acid site. For example it is straightforward that polar molecules such as methanol will have a strong interaction with this site.
In regimes of high loading on the catalyst the amount of acid sites is limited and competitive adsorption can occur. In those cases the adsorption energy can give an indication on which molecules will be directly interacting with the acid site and which ones will be rather co-adsorbed.

Herein, adsorption of methanol, DME and benzene in both H-SAPO-5 and H-SSZ-24 is studied. Adsorption on both the Brønsted acid site and the neighbouring site, i.e. on top of bridging oxygens that are not connected to the acid-site, is considered. This neighbouring site can be a very important point of reference. The reference for the adsorption energies is the adsorbate in gas phase and not interacting with the framework. To evaluate the preference of a molecule to reside on the acid site instead of moving freely inside the pores of the catalyst the co-adsorbed state is a good reference point since it will incorporate the interactions between the adsorbate and the framework.

The next step which has to occur before a reaction can happen is the formation of a pre-reactive complex. This means that next to methanol, which will preferentially reside on the acid site, a hydrocarbon pool species will be co-adsorbed simultaneously on a neighbouring site. This co-adsorption of benzene forms the pre-reactive complex.[112] Since this is the starting point for reaction it is an interesting complex to examine. In this contribution the co-adsorption complexes for one methanol and one benzene molecule are considered. The effect of adding a second methanol molecule is also evaluated.

4.1 Methanol adsorption

For the adsorption of methanol and other alcohols in zeolites there is still discussion about the exact structure of the adsorption complexes. This adsorption has received attention of experimental and theoretical research.[113] [112] There are three possible orientations of methanol which are depicted in Figure 4.1. The main point of discussion is whether or not the methanol molecule becomes protonated (i.e. chemisorbed) or if the interaction with the zeolite is due to hydrogen bonds with the catalyst (i.e. physisorbed).
The work of Stich et al. in H-SSZ-13 used MD simulations to investigate the adsorption of methanol. They concluded that there were a lot of local minima and thus that MD simulations are almost necessary to have an accurate description of this interaction. The barrier for the protonation of a single methanol was found to be too high and they concluded that methanol would only be protonated under higher loadings.[114] Cluster calculation performed by Hemelsoet et al. in the CHA topology showed that for static calculations the optimal structure for adsorption of an alcohol was an 'end-on' adsorption which involved both a strong hydrogen bond between the Brønsted proton and the oxygen of the alcohol and two weaker hydrogen bonds between the proton of the alcohol and neighbouring oxygens, similar to structure (b) in Figure 4.1.[87]

The adsorption of methanol in the two isostructural materials H-SAPO-5 and H-SSZ-24 has been examined. Since H-SSZ-24 has the highest acid strength it is clear that interaction with the acid site will be stronger in this catalyst. As mentioned before, the adsorption on a neighbouring site is investigated as well. The results are shown in Table 4.1.

Table 4.1: Adsorption energies in kJ/mol of methanol in H-SAPO-5 and H-SSZ-24 on both the acid site and a neighbouring site. The adsorption energies are split up in the contributions of the electronic and dispersion interaction.

methanol		$\Delta E_{ads,total}$ [kJ/mol]	$\Delta E_{ads,electronic}$ [kJ/mol]	$\Delta E_{ads,dispersion}$ [kJ/mol]
H-SAPO-5	acid site	-83.0	-56.8	-26.2
	neighbouring site	-44.4	-14.0	-30.3
H-SSZ-24	acid site	-98.5	-75.1	-23.4
	neighbouring site	-37.7	-12.0	-25.7

Since the adsorption on the acid site is governed by the acid strength of the site it is obvious that in the more acidic catalyst, H-SSZ-24, methanol will have the strongest

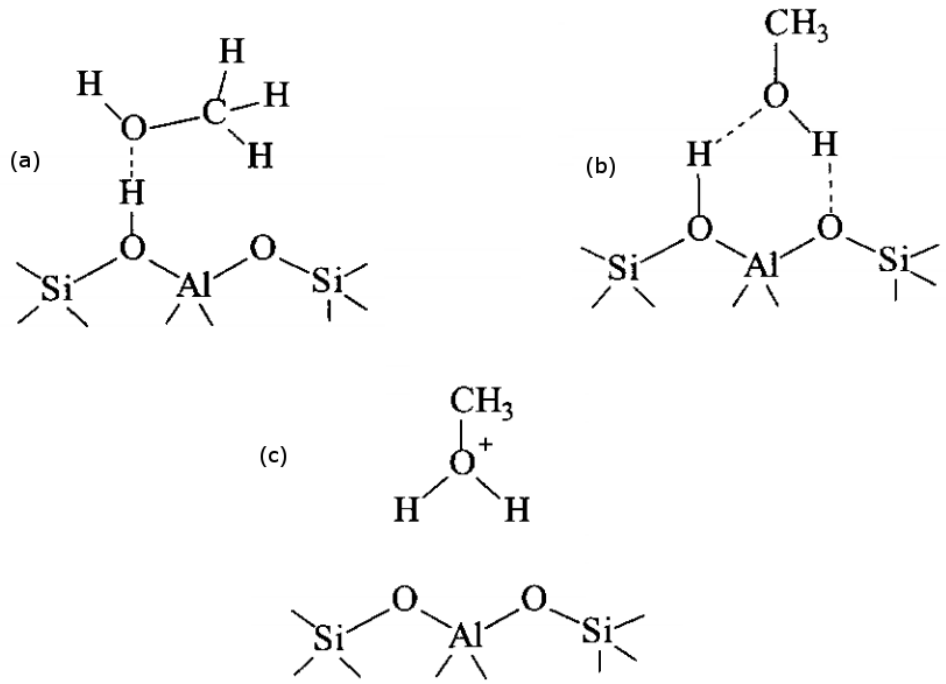

Figure 4.1: Three adsorptions orientations of methanol on an acid site. An orientation with one hydrogen bond between the oxygen of methanol and the acid site (a) an orientation with an additional hydrogen bond between the proton of methanol and the zeolite (b) an orientation with a protonated methanol molecule (c) [113]

adsorption energy. The main difference in their interaction strength is in the electronic contribution, which confirms this theory. The difference in dispersion interaction is only very small. These results are in line with a previous study on a finite cluster in H-SAPO-34.[115] Since H-SAPO-5 has a similar acid strength as H-SAPO-34 it was expected that these results would be similar. The main difference is that the dispersion interaction calculated in this thesis is smaller, which is likely due to the larger pore sizes in the AFI-topology leading to larger adsorbate-framework distance. The results in H-SAPO-34 indicated a dispersion interaction of 30-40 kJ/mol, depending on the proton position.[115]

The adsorption of methanol on the neighbouring site is slightly more favorable in H-SAPO-5, but in but both catalysts weaker than adsorption on the acid site. This is due to the absence of specific interactions with the proton on this site, therefore there is no influence of the acidity of the catalyst. The adsorption is governed by interaction with the neighbouring oxygens which is very similar in both catalysts. The alternation of aluminum and phosphorus atoms in H-SAPO-5 results in a higher polarity of the material which results in a stronger interaction with methanol. The chemical composition is

thus the reason for the difference, but this effect is rather limited. The slightly more polar framework interacts stronger with a polar molecule, this is evident since these interactions amplify each other.

As can be seen from Figure 4.2 the most stable structure is not a protonated methanol molecule, but a physisorbed methanol molecule with two hydrogen bonds with the catalyst. This is the case for both H-SAPO-5 and H-SSZ-24. This is in agreement with the previous results found by Stich et al. [114]
Another important characteristic is the distance between the methanol molecule and the proton of the acid site. As shown in Figure 4.2 this distance is 1.47 Å in H-SAPO-5 and for H-SSZ-24 it is 1.43 Å. This parameter is not as quantitative as the adsorption energy, but it does also confirm the stronger interaction which is present in H-SSZ-24.

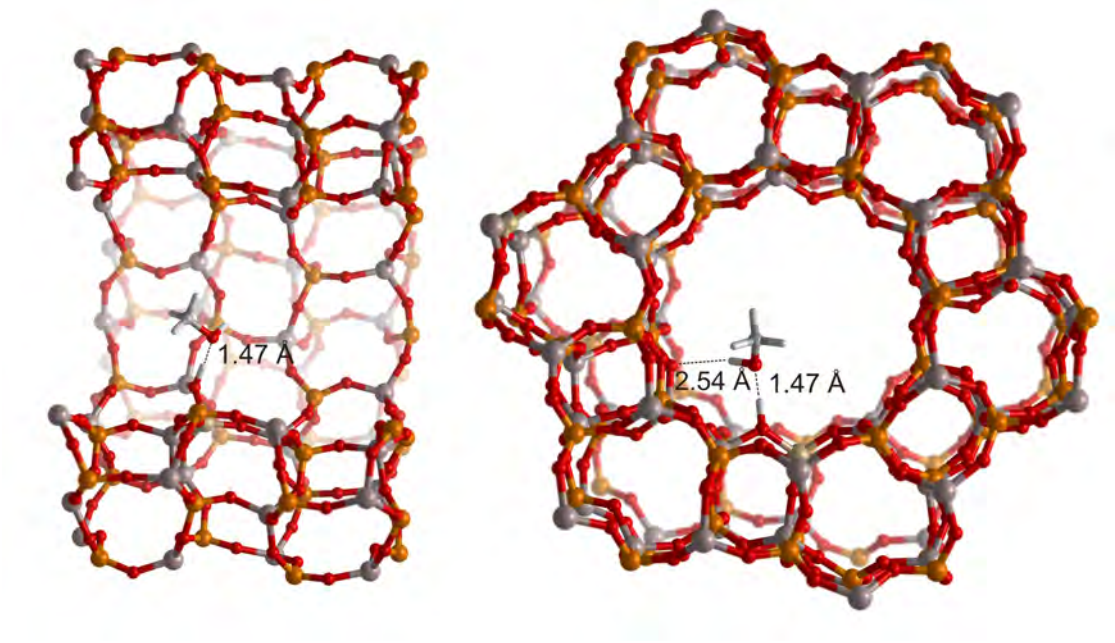

Figure 4.2: Adsorption complex of methanol on the acid site in H-SAPO-5 shown in side view and along the c-axis of the catalyst

In Figure 4.3 the adsorption of methanol is shown on the neighbouring site. There is only one hydrogen bond with the catalyst and the proton of methanol. This hydrogen bond is clearly weaker than the hydrogen bond with the acid site, but it does have a stronger interaction than the secondary hydrogen bond which was present in the complex on the acid site, this can be seen by comparing the bond lengths. The secondary hydrogen bond has a length of 2.54 Å while for adsorption on the neighbouring site the bond length is 2.31 Å.

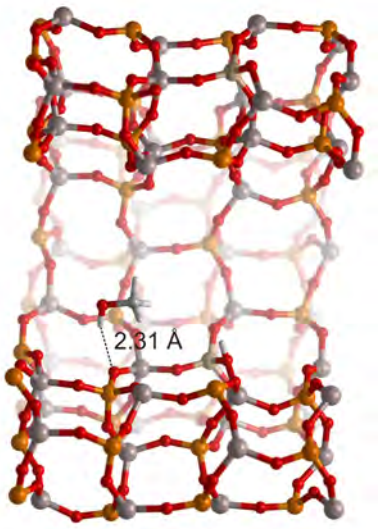

Figure 4.3: Adsorption complex of methanol on the neighbouring site in H-SAPO-5 shown in side view

4.2 DME adsorption

Dimethylether (DME) is known to form an equilibrium mixture with methanol and water during the early stages of MTO conversion. It is also the first product which is formed in the MTO process. There is discussion whether DME or methanol the reactive species is for the methylation reactions.[23] This will not be further investigated in this thesis, but it is clear that if DME is present in the mixture it is also one of the possible species to be adsorbed on the acid sites of the catalyst.

The adsorption energies of DME on the acid site and a neighbouring site for both the AFI-structured catalyst are shown in Table 4.2. The large stabilizing effect of the acid site is again visible. The effect is even stronger for DME than for methanol. This is most likely due to the electron releasing effect of the additional methyl group bonded to the oxygen atom. Even though there is no secondary hydrogen bond present in this adsorption complex the electronic effect of the acid site is still stronger than for methanol. The dispersion interactions are again very similar in all cases, they are slightly larger than those for methanol, which is to be expected due to the larger volume of DME. The interaction with the acid site is very strong, but apparently there is no influence of the acidity on this interaction strength.

The adsorption of DME on the acid site in H-SAPO-5 is shown in Figure 4.4 and the adsorption on the neightbouring site in Figure 4.5. The length of the hydrogen bond with the acid site in H-SAPO-5 is 1.44 Å while it is 1.4 Å in H-SSZ-24, indicating that

Table 4.2: Adsorption energies in kJ/mol of DME in H-SAPO-5 and H-SSZ-24 on both the acid site and a neighbouring site. The adsorption energies have been split up in the contributions of the electronic interaction and dispersion interaction.

DME		$\Delta E_{ads,total}$ [kJ/mol]	$\Delta E_{ads,electronic}$ [kJ/mol]	$\Delta E_{ads,dispersion}$ [kJ/mol]
H-SAPO-5	acid site	-112.7	-78.8	-33.9
	neighbouring site	-52,3	-21,9	-30.3
H-SSZ-24	acid site	-113.8	-83.7	-30.1
	neighbouring site	-43.8	-18.1	-25.7

these hydrogen bonds are very strong. Adsorption on a neighbouring site is stronger in H-SAPO-5, this is similar to the adsorption of methanol on the neighbouring site discussed before. The adsorption of a polar molecule on a more polarized structure is stronger. The orientation of DME in the pores of the catalyst depends on whether it is adsorbed on the acid site or not. As can be seen from Figure 4.5, DME will orient itself upright in the catalyst pores in order to have as much interaction with the framework as possible. If there is however interaction with the acid site, this interaction will completely dominate all other interactions and the strong hydrogen bond with the proton of the catalyst will determine the orientation of DME.

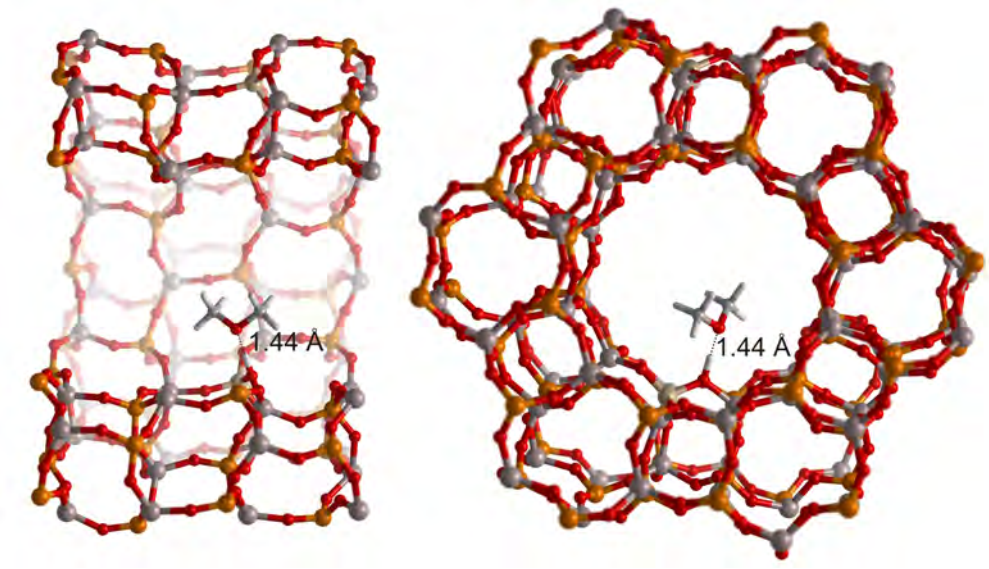

Figure 4.4: Adsorption complex of DME on the acid site in H-SAPO-5 shown in side view and along the c-axis of the catalyst

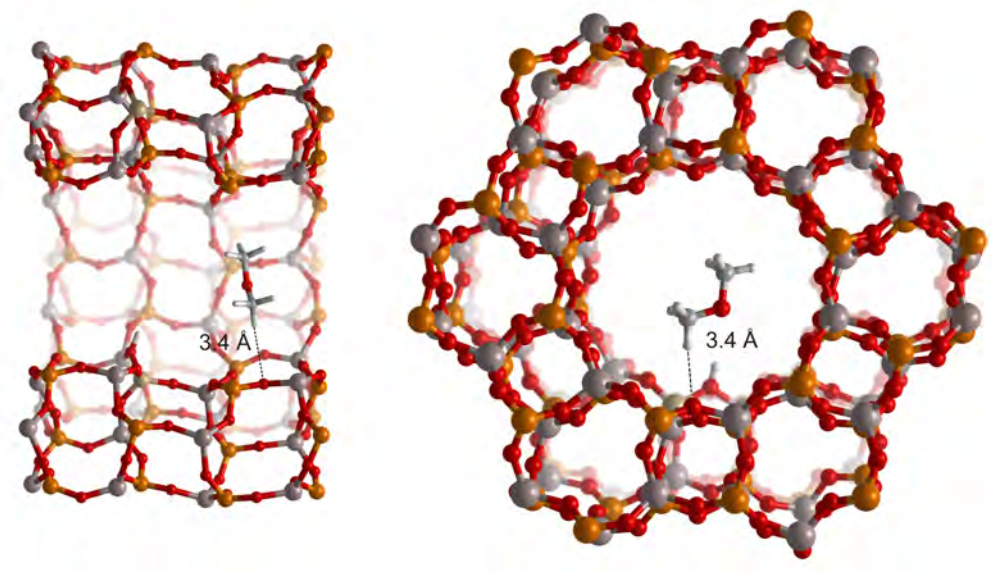

Figure 4.5: Adsorption complex of DME on the neighbouring site in H-SAPO-5 shown in side view and along the c-axis of the catalyst

4.3 Benzene adsorption

The other important species which are present inside the pores of the catalysts are of course the hydrocarbons. In this thesis work benzene was chosen as the molecule to represent an aromatic hydrocarbon pool species. Aromatics are a large fraction of the products formed in AFI-structured catalysts.[116] Benzene is an apolar molecule and thus dispersion interactions are more likely to be dominating the total adsorption energy.

Adsorption on both the acid site and a neighbouring site has been considered. The obtained results are shown in Table 4.3. As expected there is a big difference between the interaction of benzene and methanol with the framework. The heavier benzene molecule has stronger dispersion interactions than DME and methanol, but because it is a apolar molecule there is no large stabilizing electrostatic interaction.

There is still a slight preference for benzene to reside on the acid site when compared to a neighbouring site, especially in H-SSZ-24. Most likely due to an interaction between the acid site and the $\pi - orbitals$ of benzene. The difference in adsorption energy between the two sites is however relatively small, especially when it is compared to the difference for methanol or DME. This could indicate that the acid sites will preferentially be occupied by methanol or DME. Benzene will thus be the molecule that is co-adsorbed on a neighbouring site while methanol resides on the acid site. In a previous study on AlPo-5 and SSZ-24 a higher heat of adsorption was observed for benzene on SSZ-24.[117]

Table 4.3: Adsorption energies in kJ/mol of benzene in H-SAPO-5 and H-SSZ-24 on both the acid site and a neighbouring site. The adsorption energies have been split up in the contributions of the electronic interaction and dispersion interaction.

benzene		$\Delta E_{ads,total}$ [kJ/mol]	$\Delta E_{ads,electronic}$ [kJ/mol]	$\Delta E_{ads,dispersion}$ [kJ/mol]
H-SAPO-5	acid site	-83.0	-17.3	-65.7
	neighbouring site	-79.8	-16.1	-63.7
H-SSZ-24	acid site	-88.7	-24.4	-64.3
	neighbouring site	-72.6	-11.3	-61.3

This effect is also found in these simulations for the adsorption on the acid site, but not for the adsorption on a neighbouring site.

The orientation of benzene in the pores of the catalyst is shown in Figure 4.6 for the acid site and in Figure 4.7 for the neighbouring site. There is clearly a difference in orientation between the two sites. While being adsorbed on the acid site there is an interaction of the π-orbitals of benzene with the 1s orbitals of the proton. When this interaction is not present, such as on the neighbouring site, the benzene molecule will reorient itself to stand upright in the pores in order to have as much interaction with the framework as possible. This behavior is very similar to what was found for the polar molecule DME.

The distance between benzene and the proton is very similar in H-SSZ-24 and H-SAPO-5, they are respectively 2.16 and 2.23 Å. This does clearly show that there definately is some interaction between the proton and the π-orbitals of benzene, but the adsorption energies prove that this interaction is smaller than for polar adsorbates.

The closest distance between benzene on the neighbouring site and the framework was around 3,17 Å for both catalysts as shown in Figure 4.7. This is the distance between a hydrogen atom of benzene and an oxygen atom of the catalyst. This means that there is still enough free space inside the pores for substituents onto benzene.

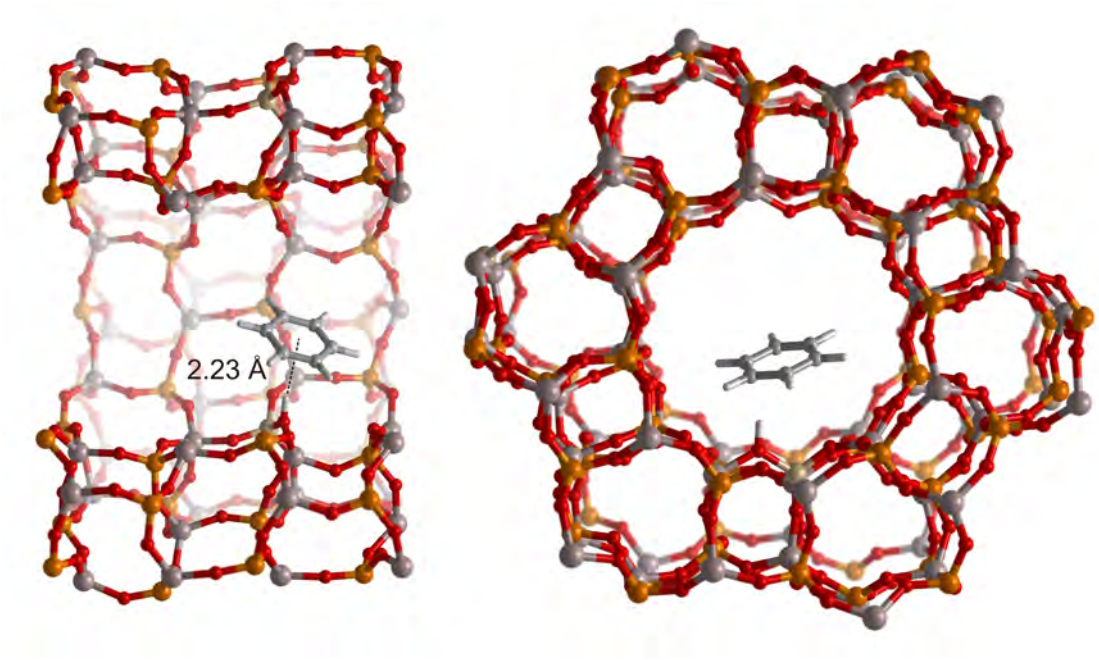

Figure 4.6: Adsorption complex of benzene on the acid site in H-SAPO-5 shown in side view and along the c-axis of the catalyst

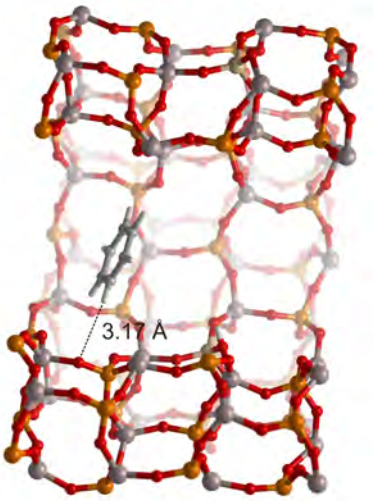

Figure 4.7: Adsorption complex of benzene on the neighbouring site in H-SAPO-5 shown in side view

4.3.1 Adsorption on a methoxy group

As discussed is section 4.1, there exist mechanisms for the methylation of benzene which use a step-wise mechanism. In this mechanism there is first the formation of a surface-

bound methoxy group. Benzene will then co-adsorb on top of this group and react further from there. Therefore the adsorption of benzene on top of a methoxy group is also very interesting. The optimized structures are shown in Figure 4.8.

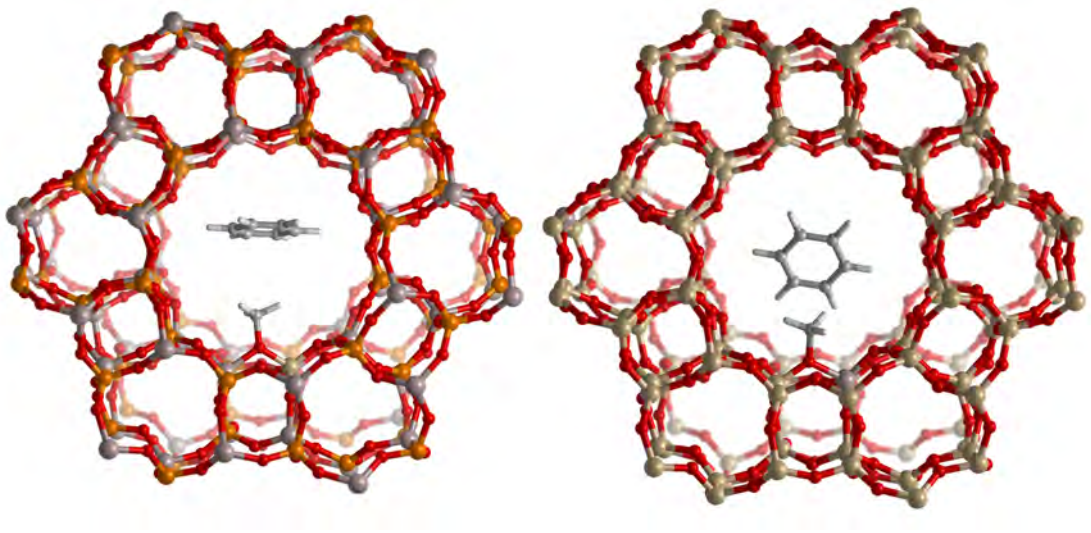

Figure 4.8: Adsorption of benzene on top of a surface-bound methoxy group in SAPO-5 (left) and SSZ-24 (right) shown along the c-axis of the catalyst

The orientation of the benzene molecule in both catalyst is different. This suggests a difference in the contribution of the different interactions. In H-SAPO-5 the benzene molecule is oriented with its π-orbitals on top of the methoxy group. This interaction is very similar to the interaction discussed before between benzene and the acid site which contained a proton. However in H-SSZ-24 the benzene molecule is oriented in a similar way as benzene usually does on a neighbouring site. This orientation suggests that the interaction with the framework is more important than the interaction with the methoxy group. The optimalization had started from a structure where benzene was oriented on top of the methoxy group for H-SSZ-24 and for H-SAPO-5 the optimization had started from a point where benzene was not oriented on top of the methoxy group. The shift in orientation shows that the orientation on top of the methoxy group is indeed more stable.

The distance between the methoxy group and benzene is smaller in H-SSZ-24 (2.82 Å 2.91 Å), which could indicate a stronger interaction with the methoxy group. Some caution is however recommended since the orientation of benzene is different. A more quantitative approach is to look at the adsorption energies. The adsorption energies calculated for benzene on the catalyst with a surface bound methoxy group are given in Table 4.4. For easy reference the previous results for adsorption of benzene on the acid

site and on a neighbouring site are also given.

Both the orientation of benzene and its adsorption energy in H-SAPO-5 are very similar to the adsorption of benzene on an acid site. For benzene in H-SSZ-24 the orientation is more similar to benzene adsorbing on a neighbouring site. The adsorption energy is however higher than the pure adsorption on a neighbouring site. In particular the electronic contribution to the adsorption is higher, but not as high as in the case of adsorption on an acid site. The interaction with the surface bound methoxy group are more similar to the adsorption in H-SAPO-5. This could indicate that the influence of the acid strength is much lower when a methoxy group is present instead of a proton. While the adsorption energies for benzene in H-SAPO-5 are very similar for all investigated possibilities, the adsorption in H-SSZ-24 does show differences. There is a clear preference for the acid site, followed by adsorption on a methoxy group and the weakest interaction is with the neighbouring site.

Table 4.4: Adsorption energies in kJ/mol of benzene on a methoxy group, on the acid site and on a neighbouring site in H-SAPO-5 and H-SSZ-24. The adsorption energies have been split up in the contributions of the electronic interaction and dispersion interaction.

benzene		$\Delta E_{ads,total}$ [kJ/mol]	$\Delta E_{ads,electronic}$ [kJ/mol]	$\Delta E_{ads,dispersion}$ [kJ/mol]
H-SAPO-5	methoxy	-78.9	-17.5	-61.4
	acid site	-83.0	-17.3	-65.7
	neighbouring site	-79.8	-16,1	-63.7
H-SSZ-24	methoxy	-81.8	-18.7	-63,1
	acid site	-88.7	-24.4	-64.3
	neighbouring site	-72.6	-11.3	-61.3

4.4 Co-adsorption of benzene and methanol

Co-adsorption is arguably even more important than the adsorption on its own and this is especially true for benzene. As discussed in the previous sections methanol will preferentially reside on the acid site. The pre-reactive complex for the methylation of benzene involves methanol on this acid site and benzene co-adsorbed on a nearby site.

The adsorbed species are shown in Figure 4.9. A similar effect for methanol on the

acid site is visible, the more acidic H-SSZ-24 catalyst has a stronger interaction with methanol and thus a shorter hydrogen bond. Another important difference between the two catalysts is the orientation of methanol. In H-SSZ-24 methanol clearly has some interaction with benzene. The methyl group is rotated towards benzene. This is thus a much more reactive position already. It is important to note that to reach this structure we started the optimization from a point where methanol was not oriented towards benzene. It is clearly energetically favorable for methanol to have this interaction with methanol. One does have to keep in mind that these static optimizations always show local minima and therefore some caution is advised.

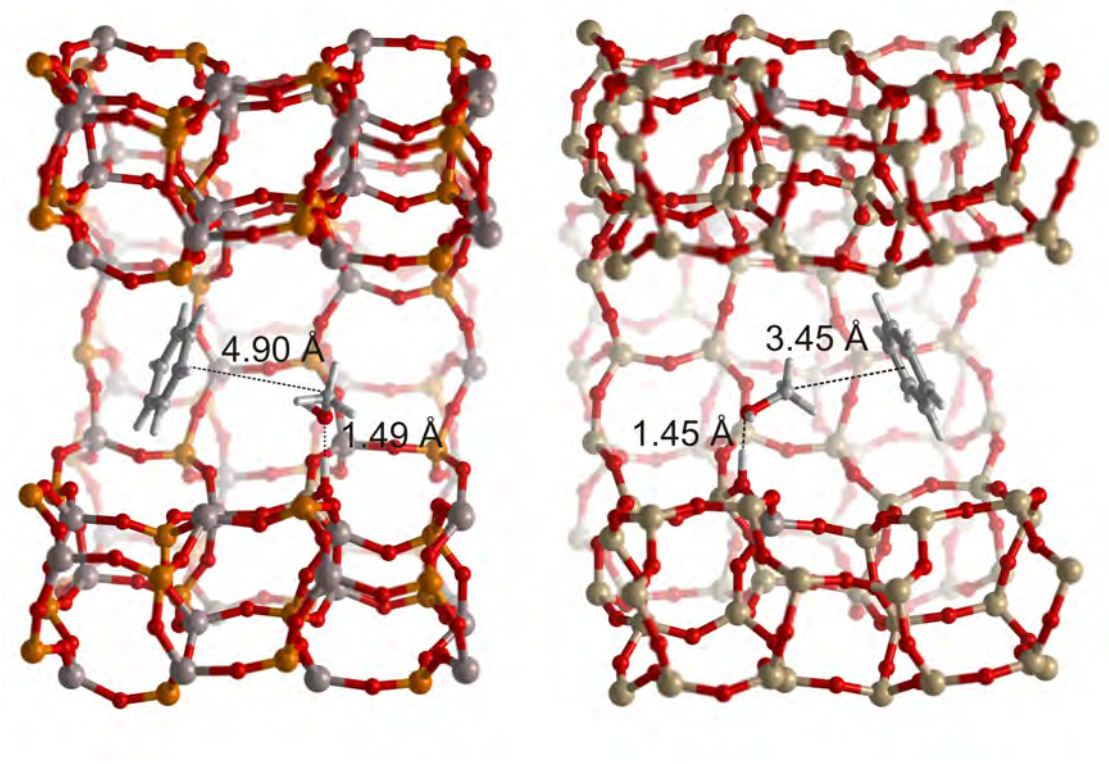

Figure 4.9: Adsorption complex of methanol and benzene in H-SAPO-5 (left) and H-SSZ-24 (right) shown in side view

Depending on the point of reference, multiple characteristics can be calculated starting from this point onwards. A first possibility is to evaluate the ΔE_{co-ads} of benzene. This means the energetic difference for the co-adsorption of benzene from the gas phase onto a framework where methanol is already adsorbed on the acid site. The energy profile for the sequence of these steps is schematically depicted in Figure 4.10. A second option is to evaluate the ΔE_{co-ads} of methanol, i.e. the adsorption energy for methanol from the gas phase onto the catalyst with benzene already adsorbed on the neighbouring site. Although the second option might not be what is actually happening during the

process it provides insight on the additional stabilization the benzene molecule provides for the adsorbed methanol. The results are shown in Table 4.5, because it is important to compare these values with the adsorption without presence of other molecules they are added to the table.

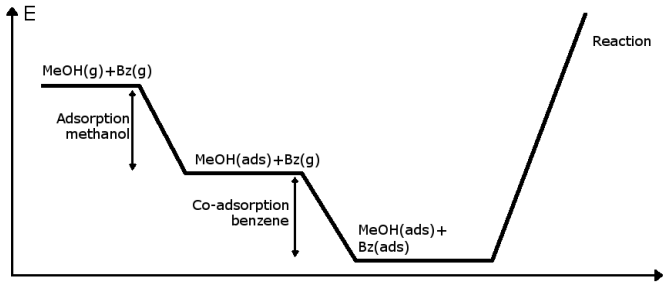

Figure 4.10: sketch of the energy profile of the different adsorption steps leading up to reaction

Table 4.5: Co-adsorption energies in kJ/mol of methanol in the presence of benzene and vice versa, together with the results of the adsorption without presence of other species

Co-adsorption	$\Delta E_{co-ads,meth}$ [kJ/mol]	$\Delta E_{ads,meth}$ [kJ/mol]	$\Delta E_{co-ads,benz}$ [kJ/mol]	$\Delta E_{ads,benz}$ [kJ/mol]
H-SAPO-5	-99.5	-83.0	-84.6	-79.8
H-SSZ-24	-105.3	-98.5	-80.6	-72.6

The presence of other guest molecules clearly results in larger co-adsorption energies compared to the pure adsorption. The effect is however limited to 10 kJ/mol, except for the co-adsorption of methanol in H-SAPO-5. The difference between the $\Delta E_{co-ads,methanol}$ and the $\Delta E_{ads,methanol}$ approximates 17 kJ/mol.

4.5 Co-adsorption of benzene and two methanol molecules

As discussed before there is evidence that higher loadings of methanol have a large effect on the reactivity of the methanol molecules. In particular the tendancy of methanol to form clusters which are more likely to abstract a proton from the catalyst is interesting. A single methanol molecule is rather unstable when it is protonated. A methanol dimer however has a larger affinity for the proton.[108]

Two possible clusters were studied, in the first one the methanol molecules are allowed to form a cluster and will form a network of hydrogen bonds as shown in Figure 4.11 the

second option is to separate the methanol molecules so they can not interact with each other. In Figure 4.11 all the relevant bond lengths are given as well. In this hydrogen bonded network the protons are able to be exchanged simultaneously between all the interacting molecules. The proton of the acid site will be transfered to the first methanol molecule which will in turn transfer its own proton to a next methanol molecule. This behavior is typical for protonic solvents and drastically increases the proton mobility.

Something which is immediately visible is that the methanol cluster with only two methanol molecules is already having a much stronger attraction on the proton of the catalyst. This is especially true for H-SSZ-24, which is logical due to its higher acid strength. The distance between the proton of the catalyst and the oxygen of methanol is only 1.45 Å for H-SAPO-5 while the distance between that same proton and the oxygen atom of the catalyst is 1.29 Å. This means that the proton is still bonded more strongly to the catalyst than the methanol cluster, but it is certainly close to a transition between the two.

In H-SSZ-24 the methanol cluster abstracts the proton almost completely from the catalyst. This further confirms the higher reactivity of this catalyst. The interaction between the proton and the catalyst is however still strong. A full abstraction of the proton to a cluster of methanols which would be able to move freely inside the pores is still unlikely. This is in agreement with theoretical work of Moors et al.[108] They used MD simulations and investigated the effect of methanol loading on the methylation of benzene in H-ZSM-5. They showed that clusters with three methanol molecules are the most stable complexes. However they also found that the methylation barrier increases as the number of methanol molecules in the cluster increases.

When the methanols are separated they are no longer able to interact with each other, but the addition of this second methanol can has its influence on the adsorption. In Figure 4.12 the corresponding adsorption complexes are shown. The complex found here is not very different from the one found when only one methanol molecule and one benzene molecule was considered. This indicates that the second methanol molecule is indeed purely a 'spectator' molecule.

The corresponding adsorption energies are a more quantitative description than the bond lengths. Similar to the complex of one methanol and one benzene molecule there are again multiple points of reference which will provide different information. A first option is to look at the co-adsorption of methanol from the gas phase onto the complex where there is already a methanol and a benzene molecule present. It is assumed that this methanol molecule will already reside on the acid site, which is a very reasonable assumption as shown in Section 4.1. A second option is to look at the co-adsorption of benzene from the gas phase onto a complex of two methanol molecules which are

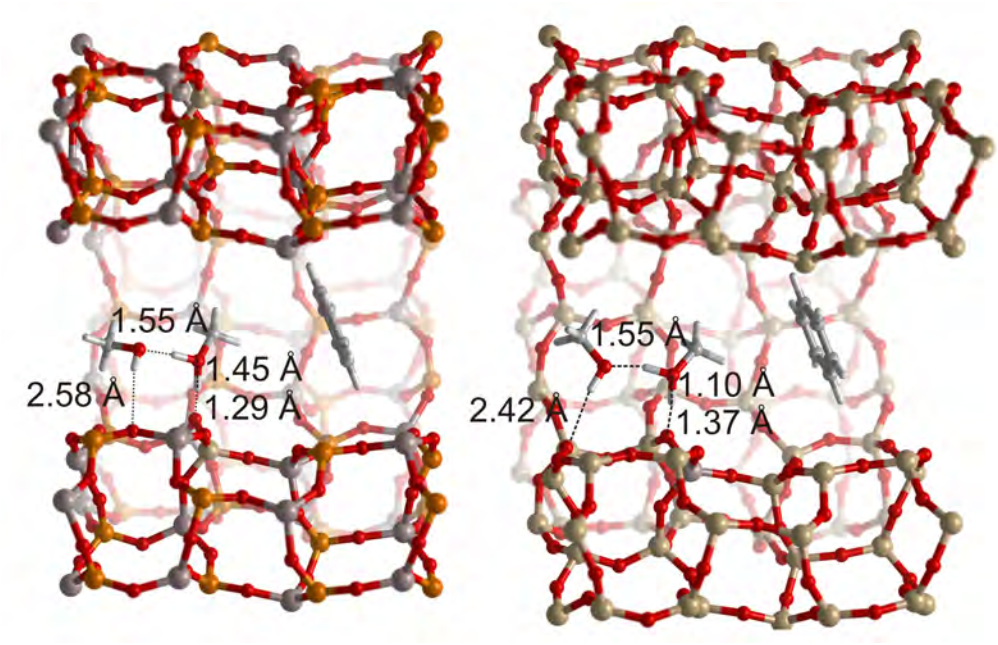

Figure 4.11: Adsorption complex of 2 methanol molecules and benzene in H-SAPO-5 (left) and H-SSZ-24 (right) shown in side view, the methanol molecules are allowed to form a cluster and a network of hydrogen bonds

already present in the pores of the catalyst. An overview of the entire energy diagram of this sequence of adsorptions is given in Figure 4.13. Thus the adsorption of benzene in between two separated methanol molecules or next to a cluster. Both results are shown in Table 4.6, the previously calculated adsorption energies are given as well for comparison in Table 4.7.

Table 4.6: Overview of the adsorption energies for the co-adsorption of methanol and benzene (kJ/mol)

Co-adsorption		$\Delta E_{co-ads,methanol}$ [kJ/mol]	$\Delta E_{co-ads,benzene}$ [kJ/mol]
H-SAPO-5	methanol cluster	-82.0	-83.9
	separated methanol	-44.8	-96.0
H-SSZ-24	methanol cluster	-84.3	-79.6
	separated methanol	-32.1	-82.5

Table 4.7: Points of reference for comparison with the co-adsorption energies of methanol and benzene. The adsorption energy for methanol without presence of other molecules are given for both the acid site and a neighbouring site, together with the adsorption energy of benzene on a neighbouring site

reference points	$\Delta E_{ads,meth,acid}$ [kJ/mol]	$\Delta E_{co-ads,meth}$ [kJ/mol]	$\Delta E_{ads,benz,neighbour}$ [kJ/mol]
H-SAPO-5	-83.0	-44.4	-79.8
H-SSZ-24	-98.5	-37.7	-72.6

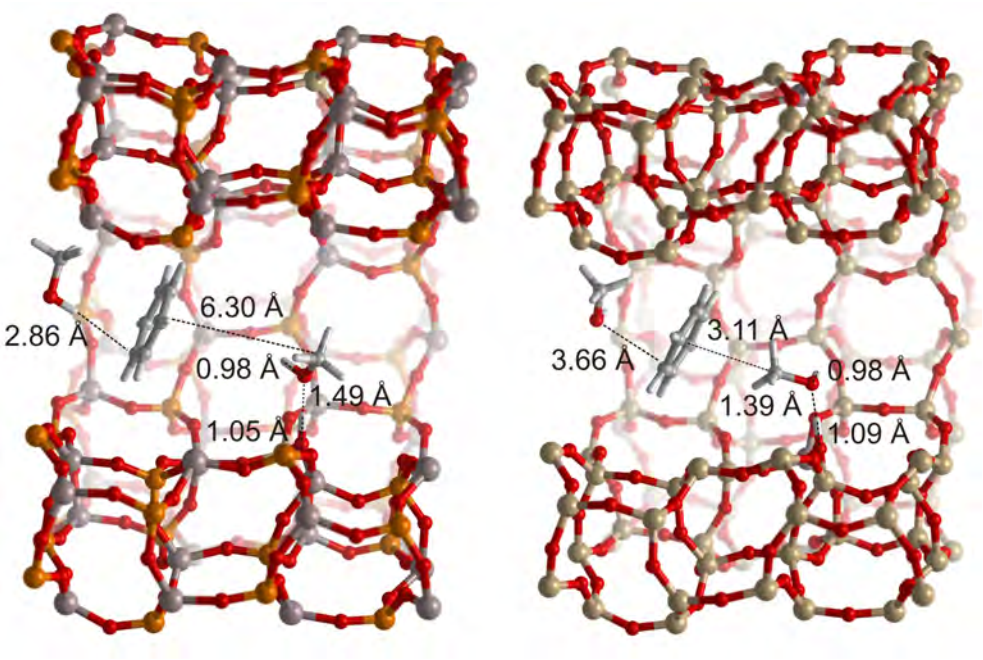

Figure 4.12: Adsorption complex of 2 methanol molecules and benzene in H-SAPO-5 (left) and H-SSZ-24 (right) shown in side view, the methanol moleculs are not allowed to interact with each other

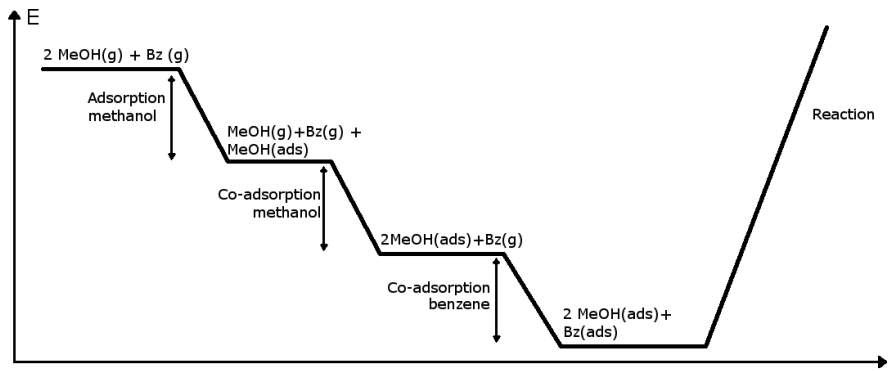

Figure 4.13: sketch of the energy profile of the different adsorption steps leading up to reaction involving 2 methanol molecules and one benzene molecule

It is remarkable that the co-adsorption energy of methanol is of the same order of magnitude as an adsorption on the acid site in the case of cluster forming. There are indeed two new hydrogen bonds formed, namely between the two methanol molecules and from the second methanol to the framework, but on the other hand one hydrogen bond from the first methanol to the framework is broken. Although the absolute numbers

for cluster formation of methanol are very similar, the relative difference between the formation of a cluster and the separation of the methanol molecules is very different. This can be seen by comparing the adsorption energies for the co-adsorption of methanol. In H-SSZ-24 the difference between these two is clearly larger. This indicates a stronger preference for cluster formation.

The adsorption energy of methanol without formation of a cluster is very similar to the adsorption of methanol on a neighbouring site. It is only a bit smaller for H-SSZ-24. They are however not bonded to the framework with any hydrogen bonds at all. This indicates that the interaction with the framework in both H-SAPO-5 and H-SSZ-24 is rather small and thus the methanol molecules will be able to move freely inside the pores of the catalyst.

For the co-adsorption of benzene the most important interactions are dispersion interactions. Therefore it is clear that there will be more interaction when benzene is placed in the middle between two methanol molecules since it is able to interact with both of them in this way. The stabilizing effect of a nearby cluster is small, but the effect of two methanol molecules surrounding benzene is 10-15 kJ/mol.

The stabilizing effect of two methanols surrounding benzene is however not as big as the stabilizing effect for the formation of a network of hydrogen bonds in a methanol cluster. The disadvantage of this methanol cluster is that it will drastically limit the freedom of the methanol molecules. This cluster formation is thus entropically disfavored, this entropic effect can be evaluated, but this is not done in this thesis. Dynamic simulations on H-ZSM-5 have shown that clusters can break and form, but in general this cluster formation is more likely to happen.[108] The weak hydrogen bond between the co-adsorbed methanol molecule and the framework will however no longer be stable at these higher temperatures.

4.6 Conclusions

The influence of the acidity on the adsorption is evaluated by comparing two AFI-structured catalysts, namely H-SAPO-5 and H-SSZ-24. Adsorption is a very important process which has to occur before the catalyzed reaction can occur. The adsorption of methanol, DME and benzene is considered by the use of static structure optimizations and energy calculations. Benzene is used to represent the active hydrocarbon pool species.

The polar molecules, DME and methanol, show a strong preference to reside on the acid site compared to a neighbouring site. This preference is even stronger in the more acidic H-SSZ-24 catalyst, which shows that this interaction increases with increasing

acid strength. Benzene showed a more moderate preference to reside on an acid site in H-SAPO-5, though a stronger preference was also observed in H-SSZ-24. There is still some interaction between the π-orbitals of benzene and the Brønsted proton, which explains this preference. The difference between polar molecules and benzene is due to the fact that for benzene the adsorption is dominated by dispersion interactions, which are influenced by the volume of the molecules and not the acid strength. For polar molecules the electronic interaction is much more important as they are able to form hydrogen bonds with the framework. These hydrogen bonds are a much stronger interaction than the relatively weak dispersion interactions.

The next step to occur before reaction is the formation of a co-adsorption complex, i.e., the second reactant will have to co-adsorb in the framework where there is already one reactant present. Co-adsorption of benzene and methanol is considered, the co-adsorption energy is stronger than the pure adsorption in both cases. The presence of another reactant has thus a stabilizing effect. The formation of a methanol dimer is investigated as well, because under industrial conditions and high partial pressure of methanol there will be multiple methanol molecules present surrounding the acid site. The co-adsorption simulations show that a methanol dimer is able to substract a proton from the catalyst, especially in HSSZ-24 and that this cluster formation is energetically favored. The pure adsorption of methanol showed a strong physisorbed methanol molecule, bonded to the framework with hydrogen bonds, but chemisorption only occurred in the presence of a second methanol molecule.

Chapter 5

Dynamic study of the paring and side-chain mechanism in H-SAPO-5

Aromatic compounds are well known to be active hydrocarbon pool species for the MTO process in certain catalysts, this was already evident from the experiment by Mole and co-workers in 1983.[38] There exist however multiple possible mechanisms with aromatic intermediates. A lot of theoretical and experimental work has been done to distinguish between these mechanisms.[23] As discussed in section 2.2 there exist three main routes, namely the side-chain mechanism, the paring mechanism starting with a ring contraction and the paring mechanism starting with a ring expansion.[50]

For large pore catalysts such as H-SAPO-5 it has been established that highly methylated benzene molecules are the most reactive aromatic species.[46] Multiple methylation steps will subsequently lead to higher substituted, more reactive methylbenzenes until eventually $heptaMB^+$ is formed. This compound forms the focus of this part of the thesis research and the reactions starting from this reactive intermediate will be investigated through advanced dynamical simulations. The first step for each mechanism will be simulated in this thesis since it is crucial to discriminate between the different mechanisms. In Figure 5.1 an overview is given of the three reactions starting from $heptaMB^+$ as studied in this thesis.

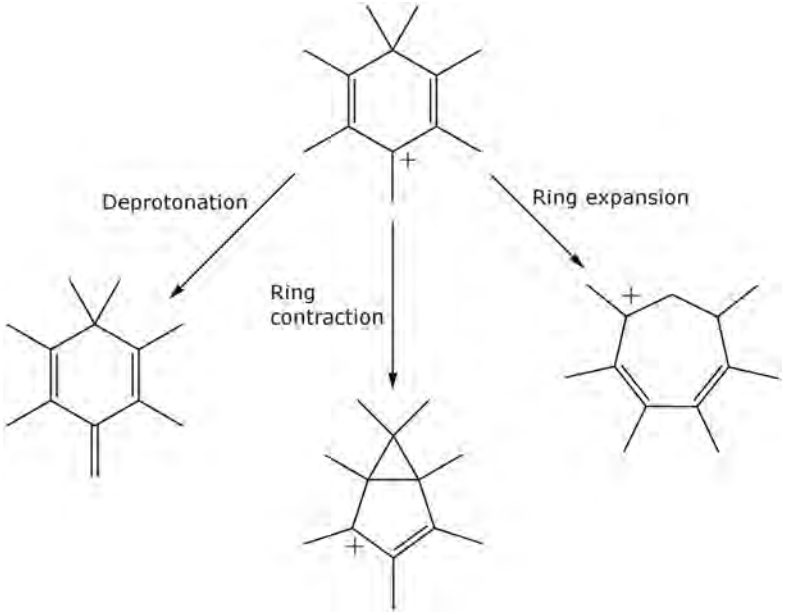

Figure 5.1: Overview of the different reactions which are simulated in this thesis

5.1 Deprotonation of the heptamethylbenzenium ion

The reaction leading up to the side chain mechanism is the deprotonation of $heptaMB^+$. This results in an aromatic ring with an exo-cyclic double bond. Further methylation occurs on this bond to form an ethyl or iso-propyl side-chain. Next, either ethylene or propylene is eliminated. This is shown in Figure 5.2.

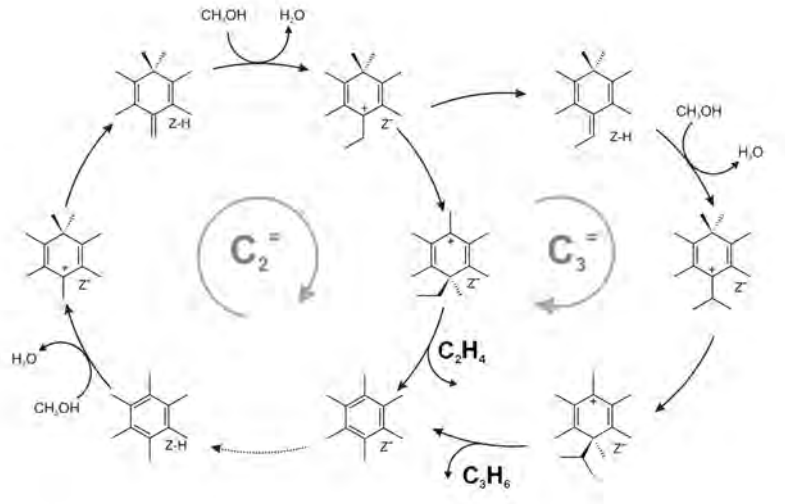

Figure 5.2: The side-chain mechanism with production of ethylene/propylene [60]

A theoretical study by De Wispelaere et al. in H-SAPO-34 has shown that a complete catalytic cycle for this mechanism with low barriers exists.[60] One of the most difficult steps in the catalytic cycle is the deprotonation of the $heptaMB^+$ ion. The problem here is mainly the fact that it is a very endothermic step, resulting in an equilibrium constant of $4.0*10^{-1}$. Hence, under equilibrium conditions, $heptaMB^+$ will rather maintain its protonated form. This result was also experimentally found by Bjørgen et al. using solid-state NMR in H-Beta.[53] H-SAPO-5 has its similarities with both catalysts, the chemical composition and the acid strength of the catalyst is very similar to H-SAPO-34 and the pore size is a bit smaller, but still similar to H-Beta. It is thus reasonable to assume that the equilibrium for this reaction will very likely favor the protonated form.

First static calculations were performed to have a clear estimate for the ΔE_r of the reaction. Finding optimized structures for both $heptaMB^+$ and 1,2,3,3,4,5-hexamethyl-6-methylene-1,4-cyclohexadiene (HMMC) proved to be difficult. Finding a stable structure for HMMC close to the acid site was not possible because there was an immediate rearrangement to form $heptaMB^+$ during the geometry optimization. Therefore, HMMC was rotated away from the acid site so that the proton transfer reaction was not possible. This was already a first indication that the equilibrium is most likely shifted towards $heptaMB^+$ In addition, there did not seem to be a large activation energy for the proton transfer from the framework to HMMC, which is the reverse reaction of the studied reaction. The calculated energy difference between the two structures is 106.4 kJ/mol. This difference suggests that the equilibrium is almost completely shifted towards the side of $heptaMB^+$. Thus, if the deprotonation step is highly endothermic, as the static calculations suggest, it will be an important bottleneck in the side chain mechanism.

5.1.1 Dynamic simulation of the reactants

Metadynamics will be used in order to achieve sufficient sampling of the reaction barrier in a reasonable timeframe. Before this can be done the system has to be equilibrated. An important decission has to be made concerning the presence of solvent molecules in the unit cell. It has been shown from ab initio molecular dynamics studies that the addition of polar protic solvents can facilitate the proton transfer.[118] In the MTO process water and methanol are readily available in the catalyst pores. These can act as a link between the framework and $heptaMB^+$ to transfer the proton. The presence of these mobile molecules has the advantage that there is no longer the need for $heptaMB^+$ to orient itself towards the acid site. More mobile molecules such as methanol and water can act as an intermediary for proton transfer between $heptaMB^+$ and the acid site.[60]

In this work the choice was made to add two methanol molecules to facilitate the proton transfer. The optimized structures of a methanol cluster in the previous chapter showed

the tendency of this dimer to substract the proton from the catalyst. The reasoning is that if two methanol molecules are able to subtract a proton from the framework they will also be likely to assist the framework with the substraction of a proton from $heptaMB^+$ thanks to their proton affinity and mobility.

A molecular dynamics simulation in the NPT ensemble is used to equilibrate the volume of the unit cell. During this period it was observed that $heptaMB^+$ is mostly located close to the acid site. Moreover, as Figure 5.3 displays, the plane of the aromatic ring is similarly oriented in the channel as benzene adsorbed on the acid site (see Section 4.3). Due to the large number of methyl groups, it is more difficult for $heptaMB^+$ to be oriented like benzene adsorbed on a neighboring site. The temperature is set at 623 K and is controlled with a CSVR thermostat with a time constant of 300 fs, the pressure is set at 1 bar and with the default time constant of 100 fs. There will be an initial period of the simulation where the different parameters have not yet converged, therefore the simulation time needs to be sufficiently long. The temperature of the simulation as a function of the time is given in appendix A (Figure A.1). This plot indicates that the first 2 ps are used to balance the system temperature and after that point an equilibrated state is obtained. The potential energy is another parameter that has to converge. This is also given in appendix A together with the conserved quantity (Figure A.2).

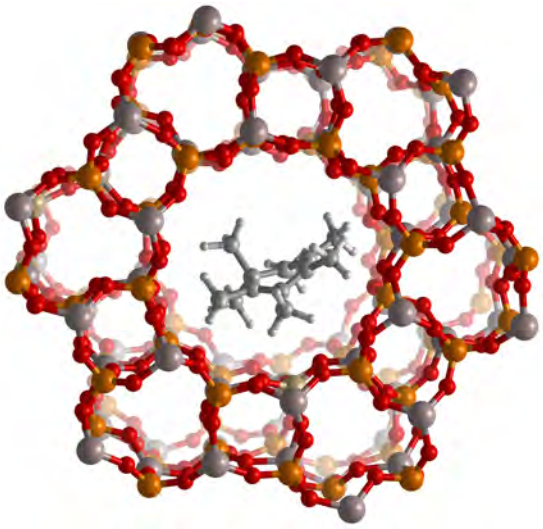

Figure 5.3: Heptamethylbenzenium inside the pores of H-SAPO-5

The conserved quantity is in theory a constant during the simulation and drift of this quantity indicates the error that is made during the simulation. Small errors such as the finite time step will lead to a drift in the conserved quantity. If the drift is small compared to the variations of the potential energy there is an acceptable level of accuracy. The drift in this simulation is an order of magnitude smaller than the variations of the

potential energy, which is acceptable.

The goal of these simulations in the NPT ensemble is to obtain a good estimate of the unit cell parameters at the operating conditions (temperature, pressure). The fluctuations of the volume are shown in appendix A (Figure A.3), the volume varies between 2800 $Å^3$ and 3000$Å^3$. In reality the system will be set at a certain pressure and the framework will be able to 'breathe' and parts of the framework will expand while others are compressed. This breathing of the framework is visible in Figure A.3. For the metadynamics simulations however we will work in the NVT-ensemble, therefore a good average volume for the unit cell is calculated from these results.

Since the first 2 ps are used to equilibrate the system these results are not used in the calculation of the average volume. The resulting average is 2914 $Å^3$. A similar averaging is done for all the cell parameters. The angles of the unit cell obtained from the simulation are very close to 90 degrees and 120 degrees. The angles for the metadynamic simulation are set at these exact values and a rescaling of the averaged cell lengths is performed to match the calculated average volume. The cell lengths which will be used for the metadynamics simulation are 14.12, 14.09 and 16.93 Å.

5.1.2 Simulation of the deprotonation reaction

To simulate the reaction metadynamics is used. Because the goal of the simulation is only to find the equilibrium thermodynamic properties of the reaction, the masses of the molecules become irrelevant in the Hamiltonian. Changing masses will only influence the dynamic behavior of the simulation, but not the underlying themodynamic properties. This means that the masses of some atoms can be varied to obtain an easier and faster simulation.[119] In particular for this simulation it can be important to change the mass of the proton which will be transfered from $heptaMB^+$ to the framework. This is because hydrogen has a very low mass and thus very little inertia. During the metadynamics simulation Gaussian hills are added which disturb the local equilibrium. Due to the low inertia of the proton it is very susceptible to these changes on the potential energy surface, which may cause the system to break.

A first simulation is performed without changing the mass of hydrogen. However after a certain time of simulation some nonphysical situations are observed. The proton suddenly breaks from $heptaMB^+$ and migrates in the voids of the catalyst pores without being bonded to anything else. It is already known that the reaction will be relatively difficult, this state of the system is thus clearly unrealistic. There are multiple options to avoid this kind of behavior. A first obvious solution is reducing the height of the Gaussian hills. This has as disadvantage that it will considerably increase the necessary time for simulation. A second option is to increase the mass of hydrogen in order to give

more inertia to this atom.

Two different simulations are performed, one where hydrogen has been given a mass of 12 g/mole and one where hydrogen has the mass of tritium, being 3 g/mole and a slightly reduced height of the Gaussian hills. There should not be a difference between both simulation for the calculation of equilibrium thermodynamics properties, but in the first simulation the mobility of hydrogen is slowed more than in the second one.

Simulation with mass_H = 12 g/mole

The first simulation was performed for 51 ps. The selected collective variable (See Figure 5.4) is a difference of coordination numbers. Namely the difference between the coordination number of the carbon atom with the weighted hydrogen (CN1) and the coordination number of this weighted hydrogen with all the possible oxygen atoms to transfer to (CN2). In particular, the two oxygen atoms of the two methanol molecules and the four oxygen atoms surrounding the silicon atom at the acid site are taken into account for CN2.

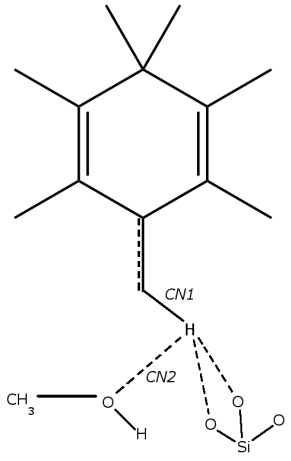

Figure 5.4: An illustration of the collective variable used to simulate the deprotonation reaction

The simulation was started with the addition of Gaussians with a hill height equal to 2.4 kJ/mol. After every recrossing of the reaction barrier the height of these hills has been halved until it reached 0.4 kJ/mol.

Multiple ways of crossing this barrier were observed during the simulation. A first

possibility is methanol which gives its proton to a second methanol molecule to which it is hydrogen bonded. A snapshot of this is shown in Figure 5.5. Initially, methanol resides close to $heptaMB^+$ interacting with the proton, but unable to substract it. It is only when the second methanol forms a hydrogen bridge with the first one that it is able to stabilize the positive charge enough for the transfer to occur. The proton affinity of a single unbonded methanol molecule is clearly much lower than when it is hydrogen bonded with the second methanol molecule, which is in line with previous work in H-ZSM-5, where it was concluded that larger methanol clusters have a higher probability of substracting a proton.[108]

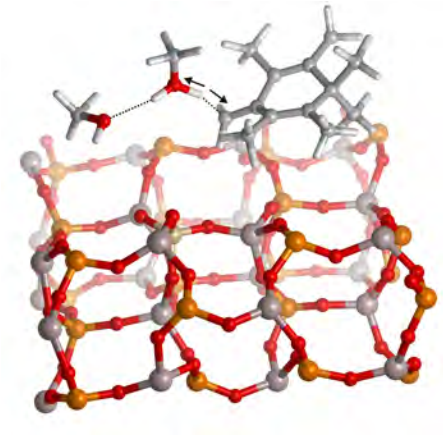

Figure 5.5: A proton of $heptaMB^+$ is transferred to a cluster of methanol molecules

A second way of transferring the proton is when methanol interacts with both the acid site and $heptaMB^+$ at the same time. The proton is then able to transfer from $heptaMB^+$ to methanol while simultaneously the proton which was originally located on methanol is transferred to the acid site. In Figure 5.6 the reaction is shown. Methanol is essentially being used as intermediary for the proton transfer between the hydrocarbon and the framework.

Other options for proton transfer would be the direct transfer from $heptaMB^+$ to the acid site or transfer to a single isolated methanol molecule. These possibilities were not observed during the simulation and are probably highly activated. The direct transfer from $heptaMB^+$ to the catalyst is hampered due to the fact that a bulky molecule such as $heptaMB^+$ would have to be rotated to the exact angle where it has the possibility to transfer its proton. Protic solvents are readily available during the MTO process and provide much easier access to the acid site. The transfer to a single methanol molecule is a similar discussion as in the previous chapter concerning the adsorption of a single methanol molecule. Methanol on its own has a too low proton affinity to be a very stable molecule when it is protonated.

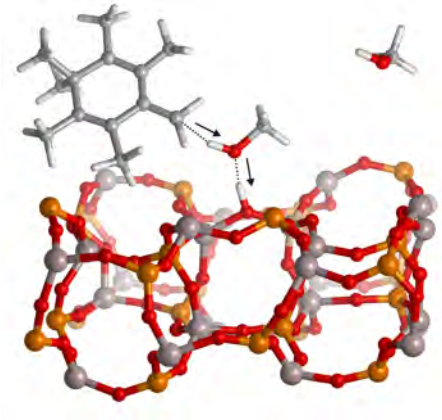

Figure 5.6: A proton of $heptaMB^+$ is transferred to methanol, which transfers its own proton to the acid site

The free energy profile that was calculated for the deprotonation of $heptaMB^+$ is shown in Figure 5.7. There are obviously still some rough bumps in the profile which indicate that further simulation of the system is necessary. The results are however good enough to get an idea of the probability for this reaction to occur.

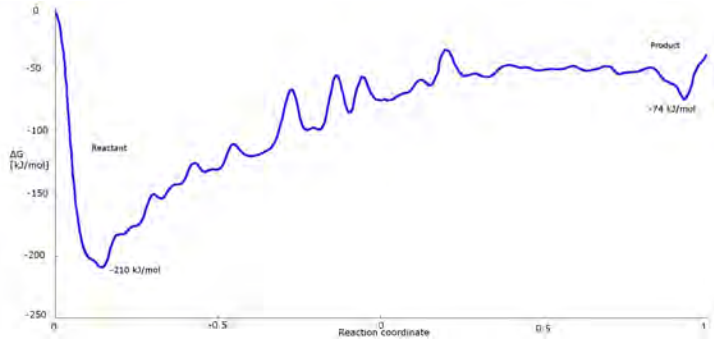

Figure 5.7: The calculated free energy profile for the deprotonation of $heptaMB^+$

Another remarkable element of the profile is the shape. Although the shape of the reaction profile is dependent on the chosen reaction coordinate it is clear that there is a large reactant valley for the system while the product valley is very small. The transition state is clearly very similar to the product state. This was also visible without this profile when looking at the simulation itself. There are many instances where methanol is located very close to $heptaMB^+$, but the carbon-hydrogen bond length would remain very stable and the simulation fell frequently back into the reactant state. This is in line with Hammond's postulate, which states that if the transition state and another state of the reaction are very similar to each other in terms of energy, they will also have a

similar structure.[120] This is often represented by Figure 5.8 and referred to as a late or early transition state. One can see that when the energy of the transition state is close to that of the reactant state it will also be very close to this state on the reaction coordinate, which is called an early transition state. Highly endothermic reactions, such as this deprotonation reaction, often have a late transition state.

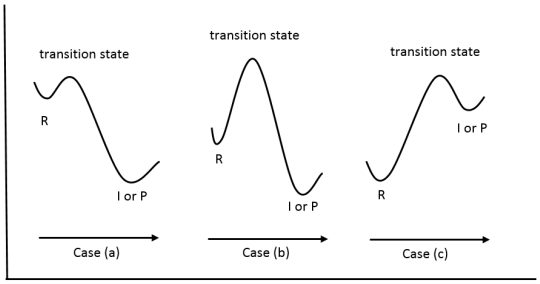

Figure 5.8: Representation of Hammond's postulate

Due to the fact that in metadynamics there is not a single point that can be denoted as saddle point (a point with one single negative frequency), there is also no exact point which can be refered to as the transition state. Therefore a certain interval of the reaction coordinate should be defined as the transition state. In this case, due to the late transition state, the transition state region was chosen as the ensemble of states where the collective variable is 0.4. The effect of this choice was evaluated by varying the position between 0.35 and 0.45. However, the resulting variance was only 5 kJ/mol and hence, did not lead to a significantly different free energy barrier. The calculated reaction barrier at 623 K for the forward reaction is 177.9 kJ/mol and for the reverse reaction it is 41.8 kJ/mol. This leads to a forward reaction rate constant of $1.6 \times 10^{-2} s^{-1}$ and a backward reaction rate constant of $4.1 \times 10^{9} s^{-1}$. The obtained reaction barrier is much higher than the one obtained in H-SAPO-34 in a previous study.[60] This can be due to multiple effects, obviously the catalyst is different but another reason for this difference could be that metadynamics is used in this work, while static ONIOM calculations were used in the previous study. Static calculations do not take the entropic contributions fully into account. The difference in DFT functional or a not fully converged metadynamics simulation are other possible explanations. The most probable reason is that the different catalyst topology leads to an inferior stabilization and thus a higher activated reaction.

Simulation with mass_H = 3 g/mol

In the second case hydrogen was simulated with a fictive mass of 3 g/mol. The mass is not increased as much as before to remain closer to the real case, even when in theory

there should be no difference in the static thermodynamic properties. The height of the hills that were added at the start of the reaction are 2 kJ/mol. Such low gaussians are needed to ensure that the dynamics of the sytem are not disturbed too much. Hydrogen has a very low inertia and is therefore very susceptible to these sudden addition of forces. Additionally, the CV used in this simulation is the difference of the CN of the carbon atom and the weighted hydrogen and the CN of this weighted hydrogen and the oxygen atom of one specific methanol molecule, shown respectively as CN1 and CN2 in Figure 5.9. The other oxygens atoms were no longer taken into account because there exist states where the proton of methanol and $heptaMB^+$ are swapped and it would be very hard to return to the product state starting from there. The CV used in the previous simulation would then reach high values and the simulation would be stuck in the product side.

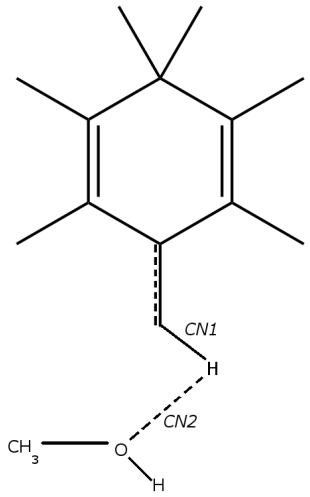

Figure 5.9: The choice of CV for the deprotonation of heptamethylbenzenium, considering only one oxygen atom of a specific methanol molecule

The system has been simulated for 35 ps and the obtained reaction profile is shown in Figure 5.10 together with the reaction profile obtained in the previous section.

The transition state was again taken at 0.4 as the profile is very similar to the simulation in the previous section. The obtained barrier for this simulation is 166.6 kJ/mol, which is slightly lower than the previous barrier. The barrier for the reverse reaction is 62.8 kJ/mol which is significantly higher than the 41.8 kJ/mol which was calculated before. This was already visible in Figure 5.10, in this second simulation the product state has been simulated a lot more. This could indicate that the previous simulation had not fully converged, which is also visible in the much rougher reaction profile obtained from that

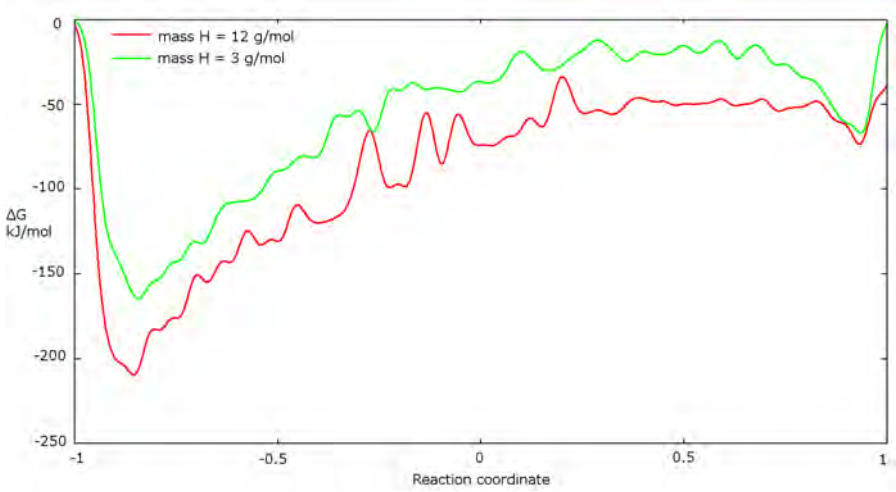

Figure 5.10: The reaction profiles for the deprotonation of heptamethylbenzenium of both simulation compared with each other, in green the simulation with $m_H = 3$ g/mol and the red curve is for the simulation with $m_H = 12$ g/mol.

simulation. Another reason for the difference in the product state for these simulations is the difference of CV. The first simulation also took the distance to the other oxygen atoms into account. Therefore it actually allowed the CV to reach higher values than 1, in the second simulation this was changed because it resulted in the simulation of states which were not of interest for this thesis. When only a single oxygen atom is part of the CV the analysis is more straightforward. In Figure 5.10 it is also visible that for the first simulation there are states where the CV reaches a value larger than 1, while this is not possible in the second simulation. The reason for the difference is thus not the difference in simulated mass of the proton, but the convergence of the simulation and more importantly the slightly different CV. This CV is only different for the product side of the simulation, as can be seen from Figure 5.10 the reactant side of the profile and the free energy barriers are similar in both simulations. These simulations result in a reaction rate constant for the forward reaction of $1.4 \times 10^{-2} s^{-1}$ and a reaction rate constant for the backwards reaction of $7.0 \times 10^{7} s^{-1}$. The equilibrium constant of the reaction K_{eq} is 2.0×10^{-9}.

From the static energy calculations we obtained an energy difference of 106.4 kJ/mol between both states. The dynamic simulation, where only a single methanol molecule was part of the CV, resulted in a free energy difference of 103.8 kJ/mol. All together, the simulation with a single methanol molecule in the CV has converged better as shown by the smoother reaction profile and the better resemblance with the static energy optimizations. The results of this simulation are therefore considered to be more accurate.

5.2 Ring contraction of heptamethylbenzenium

For the ring contraction mechanism there are two steps that prove to be difficult, namely the ring contraction and later in the mechanism the regeneration of the six-membered ring. Due to time limits there are only a few steps of the mechanism that can be investigated into more detail. The choice for this work is to start again from $heptaMB^+$ and investigate the ring contraction towards the bicyclic structure, which is shown in Figure 5.11.

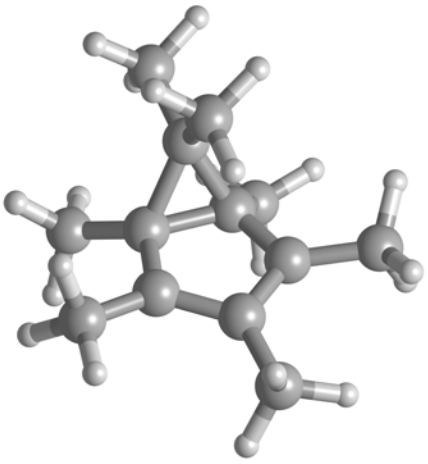

Figure 5.11: The bicyclic structure, which is the the result of a ringcontraction of $heptaMB^+$

Static calculations showed that the bicyclic structure is less stable, the ΔE_r is 13.6 kJ/mole. This is a smaller ΔE_r than obtained in a previous study in H-ZSM-5, but the number of methyl substituents on the benzene ring was lower in that work as well.[61] This is very different to the deprotonation where the product state was heavily disfavored compared to the reactant. This static energy difference does however not give us information about the free energy barrier at 623 K. Therefore, metadynamics will be applied.

5.2.1 Dynamic simulation of the reactant

The ring contraction reaction involves the breaking and formation of several strong C-C bonds. Therefore it is reasonable to assume that the free energy barrier will be substantial. It will be necessary to perform metadynamics simulations if one wants to sample enough transitions of the reaction barrier. A similar procedure as for the simulation of the deprotonation is applied. The first step is to determine the parameters of the unit cell. The system has to be equilibrated to fit the framework and $heptaMB^+$

at a temperature of 623 K. A simulation in the NPT ensemble with a pressure of 1 bar controlled by a barostat with a time constant of 100 fs is performed. The orientation of the $heptaMB^+$, close to the acid site, is mostly similar to the orientation observed for benzene adsorbing on the acid site as discussed in Section 4.3. The temperature is being controlled by a CSVR with a time constant of 300 fs. The volume is expected to be very similar to the one obtained for the deprotonation reaction, because the only difference is that there is no methanol present this time, but the small volume of these molecules should not have a large influence.

The temperature of the system is one of the important characteristics of the system which indicates the convergence of the simulation. The results are shown in appendix A (Figure A.4). After about 2500 fs the temperature of the simulation reaches an equilibrium state, fluctuating around 623 K. The next parameter to evaluate is the potential energy of the system. This one is illustrated in combination with the conserved quantity of the system in appendix A (Figure A.5). The potential energy is also converged after about 2500 fs which is similar to the temperature.

The conserved quantity of the system is rising during the simulation, but as discussed before the 'drift' of this quantity is small compared to the fluctuations in the potential energy. The error is sufficiently small to obtain an accurate simulation.

After checking the convergence of the cell parameters an average of 2913 $Å^3$ was obtained for the volume, which is only slightly smaller than the unit cell which contains the additional two methanol molecules. The cell vectors are again rescaled similar to what was explained in the section about the deprotonation because the cell angles are set at the exact value of 90, 90 and 120 degrees. The cell lengths which will be used for the metadynamics simulation are 14.12, 14.09 and 16.93 Å.

5.2.2 Simulation of the ring contraction

The collective variable that was chosen for this reaction is the coordination number between the two carbon atoms that have to form a bond in order to obtain the bicyclic structure, carbon atoms number 2 and 6 in Figure 5.12. An overview of the reactant and the different product states is shown in Figure 5.13. There are two main product states, one with a bicyclic structure and one with a isopropyl side-chain. The simulation started with the addition of hills with a height of 5 kJ/mol and the height was subsequently halved after every recrossing of the reaction barrier, at the end of the simulation the height of the hills was 1.3 kJ/mol.

A first set of simulations without any further constraints showed that the formation of this iso-propyl group occured relatively easily. It also showed that this iso-propyl group is very mobile and performs a 'ring walk' on the five equivalent positions of the

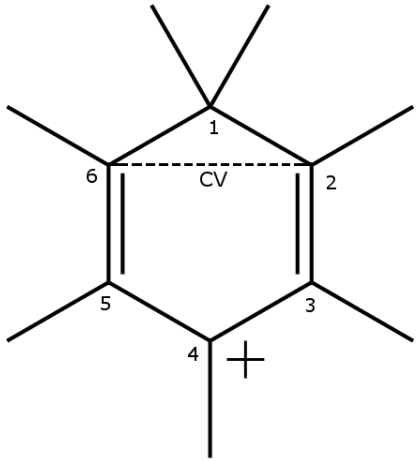

Figure 5.12: Overview of the collective variable for the simulation of the ring contraction

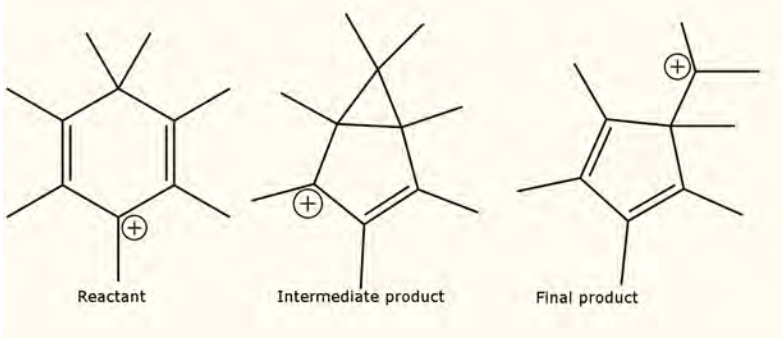

Figure 5.13: Overview of the reactant and product states of the ring contraction

five-membered ring (see Figure 5.14). This means that it forms and breaks bonds with the different carbon atoms of the ring and is able to migrate from one carbon atom to the next one. This phenomenon has been described before by Arstad et al. They found a low reaction barier for this migration of the isopropyl side-chain.[50] This ring walk was not included in the collective variables, but the fact that it is visible during the simulation further suggests the low barrier for this reaction. This indicates that the iso-propyl group is not bonded very strongly to the ring and that probably elimination reactions from this state can occur easily.

Even though this ring walk is very interesting to observe, it made the side-chain migrate towards a position from where reaction with the defined collective variables was not possible. This is because the collective variables only include two specific carbon

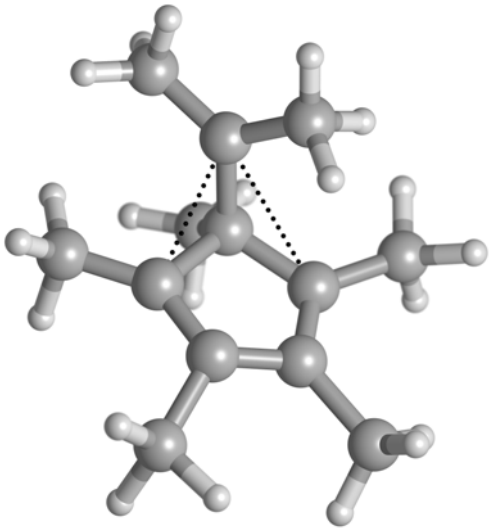

Figure 5.14: Illustration of the bonds forming and breaking during the ring walk of the iso-propyl side-chain

atoms. However the structure is identical after the transfer of the isopropyl chain to the next carbon atom and reaction should be equally likely from this position. Therefore, additional walls were placed to ensure that the side chain group was always in a position from where the reverse reaction is possible without restricting it to form the iso-propyl group. A repulsive wall was placed between the carbon atom with number 1 and the carbon atoms with numbers 3,4 and 5, the ring walk is thus no longer possible. A bond with one of these atoms is not wanted, the quadratic wall with a force constant of 650 MJ/mol will ensure that the side-chain remains bonded to one of the original two carbon atoms.

Due to the structural change it is difficult to sample transitions between reactant and product. Not only is there the formation of the C-C bond described by the collective variable, but during the transition there is also a change in the dihedral angle of carbon atoms 1,2,3 and 4 in Figure 5.12. A lot of atoms will have to move at the same time for the reaction to occur. Furthermore, when the simulated molecule is in the intermediate bicyclic product state it has the possibility to form the isopropyl side-chain. From this state there is no direct route back to the product. The consequence is that crossing of the reaction barrier occurs less frequently than expected. The system has been simulated for 80 ps, but only a limited number of crossings of the reaction barrier had occurred (there was only five times a crossing of the barrier). The reaction profile of the final three runs is shown in Figure 5.15. Every run represents a simulation time of 20 ps, but it is clear that the simulation did not yet converge because the profile still changes a lot.

The reason for this is that the simulation gets stuck in certain states and is not able to recross the barrier even when the local minimum is being filled.

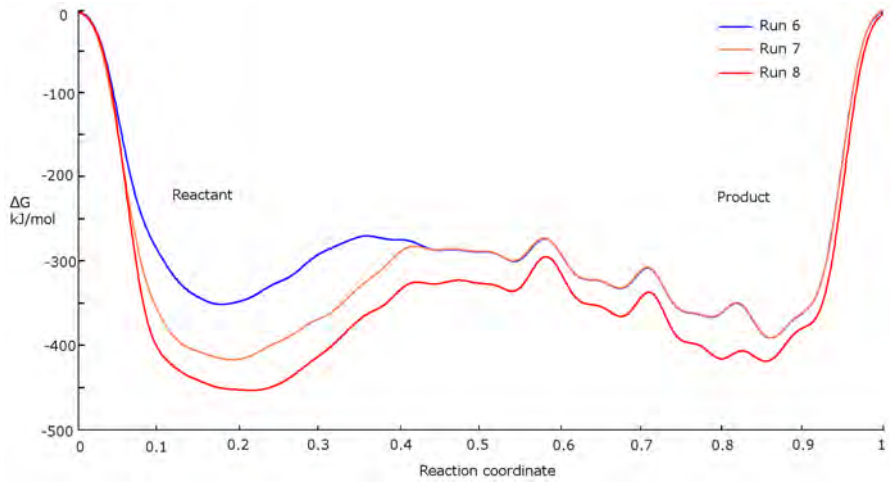

Figure 5.15: The reaction profile of the ring contraction for the final three runs

Clearly, run 6 is very different from the final two runs and this is also notable in the resulting free energy barriers. For run 6 the calculated barrier is 96.5 kJ/mol, for run 7 it is 146.8 kJ/mol and for run 8 it is 141.1 kJ/mol. Though the final two results are very similar they were calculated from a simulation that had not yet fully converged. They are however also very similar to previously reported results by Arstad et al. who reported a reaction barrier of 139 kJ/mol.[50] The free energy barriers at 623 K for the reverse reaction are 132.5 kJ/mol for run 6, 116.3 kJ/mol for run 7 and 104.3 kJ/mol for run 8. Run 8 is chosen as the most accurate description, because it is the one that has run the longest and has converged best. The obtained reaction rate constant for the forward reaction is $1.9 \times 10^{1} s^{-1}$ and a reaction rate constant for the backwards reaction of $2.3 \times 10^{4} s^{-1}$. This results in an equilibrium constant K_{eq} of 8.2×10^{-4}. The difficulties arising in this simulation can not be solved by simulating longer. A better approach would be to take a second collective variable into account. As discussed there are two product states, an intermediate one where there is a bicyclic structure and one with a isopropyl side-chain (see Figure 5.13). The reaction is also not only characterized by the change in bond length described by the current collective variable but also by a change in the dihedral angle. This dihedral angle is however not fixed in the product state. When the isopropyl side-chain is formed, the dihedral angle is allowed to vary within a large range.

There are two suggestions for a second collective variable, the first one involves the dihedral angle which changes during the actual reaction and the second one is to take the C-C bonds for the product state into account in order to distinguish between the two

different product states. In this one dimensional simulation it is impossible to determine if the bicyclic structure is certainly a minimum. The static optimizations were able to find this minimum and during the simulation the system stays in this state for a long time, but only by adding a second collective variable it would be possible to be certain.

The dihedral angle of carbon atoms with numbers 1,2,3 and 4 from Figure 5.12 is chosen as a second CV the expected two dimensional potential energy surface is shown in Figure 5.16. In the product state the dihedral angle is fixed at 0 degrees, when reaction occurs carbon atom number 1 will leave the plane of the cyclic structure and the dihedral angle will have a fixed value for the bicyclic product state. If the bicyclic structure is broken and the isopropyl side-chain is formed the dihedral angle is allowed to vary to a larger extend. The reaction is thus described as a two step mechanism and the product states differ in their ability to change the dihedral angle. An angle is however not very easy to use for practical purposes.

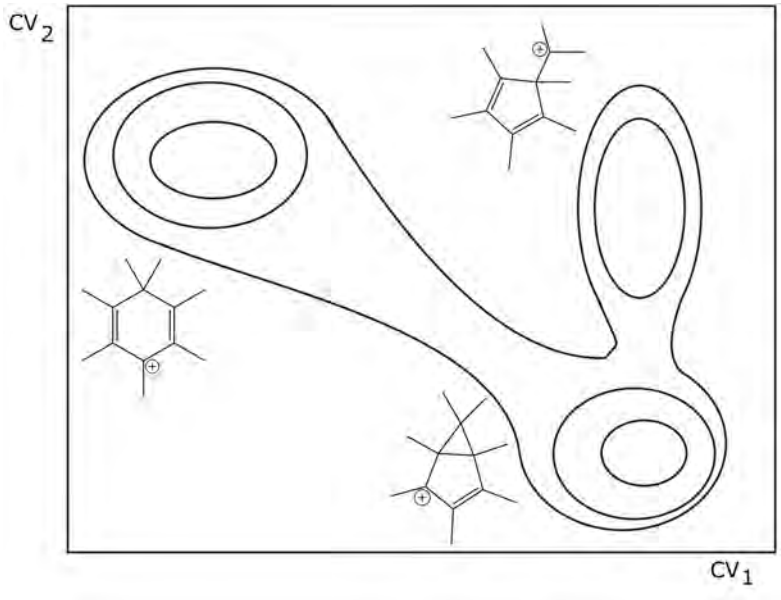

Figure 5.16: The expected two dimensional potential energy surface for the ring contraction with the dihedral angle as CV_2 and the original difference of coordination numbers as CV_1

The second option is to distinguish clearly between the two product states. To do this the CN between the double substituted carbon atom and its two neighbouring carbon ring atoms is used. One of theses bonds is only broken in case an isopropyl side-chain is formed. In Figure 5.17 the expected potential energy surface is shown. The addition of this second CV will aid to make the system change between both product states, this is necessary because the reverse reaction can only occur starting from the bicyclic

structure.

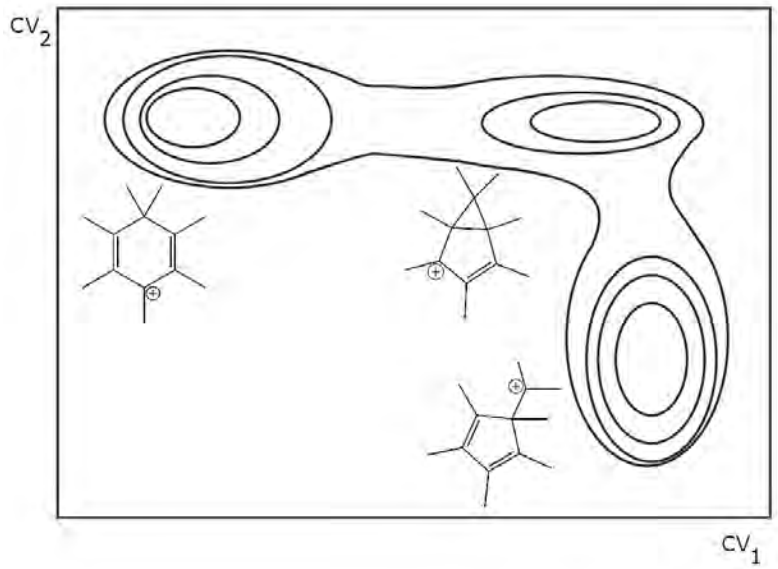

Figure 5.17: The expected two dimensional potential energy surface for the ring contraction with the new CN which describes the breaking of the bicyclic structure as CV_2 and the original difference of coordination numbers as CV_1

5.3 Ring expansion of heptamethylbenzenium

The final reaction that was investigated is the ring expansion of $heptaMB^+$. The ring expansion mechanism has received less attention in literature compared to the previously discussed mechanisms. Arstad et al. reported that in the full catalytic cycle the elimination of the products is the bottleneck, closely followed by the expansion of the six-membered ring structure to the seven-membered ring.[50] They reported a barrier of 231 kJ/mol for the latter reaction and a ΔE_r of 64 kJ/mol in the gas phase. This is the reaction that is studied in this thesis and depicted in Figure 5.18.

This is a complex reaction, it involves a proton transfer from one of the gem-methylated groups to a carbon atom in beta position and simultaneously the breaking of a carbon-carbon bond and the formation of another one (see Figure 5.18) In Figure 5.19 the product is shown after a static optimization on H-SAPO-5. It is a very large compound, but the pores of H-SAPO-5 provide enough free space.

A static optimization of the reactant and product side for this reaction in H-SAPO-5 leads to a ΔE_r of 65 kJ/mol, which is very close to the results reported by Arstad et al. of 64 kJ/mol in gas phase.[50] Seemingly there is almost no influence of the catalyst

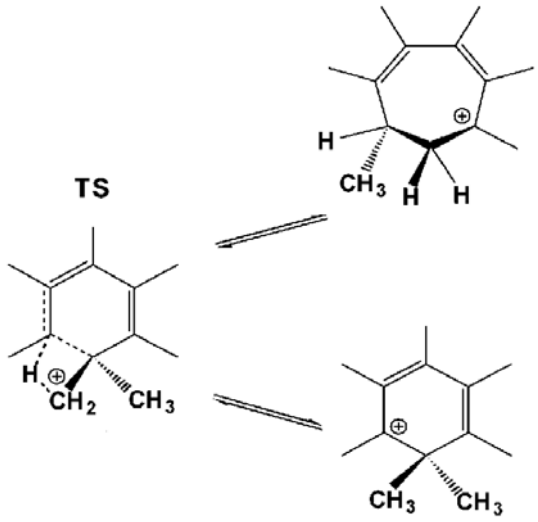

Figure 5.18: The ring expansion of $heptaMB^+$ [50]

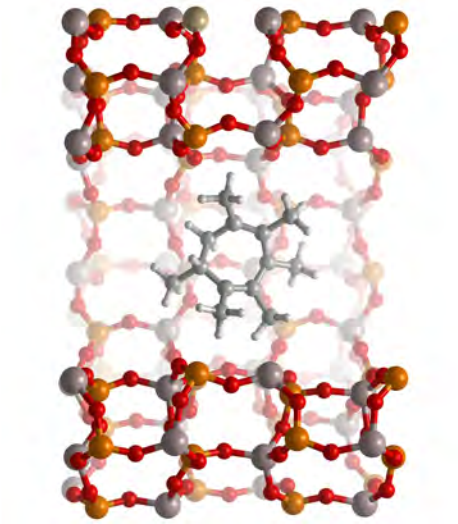

Figure 5.19: The methylated cycloheptatriene structure which is the product of a ring expansion of $heptaMB^+$ on H-SAPO-5

surroundings on the stability of the reactant and product. This shows already that in equilibrium conditions this product will be disfavored compared to both the reactant and the product of the ring contraction (which has a ΔE_r of 14 kJ/mol). Nonetheless this reaction is simulated because the large pores of H-SAPO-5 seems to be an optimal environment for this reaction, if it is not feasible in this catalyst it will most likely be even more difficult in catalysts with smaller pores.

5.3.1 Dynamic simulation of the ring expansion

The same starting structure for the simulation was used as for the ring contraction reaction. All parameters are identical except for the collective variables of course. A first simulation which tried to describe this system with only a single CV led to multiple errors. Due to the complexity of the reaction it is necessary to take multiple effects into account. The two CVs which are used for the simulation are shown in Figure 5.20. The proton transfer and the breaking of the carbon-carbon bond are described by two separate collective variables. The bond which will have to be formed to achieve the seven-membered ring is not taken into account in the collective variables, because it is assumed that the distribution of charges will drive the simulation towards this bond naturally.

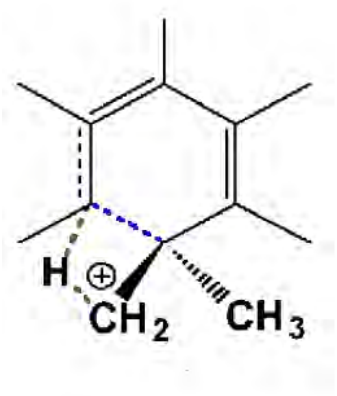

Figure 5.20: The two CVs used to simulate the ring expansion mechanism, the proton transfer is described by the green CV and the breaking of the carbon-carbon bond is described by the blue CV

Unfortunately during the simulation the desired reaction is not observed. Instead a five-membered ring structure is formed. In this product the carbon-carbon bond described by the collective variables is able to break and form thanks to the ability of the side-chain to perform a ring-walk. Clearly it is necessary to take more effects into account. Additional walls can be implemented with a limited computational cost, these walls can ensure that a ring contraction is no longer possible. Furthermore, it might be necessary to take the bond which will have to be formed into account as well. This will lead to a three dimensional simulation which is computationally less efficient and also less easy to analyze and interpret.

Although we could not yet obtain the free energy barriers for the ring expansion, the results of Arstad et al. and the static optimizations strongly indicate that this reaction is less likely to happen compared to the ring contraction.[50] Both reactions involve a large

rearrangement of atoms, but the product of the ring expansion is thermodynamically disfavored and there are strong indications that the reaction barrier will be higher as well.

5.4 Conclusions

In this chapter a critical step in the ring contraction, ring expansion and side-chain mechanism has been evaluated using advanced molecular dynamics simulations. The reactions all started from the heptamethylbenzenium ion, which is the most reactive methylbenzene in large pore catalysts such as H-SAPO-5. The three reactions are always just a single step in their respective mechanisms, but they have proven to be important bottlenecks in the full catalytic cycle in other catalysts, which is especially true for the deprotonation reaction.

Frequent sampling of the reaction at 623 K has been obtained by using metadynamics to achieve a more efficient sampling of the potential energy surface. It has proven to be a powerful tool to incorporate different reaction paths in one simulation as could be seen in the simulation of the deprotonation. There exist multiple paths leading from reactant to product state and molecular dynamics are not limited to the choice of one specific path. The free energy barriers which were obtained in this thesis work showed a slight preference for the ring contraction paring mechanism and especially the equilibrium coefficient was more beneficial for this mechanism. The tentative results are summarized in Table 5.1. These conclusions are in line with experimental results where labeling patterns predicted a paring mechanism to be the dominant pathway for olefin elimination in H-SAPO-5.[116]

Table 5.1: Summary of the results for the deprotonation and ring contraction reaction of $heptaMB^+$ at 623 K in H-SAPO-5. The free energy barrier ($\Delta G^{\ddagger}$ in kJ/mol), the reaction rate constant (k in s^{-1}) and the equilibrium constant (K_{eq}) are given.

		$\Delta G^{\ddagger}$ [kJ/mol]	k [s^{-1}]	K_{eq}
deprotonation	forward	166.6	1.4×10^{-1}	2.0×10^{-09}
	backward	62.8	7.0×10^{7}	
ring contraction	forward	141.1	1.9×10^{1}	8.2×10^{-4}
	backward	104.3	2.3×10^{4}	

Chapter 6

Conclusions

Figuring out the mechanism of the methanol conversion has proved to be very difficult due to the complexity of the MTO process. Insight into this process on the molecular scale can lead to industrial optimizations and is thus very interesting. A lot of theoretical and experimental work has been performed in this area. Thanks to experimental evidence, the hydrocarbon pool mechanism is commonly accepted as the active mechanism. Herein, hydrocarbon compounds act as co-catalysts for the process. There are two main categories of active hydrocarbon pool species, namely the alkenes and arenes. Methanol will be added onto these hydrocarbon pool species to form larger compounds. Eventually olefins will be eliminated from these larger compounds.

The catalytic cycles with alkenes and arenes as co-catalyst can work independently from each other, but they are connected by secondary reactions such as cyclization and deprotonation. This concept is called the dual-cycle concept. The relative importance of these cycles is dependent on many parameters such as the catalyst topology, catalyst acidity, reaction temperature, pressure, pore size, etc. All these factors further complicate the search for details on the true reaction mechanism. The paring and side-chain mechanism are two proposed mechanisms to describe the olefin production with aromatic compounds as co-catalyst. Methylations are important in both cycles, the difference between both mechanisms lies in the exact mechanism for the elimination of the products.

In a first part of this thesis the influence of the acidity on the adsorption is evaluated by comparing two AFI-structured catalysts, namely H-SAPO-5 and H-SSZ-24. Adsorption is a very important process which has to occur before the catalyzed reaction can occur. The adsorption of methanol, DME and benzene is considered. Benzene is used to represent the active hydrocarbon pool species. The polar molecules, DME and methanol, show a strong preference to reside on the acid site compared to a neighbouring site. This preference is even stronger in the more acidic H-SSZ-24 catalyst, which shows that this interaction increases with increasing acid strength. Benzene showed a more moderate

preference to reside on an acid site, though a stronger preference was also observed for H-SSZ-24. This difference between polar molecules and benzene is due to the fact that for benzene the adsorption is dominated by dispersion interactions, which are influenced by the volume of the molecules and not the acid strength. For polar molecules the electronic interaction is much more important as they are able to form hydrogen bonds with the framework. These hydrogen bonds are a much stronger interaction than the relatively weak dispersion interactions.

The next step to occur before reaction is the formation of a co-adsorption complex, i.e., the second reactant will have to co-adsorb in the framework where there is already one reactant present. Co-adsorption of benzene and methanol is considered, the co-adsorption energy is stronger than the pure adsorption in both cases. The presence of another reactant has thus a stabilizing effect. The formation of a methanol dimer is investigated as well, because under industrial conditions and high partial pressure of methanol there will be multiple methanol molecules present surrounding the acid site. These dimers have a higher tendency to substract a proton from the framework, a methanol dimer has a higher proton affinity than a single methanol molecule. A methanol dimer is able to form a network of hydrogen bonds and results in a very strong interaction energy.

In a second part of this thesis , the first step of three possible reaction mechanisms involving aromatic hydrocarbon pool species in H-SAPO-5 is studied. Namely, the side-chain mechanism, the paring mechanism starting with a ring contraction and the paring mechanism starting with a ring expansion are compared. Therefore, the first step of these three mechanisms is evaluated using advanced molecular dynamics methods. The first step is of course crucial in each mechanism and can indicate a difference between the possible mechanisms without simulating the entire catalytic cycles. The heptamethylbenzenium ion was chosen as starting compound, because it has been shown before that heavily methylated methylbenzenes are the most reactive aromatic compounds in large pore catalysts. The side-chain mechanism starts with a deprotonation step, leading to an exo-cyclic double bond. At 623 K the free energy barrier for this reaction is 166 kJ/mol and the K_{eq} is 2.0 $\times 10^{-9}$. The ring contraction reaction has a barrier of 141 kJ/mol and a K_{eq} of 8.2 $\times 10^{-4}$. Unfortunately a suboptimal choice of the collective variable for the ring expansion mechanism made it impossible to obtain results for this reaction. Optimization of static points indicated however that this reaction would most likely be disfavored compared to the ring contraction mechanism. When comparing these first steps of the different mechanisms the ring contraction is the most promising. It is the reaction with the lowest reaction barrier and furthermore the K_{eq} is much more favorable for this reaction. These results are in accordance with previously reported results obtained from gas phase calculations.[50]

Previous work in H-ZSM-5 and H-SAPO-34 has shown that the deprotonation reaction is the bottleneck for the side-chain mechanism. Therefore it seems evident that it will also be a bottleneck in H-SAPO-5. For the ring contraction mechanism the bottleneck in H-ZSM-5 is the recovering of the six-membered ring structure. The ring contraction itself has a comparable reaction barrier, it is only slightly lower. It might thus be interesting for future research to also investigate this recovery of the six membered ring to see if the same conclusions still hold. Ideally the full catalytic cycle is considered, however simulation of some key steps can already provide a lot of insight to compare the different cycles. The ring expansion itself seemed less promising from static calculations, but a dynamic simulation of this reaction could provide certainty about the importance of this mechanism.

Next to the arene cycle there is also the alkene cycle according to the dual-cycle concept. Experimental results indicate that this cycle is more important in H-SAPO-5 than in H-SSZ-24. The influence of the acidity on the different reaction mechanisms is still to be investigated. Similar dynamic simulations in H-SSZ-24 can provide insight into the influence of the acidity and can hopefully complement the experimental results. There are still a lot of uncertainties in the MTO process, a combination of experimental and theoretical work will be necessary to further unravel the underlying mechanism.

Appendix A

Supporting information dynamical simulations

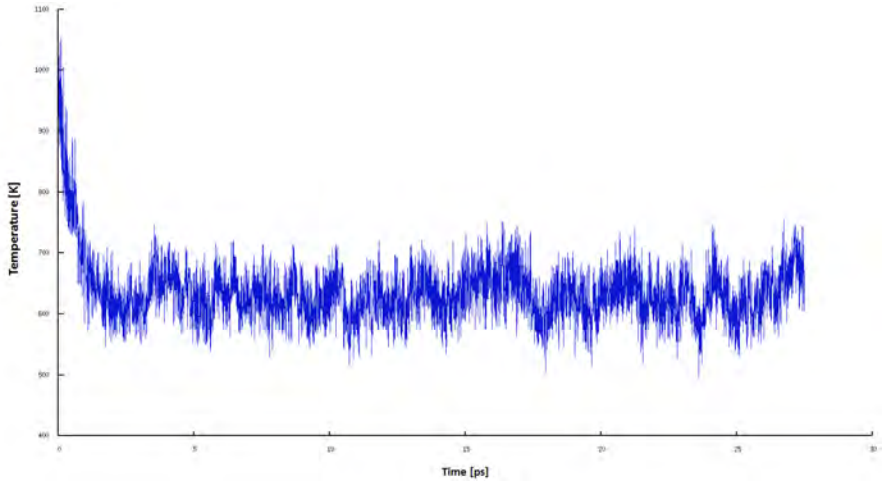

Figure A.1: The temperature as a function of simulation time in the NPT ensemble

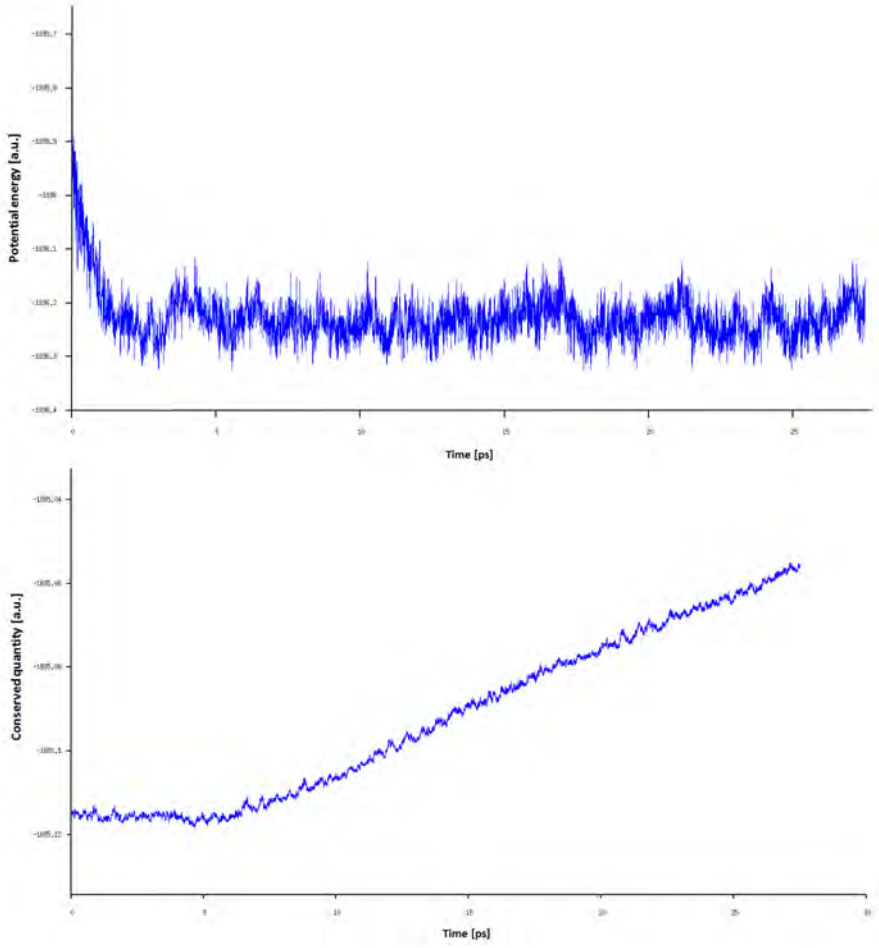

Figure A.2: The potential energy and conserved quantity of the system as a function of simulation time in the NPT ensemble

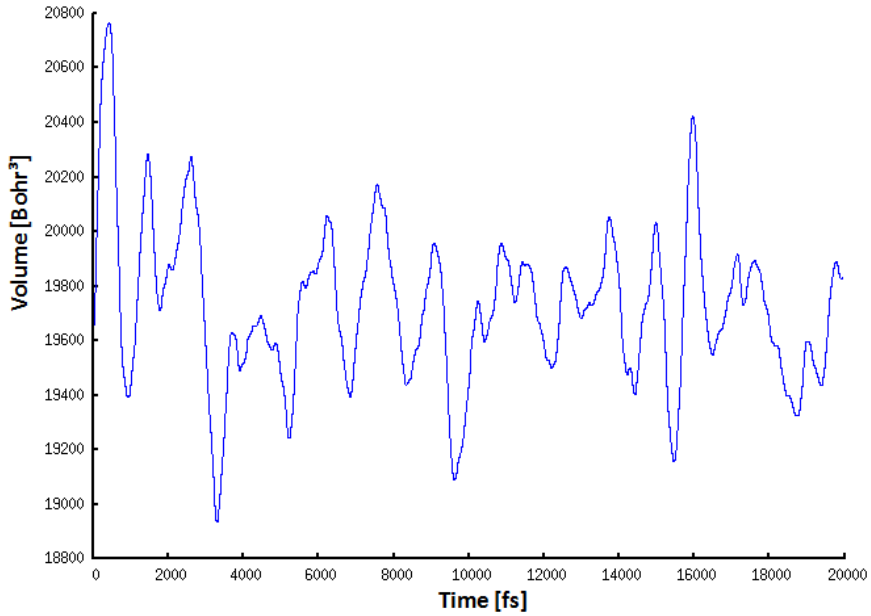

Figure A.3: The volume of the unit cell as a function of simulation time in the NPT ensemble

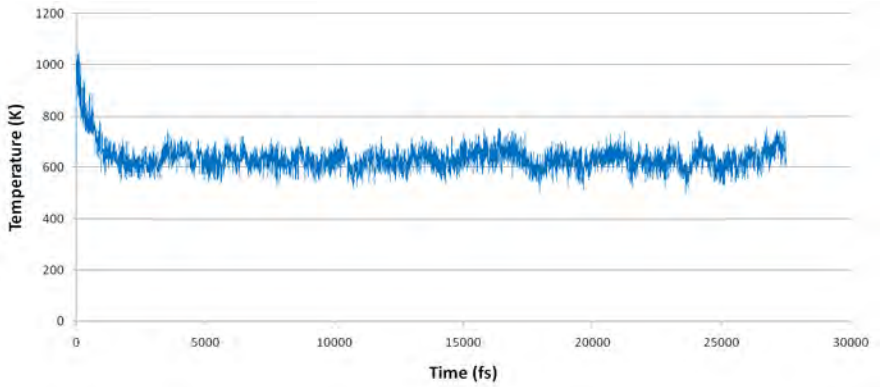

Figure A.4: The temperature as a function of simulation time in the NPT ensemble

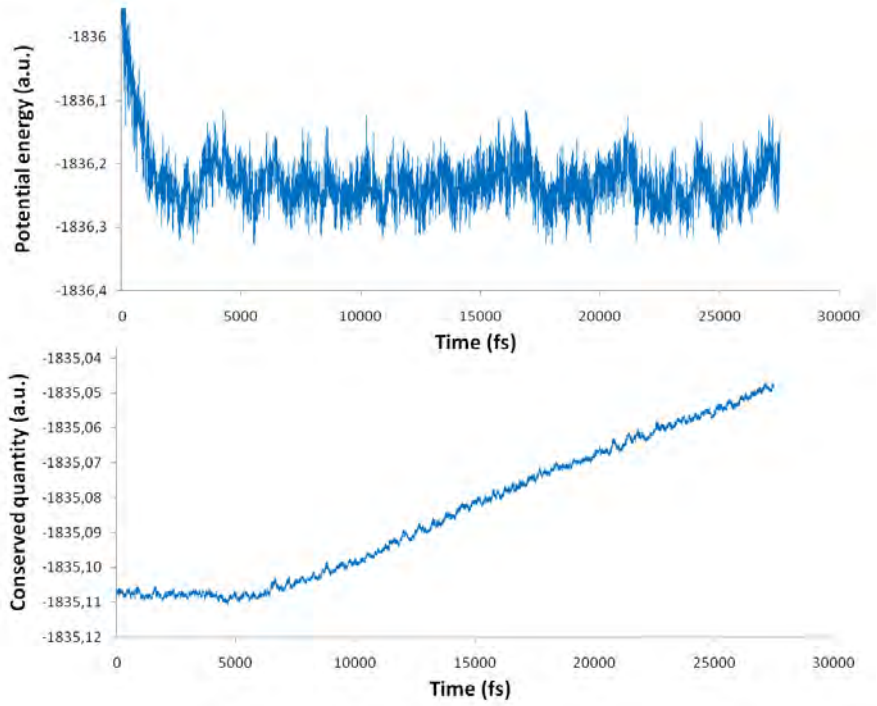

Figure A.5: The potential energy and conserved quantity of the system as a function of simulation time in the NPT ensemble

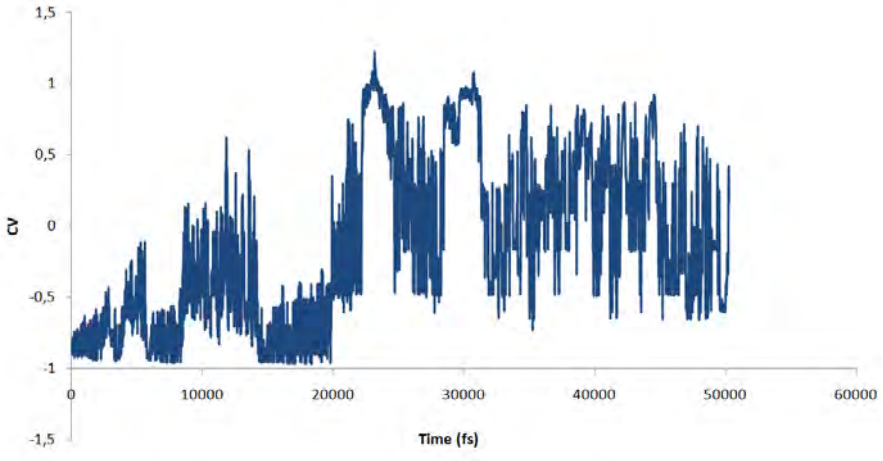

Figure A.6: The CV as a function of simulation time in the metadynamics simulation of the deprotonation with m_H=12 g/mol

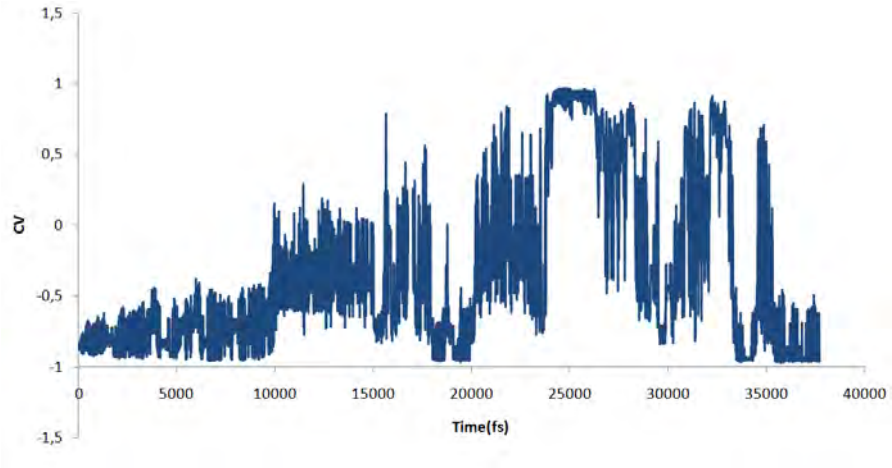

Figure A.7: The CV as a function of simulation time in the metadynamics simulation of the deprotonation with m_H=3 g/mol

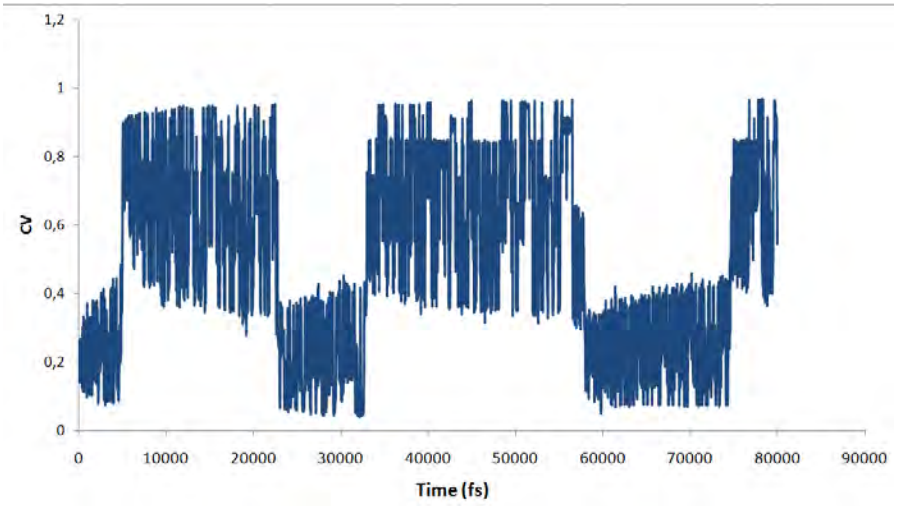

Figure A.8: The CV as a function of simulation time in the metadynamics simulation of the ring contraction

Appendix B

Poster NCCC

This appendix contains the poster which was presented on March 10 2014 at the 15th Netherlands' Catalysis and Chemistry Conference (NCCC), Noordwijkerhout (NL).

Dynamic ab initio study towards new hydrocarbon pool cycles for the MTO conversion in H-SAPO-5

Thomas Deconinck[1], Kristof De Wispelaere[1], Jeroen Van der Mynsbrugge[1], Samuel Moors[1], Marius Westgård Erichsen[2], Stian Svelle[2], Unni Olsbye[2], Karen Hemelsoet[1], Veronique Van Speybroeck[1]

[1]Center for Molecular Modeling, Ghent University, Technologiepark 903, 9052 Zwijnaarde, Belgium
[2]inGAP Centre of Research Based Innovation, Department of Chemistry, University of Oslo, N-0315 Oslo, Norway

Methanol to olefins

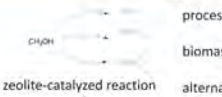

zeolite-catalyzed reaction
↓
shape selective products
diffusional limitations

process based on renewable sources

biomass → syngas → methanol

alternative source for base chemicals not depending on oil

The reaction mechanism [1],[2]

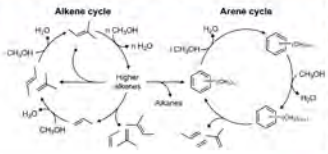

Generally accepted:
Based on a dual cycle mechanism
Hydrocarbon pool important to catalyze the reaction
No direct C-C coupling

Remaining uncertainties:
Importance of different hydrocarbon pool species
Exact olefin elimination process
Influence of the catalyst structure and acidity

AFI

7.3 x 7.3 Å²

H-SAPO-5: moderately acidic

H-SSZ-24 strongly acidic

Why AFI?
CONS: not a regulary used MTO catalyst little shape selectivity
PROS:
The ability to feed a range of different hydrocarbons [2],[3]

Good control over the concentrations inside the catalyst
↓
Experimental kinetic studies possible

GOALS:

- Gain insight into the different roles of structurally different HP species in the two materials
- Investigate the effect of composition on the reaction mechanism
- Study the adsorption complexes of methanol and hydrocarbons
- Simulate key steps of the olefin producing mechanism

Adsorption energies of methanol and benzene

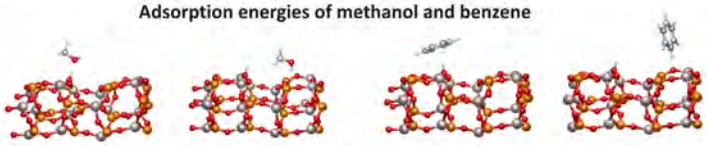

adsorption energy (kJ/mol)	H-SAPO-5	H-SSZ-24
methanol on acid site	-83,0	-98,5
methanol on neighbouring O-atom	-44,4	-37,7

adsorption energy (kJ/mol)	H-SAPO-5	H-SSZ-24
benzene on acid site	-88,3	-88,7
benzene on neighbouring O-atom	-79,8	-72,6

Method:

- ab-inito calculations with CP2K
- periodic calculations using revised PBE with D3 dispersion correction terms [6]
- GPW basis-set
- MD/Metadynamics [7,8]

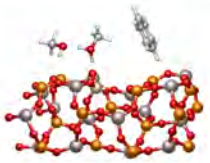

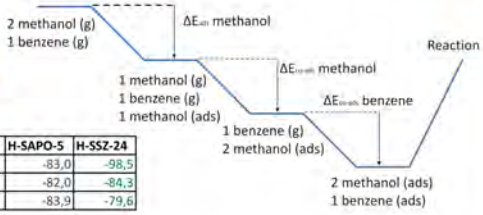

adsorption energy (kJ/mol)	H-SAPO-5	H-SSZ-24
first methanol adsorption	-83,0	-98,5
co-adsorption second methanol	-82,0	-84,3
co-adsorption benzene	-83,9	-79,6

Conclusions

- Different host-guest interaction strength due to difference in acidity
- Framework interaction very important
- Methanol cluster formation more pronounced in H-SSZ-24

Host guest interaction

H-SSZ-24

-82 kJ/mol

H-SAPO-5

-79 kJ/mol

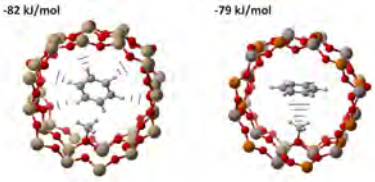

The orientation of the guest-molecule depends on the interaction strength with the framework.

Olefin production from aromatic hydrocarbon pool species [5]

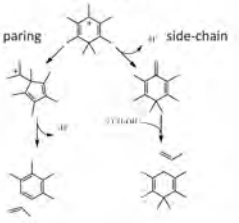

Experimental evidence suggests that the paring mechanism is dominant [2,3]

Future work:

- Investigate the paring mechanism
- Investigate why side chain mechanism is less pronounced

References:

[1] Hemelsoet K. et al., ChemPhysChem., 14 (2013) 1526
[2] Westgård E.M. et al., Catal. Today., 215 (2013) 216
[3] Westgård E.M. et al., J. Catal., 298 (2012) 94
[4] Klap G. J. et al., Chem. Mater., 11 (1999) 3497
[5] McCan D.M. et al.,Angew. Chem;, 47 (2006) 5179
[6] Grimme S., J. Comput. Chem., 27 (2006) 1787
[7] Laio A. et al., Rep. Prog. Phys., 71 (2008) 22
[8] Ensing B. et al., Accounts Chem. Res., 39 (2006) 73

Appendix C

Article in preparation

Some of the optimized structures and corresponding adsorption energies that were calculated in this thesis are used during the preparation of the following manuscript:
"How zeolitic acid strength and composition alter the reactivity of alkenes and aromatics towards methanol", Marius Westgård Erichsen, Kristof De Wispelaere, Karen Hemelsoet, Samuel L. C. Moors, Thomas Deconinck, Stian Svelle, Veronique Van Speybroeck and Unni Olsbye, 2014, in preparation

List of Figures

List of Tables

Bibliography

[1] Y.-K. Park, C. W. Lee, N. Y. Kang, W. C. Choi, S. Choi, S. H. Oh, and D. S. Park, "Catalytic cracking of lower-valued hydrocarbons for producing light olefins," *Catalysis Surveys from Asia*, vol. 14, no. 2, pp. 75–84, 2010.

[2] Analysis & projections - U.S. energy information administration (EIA) - U.S. energy information administration (EIA), http://www.eia.gov/analysis/studies/worldshalegas/ 2013.

[3] The end of cheap coal, http://www.postcarbon.org/article/406162-the-end-of-cheap-coal 2011.

[4] K. Hemelsoet, J. Van der Mynsbrugge, K. De Wispelaere, M. Waroquier, and V. Van Speybroeck, "Unraveling the reaction mechanisms governing methanol-to-olefins catalysis by theory and experiment," *European Journal of Chemical Physics and Physical Chemistry*, vol. 14, no. 8, pp. 1526–1545, 2013.

[5] "Market intelligence: MTO enjoys an advantage in china over naphtha," http://www.icis.com/resources/news/2012/08/27/9589985/market-intelligence-mto-enjoys-an-advantage-in-china-over-naphtha/ 2012.

[6] M. J. Tallman and C. N. Eng, "Propylene on purpose," http://www.kbr.com/Newsroom/Publications/Articles/Propylene-on-Purpose.pdf Dec. 2010.

[7] L.-W. Su, X.-R. Li, and Z.-Y. Sun, "The consumption, production and transportation of methanol in china: A review," *Energy Policy*, vol. 63, pp. 130–138, 2013.

[8] "Olefin production boosts demand for coal-based methanol in china :: Chemical week," http://www.chemweek.com/lab/Olefin-production-boosts-demand-for-coal-based-methanol-in-China 54949.html 2013.

[9] "China annual methanol demand to spike on MTO, MTP projects," http://www.icis.com/resources/news/2012/10/30/9604963/china-annual-methanol-demand-to-spike-on-mto-mtp-projects/ 2012.

[10] L. Tock, M. Gassner, and F. Maréchal, "Thermochemical production of liquid fuels from biomass: Thermo-economic modeling, process design and process integration analysis," *Biomass and Bioenergy*, vol. 34, no. 12, pp. 1838–1854, Dec. 2010.

[11] I. Olofsson, A. Nordin, and U. Soderlind, *Initial review and evaluation of process technologies and systems suitable for cost-efficient medium-scale gasification for biomass to liquid fuels*, Energy Technology & Thermal Process Chemistry, University of Umea, Umea, 2005.

[12] K. M. Holmgren, T. Berntsson, E. Andersson, and T. Rydberg, "System aspects of biomass gasification with methanol synthesis – process concepts and energy analysis," *Energy*, vol. 45, no. 1, pp. 817–828, 2012.

[13] K. S. Ng and J. Sadhukhan, "Process integration and economic analysis of bio-oil platform for the production of methanol and combined heat and power," *Biomass and Bioenergy*, vol. 35, no. 3, pp. 1153–1169, 2011.

[14] "Naphta catalytic cracking for propylene production," http://www.digitalrefining.com/article/1000787,Naphtha catalytic cracking for propylene production.html.Uzqmpvl uW4 2013.

[15] J. Ding and W. Hua, "Game changers of the c3 value chain: Gas, coal, and biotechnologies," *Chemical Engineering & Technology*, vol. 36, no. 1, pp. 83–90, 2013.

[16] B. V. Vora, T. L. Marker, P. T. Barger, H. R. Nilsen, S. Kvisle, and T. Fuglerud, "Economic route for natural gas conversion to ethylene and propylene," in *Studies in Surface Science and Catalysis*, C. P. Nicolaides J. H. Scholtz M. de Pontes, R. L. Espinoza and M. S. Scurrell, Eds., vol. Volume 107 of *Natural Gas Conversion IV*, pp. 87–98. Elsevier, 1997.

[17] H. Koempel and W. Liebner, "Lurgi's methanol to propylene (MTP®) report on a successful commercialisation," in *Studies in Surface Science and Catalysis*, Martin Schmal Fábio Bellot Noronha and Eduardo Falabella Sousa-Aguiar, Eds., vol. Volume 167 of *Natural Gas Conversion VIII Proceedings of the 8th Natural Gas Conversion Symposium*, pp. 261–267. Elsevier, 2007.

[18] F. J. Keil, "Methanol-to-hydrocarbons: process technology," *Microporous and Mesoporous Materials*, vol. 29, no. 1–2, pp. 49–66, 1999.

[19] J. Q. Chen, A. Bozzano, B. Glover, T. Fuglerud, and S. Kvisle, "Recent advancements in ethylene and propylene production using the UOP/Hydro MTO process," *Catalysis Today*, vol. 106, no. 1–4, pp. 103–107, 2005.

[20] A. T. Najafabadi, S. Fatemi, M. Sohrabi, and M. Salmasi, "Kinetic modeling and optimization of the operating condition of MTO process on SAPO-34 catalyst," *Journal of Industrial and Engineering Chemistry*, vol. 18, no. 1, pp. 29–37, 2012.

[21] J. F. Haw and D. M. Marcus, "Well-defined (supra)molecular structures in zeolite methanol-to-olefin catalysis," *Topics in Catalysis*, vol. 34, no. 1-4, pp. 41–48, 2005.

[22] D. Mores, J. Kornatowski, U. Olsbye, and B. M. Weckhuysen, "Coke formation during the methanol-to-olefin conversion: In situ microspectroscopy on individual H-ZSM-5 crystals with different brønsted acidity," *Chemistry – A European Journal*, vol. 17, no. 10, pp. 2874–2884, 2011.

[23] U. Olsbye, S. Svelle, M. Bjørgen, P. Beato, T. V. W. Janssens, F. Joensen, S. Bordiga, and K. P. Lillerud, "Conversion of methanol to hydrocarbons: How zeolite cavity and pore size controls product selectivity," *Angewandte Chemie International Edition*, vol. 51, no. 24, pp. 5810–5831, 2012.

[24] J. Senetar and E. Romers, *Scale-up of advanced MTO technology and integrated OCP technology*, http://www.allriskengineering.com/library files/AIChe conferences/AIChe 2011/ data/papers/P213033.pdf, 2011.

[25] K. Van Geem, *Course notes sustainable chemical production processes*, 2012.

[26] R. Kempf, *Advances in Commercialization of the UOP Advanced MTO Technology*, 2011.

[27] "Database of zeolite structures," http://www.iza-structure.org/databases/, May 2014.

[28] M. Stöcker, "Methanol-to-hydrocarbons: catalytic materials and their behavior," *Microporous and Mesoporous Materials*, vol. 29, no. 1-2, pp. 3–48, 1999.

[29] S. Devika, B. Sundaravel, M. Palanichamy, and V. Murugesan, "Vapour phase oxidation of toluene over CeAlPO-5 molecular sieves," *Journal of Nanoscience and Nanotechnology*, vol. 14, no. 4, pp. 3187–3192, 2014.

[30] K. L. Boyesen and K. Mathisen, "Exposing the synergistic effect between copper and vanadium in A1P0-5 during the selective oxidation of propene," *Catalysis Today*, vol. 229, pp. 14–22, 2014.

[31] M. Westgård Erichsen, S. Svelle, and U. Olsbye, "H-SAPO-5 as methanol-to-olefins (MTO) model catalyst: Towards elucidating the effects of acid strength," *Journal of Catalysis*, vol. 298, pp. 94–101, 2013.

[32] L.-T. Yuen, S. I. Zones, T. V. Harris, E. J. Gallegos, and A. Auroux, "Product selectivity in methanol to hydrocarbon conversion for isostructural compositions of AFI and CHA molecular sieves," *Microporous Materials*, vol. 2, no. 2, pp. 105–117, 1994.

[33] Z.-M. Cui, Q. Liu, W.-G. Song, and L.-J. Wan, "Insights into the mechanism of methanol-to-olefin conversion at zeolites with systematically selected framework structures," *Angewandte Chemie International Edition*, vol. 45, no. 39, pp. 6512–6515, 2006.

[34] Q. Wang, Z.-M. Cui, C.-Y. Cao, and W.-G. Song, "0.3 Å makes the difference: Dramatic changes in methanol-to-olefin activities between H-ZSM-12 and H-ZSM-22 zeolites," *The Journal of Physical Chemistry C*, vol. 115, no. 50, pp. 24987–24992, 2011.

[35] J. Li, Y. Wei, G. Liu, Y. Qi, P. Tian, B. Li, Y. He, and Z. Liu, "Comparative study of MTO conversion over H-SAPO-34, H-ZSM-5 and H-ZSM-22: correlating catalytic performance and reaction mechanism to zeolite topology," *Catalysis Today*, vol. 171, no. 1, pp. 221–228, 2011.

[36] D. Lesthaeghe, V. Van Speybroeck, G. B. Marin, and M. Waroquier, "Understanding the failure of direct c-c coupling in the zeolite-catalyzed methanol-to-olefin process," *Angewandte Chemie International Edition*, vol. 45, no. 11, pp. 1714–1719, 2006.

[37] R. M. Dessau and R. B. LaPierre, "On the mechanism of methanol conversion to hydrocarbons over HZSM-5," *Journal of Catalysis*, vol. 78, no. 1, pp. 136–141, 1982.

[38] T. Mole, J. A. Whiteside, and D. Seddon, "Aromatic co-catalysis of methanol conversion over zeolite catalysts," *Journal of Catalysis*, vol. 82, no. 2, pp. 261–266, 1983.

[39] T. Mole, G. Bett, and D. Seddon, "Conversion of methanol to hydrocarbons over ZSM-5 zeolite: An examination of the role of aromatic hydrocarbons using 13carbon- and deuterium-labeled feeds," *Journal of Catalysis*, vol. 84, no. 2, pp. 435–445, 1983.

[40] I. M. Dahl and S. Kolboe, "On the reaction mechanism for hydrocarbon formation from methanol over SAPO-34: i. isotopic labeling studies of the co-reaction of ethene and methanol," *Journal of Catalysis*, vol. 149, no. 2, pp. 458–464, 1994.

[41] I. M. Dahl and S. Kolboe, "On the reaction mechanism for propene formation in the MTO reaction over SAPO-34," *Catalysis Letters*, vol. 20, no. 3-4, pp. 329–336, 1993.

[42] W. Song, D. M. Marcus, H. Fu, J. O. Ehresmann, and J. F. Haw, "An oft-studied reaction that may never have been: direct catalytic conversion of methanol or dimethyl ether to hydrocarbons on the solid acids H-ZSM-5 or H-SAPO-34," *Journal of the American Chemical Society*, vol. 124, no. 15, pp. 3844–3845, 2002.

[43] Y. Jiang, W. Wang, V. R. Reddy Marthala, J. Huang, B. Sulikowski, and M. Hunger, "Effect of organic impurities on the hydrocarbon formation via the decomposition of surface methoxy groups on acidic zeolite catalysts," *Journal of Catalysis*, vol. 238, no. 1, pp. 21–27, 2006.

[44] M. Vandichel, D. Lesthaeghe, J. Van der Mynsbrugge, M. Waroquier, and V. Van Speybroeck, "Assembly of cyclic hydrocarbons from ethene and propene in acid zeolite catalysis to produce active catalytic sites for MTO conversion," *Journal of Catalysis*, vol. 271, no. 1, pp. 67–78, 2010.

[45] W. Song, John B. Nicholas, A. Sassi, and J. F. Haw, "Synthesis of the heptamethylbenzenium cation in zeolite-: in situ NMR and theory," *Catalysis Letters*, vol. 81, no. 1-2, pp. 49–53, 2002.

[46] A. Sassi, M. A. Wildman, H. J. Ahn, P. Prasad, J. B. Nicholas, and J. F. Haw, "Methylbenzene chemistry on zeolite HBeta: multiple insights into methanol-to-olefin catalysis," *The Journal of Physical Chemistry B*, vol. 106, no. 9, pp. 2294–2303, 2002.

[47] S. Svelle, F. Joensen, J. Nerlov, U. Olsbye, K.-P. Lillerud, S. Kolboe, and M. Bjørgen, "Conversion of methanol into hydrocarbons over zeolite H-ZSM-5: ethene formation is mechanistically separated from the formation of higher alkenes," *Journal of the American Chemical Society*, vol. 128, no. 46, pp. 14770–14771, 2006.

[48] U. Olsbye, M. Bjørgen, S. Svelle, K.-P. Lillerud, and S. Kolboe, "Mechanistic insight into the methanol-to-hydrocarbons reaction," *Catalysis Today*, vol. 106, no. 1–4, pp. 108–111, 2005.

[49] S. Svelle, U. Olsbye, F. Joensen, and M. Bjørgen, "Conversion of methanol to alkenes over medium- and large-pore acidic zeolites: steric manipulation of the reaction intermediates governs the Ethene/Propene product selectivity," *The Journal of Physical Chemistry C*, vol. 111, no. 49, pp. 17981–17984, 2007.

[50] B. Arstad, S. Kolboe, and O. Swang, "Theoretical study of the heptamethylbenzenium ion. intramolecular isomerizations and c2, c3, c4 alkene elimination," *The Journal of Physical Chemistry A*, vol. 109, no. 39, pp. 8914–8922, 2005.

[51] A. Sassi, M. A. Wildman, and J. F. Haw, "Reactions of butylbenzene isomers on zeolite HBeta: methanol-to-olefins hydrocarbon pool chemistry and secondary

reactions of olefins," *The Journal of Physical Chemistry B*, vol. 106, no. 34, pp. 8768–8773, 2002.

[52] R. F. Sullivan, C. J. Egan, G. E. Langlois, and R. P. Sieg, "A new reaction that occurs in the hydrocracking of certain aromatic hydrocarbons," *Journal of the American Chemical Society*, vol. 83, no. 5, pp. 1156–1160, 1961.

[53] M. Bjørgen, U. Olsbye, D. Petersen, and S. Kolboe, "The methanol-to-hydrocarbons reaction: insight into the reaction mechanism from benzene and methanol coreactions over zeolite h-beta," *Journal of Catalysis*, vol. 221, no. 1, pp. 1–10, 2004.

[54] W. Song, H. Fu, and J. F. Haw, "Selective synthesis of methylnaphthalenes in H-SAPO-34 cages and their function as reaction centers in methanol-to-olefin catalysis," *The Journal of Physical Chemistry B*, vol. 105, no. 51, pp. 12839–12843, 2001.

[55] B. P. C. Hereijgers, F. Bleken, M. H. Nilsen, S. Svelle, Karl-Petter Lillerud, Morten Bjørgen, Bert M. Weckhuysen, and Unni Olsbye, "Product shape selectivity dominates the methanol-to-olefins (MTO) reaction over H-SAPO-34 catalysts," *Journal of Catalysis*, vol. 264, no. 1, pp. 77–87, 2009.

[56] V. Van Speybroeck, K. Hemelsoet, K. DeWispelaere, Q. Qian, J. VanderMynsbrugge, B. DeSterck, B. M. Weckhuysen, and Michel Waroquier, "Mechanistic studies on chabazite-type methanol-to-olefin catalysts: Insights from time-resolved UV/Vis microspectroscopy combined with theoretical simulations," *ChemCatChem*, vol. 5, no. 1, pp. 173–184, 2013.

[57] H. Fu, W. Song, and J. F. Haw, "Polycyclic aromatics formation in H-SAPO-34 during methanol-to-olefin catalysis: Ex situ characterization after cryogenic grinding," *Catalysis Letters*, vol. 76, no. 1-2, pp. 89–94, 2001.

[58] K. Hemelsoet, A. Nollet, V. Van Speybroeck, and M. Waroquier, "Theoretical simulations elucidate the role of naphthalenic species during methanol conversion within H-SAPO-34," *Chemistry – A European Journal*, vol. 17, no. 33, pp. 9083–9093, 2011.

[59] C.-M. Wang, Y.-D. Wang, Z.-K. Xie, and Z.-P. Liu, "Methanol to olefin conversion on H-SAPO-34 zeolite from periodic density functional theory calculations: A complete cycle of side chain hydrocarbon pool mechanism," *The Journal of Physical Chemistry C*, vol. 113, no. 11, pp. 4584–4591, 2009.

[60] K. De Wispelaere, K. Hemelsoet, M. Waroquier, and V. Van Speybroeck, "Complete low-barrier side-chain route for olefin formation during methanol conversion in H-SAPO-34," *Journal of Catalysis*, vol. 305, pp. 76–80, 2013.

[61] D.M. McCann, D. Lesthaeghe, P.W. Kletnieks, D.R. Guenther, M.J. Hayman, V. Van Speybroeck, M. Waroquier, and J.F. Haw, "A complete catalytic cycle for supramolecular methanol-to-olefins conversion by linking theory with experiment," *Angewandte Chemie International Edition*, vol. 47, no. 28, pp. 5179–5182, 2008.

[62] M. Bjørgen, F. Bonino, S. Kolboe, K.-P. Lillerud, A. Zecchina, and S. Bordiga, "Spectroscopic evidence for a persistent benzenium cation in zeolite h-beta," *Journal of the American Chemical Society*, vol. 125, no. 51, pp. 15863–15868, 2003.

[63] J. F. Haw, "Zeolite acid strength and reaction mechanisms in catalysis," pp. 5431–5441, 2002.

[64] J. F. Haw, J. B. Nicholas, W. Song, F. Deng, Z. Wang, T. Xu, and Catherine S. Heneghan, "Roles for cyclopentenyl cations in the synthesis of hydrocarbons from methanol on zeolite catalyst H-ZSM-5," *Journal of the American Chemical Society*, vol. 122, no. 19, pp. 4763–4775, 2000.

[65] J. Macht, R. T. Carr, and E. Iglesia, "Consequences of acid strength for isomerization and elimination catalysis on solid acids," *Journal of the American Chemical Society*, vol. 131, no. 18, pp. 6554–6565, 2009.

[66] D. Lesthaeghe, A. Horré, M. Waroquier, G.B. Marin, and V. Van Speybroeck, "Theoretical insights on methylbenzene side-chain growth in ZSM-5 zeolites for methanol-to-olefin conversion," *Chemistry – A European Journal*, vol. 15, no. 41, pp. 10803–10808, 2009.

[67] S. Svelle, P. O. Rønning, and S. Kolboe, "Kinetic studies of zeolite-catalyzed methylation reactions: coreaction of ethene and methanol," *Journal of Catalysis*, vol. 224, no. 1, pp. 115–123, 2004.

[68] M. Bjørgen, S. Svelle, F. Joensen, J. Nerlov, S. Kolboe, F. Bonino, L. Palumbo, S. Bordiga, and U. Olsbye, "Conversion of methanol to hydrocarbons over zeolite H-ZSM-5: on the origin of the olefinic species," *Journal of Catalysis*, vol. 249, no. 2, pp. 195–207, 2007.

[69] M. Bjørgen, F. Joensen, K.-P. Lillerud, U. Olsbye, and S. Svelle, "The mechanisms of ethene and propene formation from methanol over high silica H-ZSM-5 and H-Beta," *Catalysis Today*, vol. 142, no. 1–2, pp. 90–97, 2009.

[70] D. Lesthaeghe, J. VanderMynsbrugge, M. Vandichel, M. Waroquier, and V. Van Speybroeck, "Full theoretical cycle for both ethene and propene formation during methanol-to-olefin conversion in H-ZSM-5," *ChemCatChem*, vol. 3, no. 1, pp. 208–212, 2011.

[71] S. Teketel, S. Svelle, K.-P. Lillerud, and U. Olsbye, "Shape-selective conversion of methanol to hydrocarbons over 10-ring unidirectional-channel acidic H-ZSM-22," *Chemcatchem*, vol. 1, no. 1, pp. 78–81, 2009,

[72] S. Teketel, W. Skistad, S. Benard, U. Olsbye, K. P. Lillerud, P. Beato, and S. Svelle, "Shape selectivity in the conversion of methanol to hydrocarbons: The catalytic performance of one-dimensional 10-ring zeolites: ZSM-22, ZSM-23, ZSM-48, and EU-1," *ACS Catalysis*, vol. 2, no. 1, pp. 26–37, 2012.

[73] S. Svelle, M. Visur, U. Olsbye, Saepurahman, and M. Bjørgen, "Mechanistic aspects of the zeolite catalyzed methylation of alkenes and aromatics with methanol: A review," *Topics in Catalysis*, vol. 54, no. 13-15, pp. 897–906, 2011.

[74] V. Van Speybroeck, J. Van der Mynsbrugge, M. Vandichel, Karen Hemelsoet, D. Lesthaeghe, A. Ghysels, G. B. Marin, and M. Waroquier, "First principle kinetic studies of zeolite-catalyzed methylation reactions," *Journal of the American Chemical Society*, vol. 133, no. 4, pp. 888–899, 2011.

[75] S. Svelle, C. Tuma, X. Rozanska, T. Kerber, and J. Sauer, "Quantum chemical modeling of zeolite-catalyzed methylation reactions: Toward chemical accuracy for barriers," *Journal of the American Chemical Society*, vol. 131, no. 2, pp. 816–825, 2009.

[76] B. Arstad, J. B. Nicholas, and J. F. Haw, "Theoretical study of the methylbenzene side-chain hydrocarbon pool mechanism in methanol to olefin catalysis," *Journal of the American Chemical Society*, vol. 126, no. 9, pp. 2991–3001, 2004.

[77] H. Yamazaki, H. Shima, H. Imai, T. Yokoi, T. Tatsumi, and J. N. Kondo, "Evidence for a "Carbene-like" intermediate during the reaction of methoxy species with light alkenes on H-ZSM-5," *Angewandte Chemie International Edition*, vol. 50, no. 8, pp. 1853–1856, 2011.

[78] M. Guisnet and P. Magnoux, "Organic chemistry of coke formation," *Applied Catalysis a-General*, vol. 212, no. 1-2, pp. 83–96, 2001.

[79] K. Hemelsoet, A. Nollet, M. Vandichel, D. Lesthaeghe, V. Van Speybroeck, and M. Waroquier, "The effect of confined space on the growth of naphthalenic species in a chabazite-type catalyst: A molecular modeling study," *Chemcatchem*, vol. 1, no. 3, pp. 373–378, 2009.

[80] D. Chen, K. Moljord, and A. Holmen, "A methanol to olefins review: Diffusion, coke formation and deactivation on SAPO type catalysts," *Microporous and Mesoporous Materials*, vol. 164, pp. 239–250, 2012.

[81] G. Z. Qi, Z. K. Xie, W. M. Yang, S. Q. Zhong, H. X. Liu, C. F. Zhang, and Q. L. Chen, "Behaviors of coke deposition on SAPO-34 catalyst during methanol conversion to light olefins," *Fuel Processing Technology*, vol. 88, no. 5, pp. 437–441, 2007.

[82] D. Chen, H. P. Rebo, K. Moljord, and A. Holmen, "Influence of coke deposition on selectivity in zeolite catalysis," *Industrial & Engineering Chemistry Research*, vol. 36, no. 9, pp. 3473–3479, 1997.

[83] D. Mores, E. Stavitski, M.H.F. Kox, J. Kornatowski, U. Olsbye, and B.M. Weckhuysen, "Space- and time-resolved in-situ spectroscopy on the coke formation in molecular sieves: Methanol-to-olefin conversion over H-ZSM-5 and H-SAPO-34," *Chemistry – A European Journal*, vol. 14, no. 36, pp. 11320–11327, 2008.

[84] Z. D. Zhu, M. Hartmann, and L. Kevan, "Catalytic conversion of methanol to olefins on SAPO-n (n=11, 34, and 35), CrAPSO-n, and cr-SAPO-n molecular sieves," *Chemistry of Materials*, vol. 12, no. 9, pp. 2781–2787, 2000.

[85] A. M. Prakash, M. Hartmann, Z. D. Zhu, and L. Kevan, "Incorporation of transition metal ions into MeAPO/MeAPSO molecular sieves," *Journal of Physical Chemistry B*, vol. 104, no. 7, pp. 1610–1616, 2000.

[86] I. M. Dahl, H. Mostad, D. Akporiaye, and R. Wendelbo, "Structural and chemical influences on the MTO reaction: a comparison of chabazite and SAPO-34 as MTO catalysts," *Microporous and Mesoporous Materials*, vol. 29, no. 1-2, pp. 185–190, 1999.

[87] K. Hemelsoet, A. Ghysels, D. Mores, K. De Wispelaere, V. Van Speybroeck, B. M. Weckhuysen, and M. Waroquier, "Experimental and theoretical IR study of methanol and ethanol conversion over H-SAPO-34," *Catalysis Today*, 2011.

[88] F. Bleken, M. Bjørgen, L. Palumbo, S. Bordiga, S. Svelle, K.-P. Lillerud, and U. Olsbye, "The effect of acid strength on the conversion of methanol to olefins over acidic microporous catalysts with the CHA topology," *Topics in Catalysis*, vol. 52, no. 3, pp. 218–228, 2009.

[89] Y. Kumita, J. Gascon, E. Stavitski, J. A. Moulijn, and F. Kapteijn, "Shape selective methanol to olefins over highly thermostable DDR catalysts," *Applied Catalysis a-General*, vol. 391, no. 1-2, pp. 234–243, 2011.

[90] Y.Jiang, J. Huang, V. R. R. Marthala, Y. S. Ooi, J. Weitkamp, and M. Hunger, "In situ MAS NMR–UV/Vis investigation of H-SAPO-34 catalysts partially coked in the methanol-to-olefin conversion under continuous-flow conditions and of their regeneration," *Microporous and Mesoporous Materials*, vol. 105, no. 1–2, pp. 132–139, 2007.

[91] V. Van Speybroeck, *Course notes molecular modeling of industrial processes*, 2012.

[92] J. P. Perdew, K. Burke, and M. Ernzerhof, "Generalized gradient approximation made simple," *Physical Review Letters*, vol. 77, no. 18, pp. 3865–3868, 1996.

[93] S. Grimme, J. Antony, S. Ehrlich, and H. Krieg, "A consistent and accurate ab initio parametrization of density functional dispersion correction (DFT-D) for the 94 elements h-pu," *The Journal of Chemical Physics*, vol. 132, no. 15, pp. 154104, 2010.

[94] A. Alparone, V. Librando, and Z. Minniti, "Validation of semiempirical PM6 method for the prediction of molecular properties of polycyclic aromatic hydrocarbons and fullerenes," *Chemical Physics Letters*, vol. 460, no. 1-3, pp. 151–154, 2008.

[95] G. Lippert, J. Hutter, and M. Parrinello, "The gaussian and augmented-plane-wave density functional method for ab initio molecular dynamics simulations," *Theoretical Chemistry Accounts*, vol. 103, no. 2, pp. 124–140, 1999,

[96] J. VandeVondele, M. Krack, F. Mohamed, M. Parrinello, T. Chassaing, and J. Hutter, "Quickstep: Fast and accurate density functional calculations using a mixed gaussian and plane waves approach," *Computer Physics Communications*, vol. 167, no. 2, pp. 103–128, 2005.

[97] S. Maeda, E. A., M. Hatanaka, T. Taketsugu, and K. Morokuma, "Exploring potential energy surfaces of large systems with artificial force induced reaction method in combination with ONIOM and microiteration," *Journal of Chemical Theory and Computation*, vol. 8, no. 12, pp. 5058–5063, 2012.

[98] T. Vreven and K. Morokuma, "On the application of the IMOMO (integrated molecular orbital + molecular orbital) method," *Journal of Computational Chemistry*, vol. 21, no. 16, pp. 1419–1432, 2000.

[99] R. Car and M. Parrinello, "Unified approach for molecular dynamics and density-functional theory," *Physical Review Letters*, vol. 55, no. 22, pp. 2471–2474, 1985.

[100] D. Frenkel and B. Smit, *Understanding Molecular Simulation: From Algorithms to Applications*, Academic Press, 2001.

[101] T. Bučko, L. Benco, O. Dubay, C. Dellago, and J. Hafner, "Mechanism of alkane dehydrogenation catalyzed by acidic zeolites: Ab initio transition path sampling," *The Journal of Chemical Physics*, vol. 131, no. 21, pp. 214508, 2009.

[102] T. Bučko, L. Benco, J. Hafner, and J. G. Ángyán, "Monomolecular cracking of propane over acidic chabazite: An ab initio molecular dynamics and transition path sampling study," *Journal of Catalysis*, vol. 279, no. 1, pp. 220–228, 2011.

[103] L. Benco, T. Bucko, and J. Hafner, "Dehydrogenation of propane over ZnMOR. static and dynamic reaction energy diagram," *Journal of Catalysis*, vol. 277, no. 1, pp. 104–116, 2011.

[104] "Multiscale modeling and simulation," http://www.wag.caltech.edu/multiscale/ 2014.

[105] A. Laio and F. L. Gervasio, "Metadynamics: a method to simulate rare events and reconstruct the free energy in biophysics, chemistry and material science," *Reports on Progress in Physics*, vol. 71, no. 12, pp. 126601, 2008.

[106] B. Ensing, M. De Vivo, Z. Liu, P. Moore, and M. L. Klein, "Metadynamics as a tool for exploring free energy landscapes of chemical reactions," *Accounts of Chemical Research*, vol. 39, no. 2, pp. 73–81, 2006.

[107] M. Ianuzzi, "first CP2K tutorial," http://scc.acad.bg/ncsa/articles/library/CP2K-Tutorial-Quantum-Mechanics-and-Molecular-Dynamics/presentation 2995.pdf, 2014.

[108] S. L. C. Moors, K. De Wispelaere, J. Van der Mynsbrugge, M. Waroquier, and V. Van Speybroeck, "Molecular dynamics kinetic study on the zeolite-catalyzed benzene methylation in ZSM-5," *ACS Catalysis*, vol. 3, no. 11, pp. 2556–2567, 2013.

[109] "about [CP2K open source molecular dynamics]," http://www.cp2k.org/ 2014.

[110] B. Hammer, L. B. Hansen, and J. K. Nørskov, "Improved adsorption energetics within density-functional theory using revised perdew-burke-ernzerhof functionals," *Physical Review B*, vol. 59, no. 11, pp. 7413–7421, 1999.

[111] S. Goedecker, M. Teter, and J. Hutter, "Separable dual-space gaussian pseudopotentials," *Physical Review B*, vol. 54, no. 3, pp. 1703–1710, July 1996.

[112] G. Mirth and J. A. Lercher, "Coadsorption of toluene and methanol on H-ZSM-5," *Journal of Physical Chemistry*, vol. 95, no. 9, pp. 3736–3740, 1991.

[113] R. A. van Santen, "Quantum-chemistry of zeolite acidity," *Catalysis Today*, vol. 38, no. 3, pp. 377–390, Nov. 1997.

[114] I. Stich, J. D Gale, K. Terakura, and M. C Payne, "Dynamical observation of the catalytic activation of methanol in zeolites," *Chemical Physics Letters*, vol. 283, no. 5–6, pp. 402–408, 1998.

[115] K. De Wispelaere, *Ab Initio Studie naar de Deactivering van Zeoliet- en Zeotype-katalysatoren in het MTO-proces; Master thesis*, UGent, 2011.

[116] M. Westgård Erichsen, S. Svelle, and U. Olsbye, "The influence of catalyst acid strength on the methanol to hydrocarbons (MTH) reaction," *Catalysis Today*, vol. 215, pp. 216–223, 2013.

[117] S. B. McCullen, P. T. Reischman, and D. H. Olson, "Hexane and benzene adsorption by aluminophosphates and SSZ-24: the effect of pore size and molecular sieve composition," *Zeolites*, vol. 13, no. 8, pp. 640–644, 1993.

[118] Ľ Benco, T Demuth, J Hafner, and F Hutschka, "Ab initio molecular dynamics simulation of hydration and ion-exchange processes in low al-zeolites," *Microporous and Mesoporous Materials*, vol. 42, no. 1, pp. 1–19, 2001.

[119] I.-C. Lin and M. E Tuckerman, "Enhanced conformational sampling of peptides via reduced side-chain and solvent masses," *The journal of physical chemistry. B*, vol. 114, no. 48, pp. 15935–15940, 2010.

[120] G. S. Hammond, "A correlation of reaction rates," *Journal of the American Chemical Society*, vol. 77, no. 2, pp. 334–338, 1955.